

REPORT DOCUMENTATION PAGE			Form Approved OMB No. 0704-0188	
Public reporting burden for this collection of information is estimated to average 1 hour per response, including the time for reviewing instructions, searching existing data sources, gathering and maintaining the data needed, and completing and reviewing the collection of information. Send comments regarding this burden estimate or any other aspect of this collection of information, including suggestions for reducing this burden, to Washington Headquarters Services, Directorate for Information Operations and Reports, 1215 Jefferson Davis Highway, Suite 1204, Arlington, VA 22202-4302, and to the Office of Management and Budget, Paperwork Reduction Project (0704-0188), Washington, DC 20503.				
1. AGENCY USE ONLY (Leave blank)	2. REPORT DATE 10 Sep 95	3. REPORT TYPE AND DATES COVERED		
4. TITLE AND SUBTITLE Detection of Summertime Convergence Zones In Central and Eastern North Carolina Using The WSR-88D Doppler Radar		5. FUNDING NUMBERS		
6. AUTHOR(S)  Charles Anthony Ray				
7. PERFORMING ORGANIZATION NAME(S) AND ADDRESS(ES)  AFIT Students Attending:  North Carolina State University		8. PERFORMING ORGANIZATION REPORT NUMBER  95-098		
9. SPONSORING/MONITORING AGENCY NAME(S) AND ADDRESS(ES)  DEPARTMENT OF THE AIR FORCE AFIT/CI 2950 P STREET, BLDG 125 WRIGHT-PATTERSON AFB OH 45433-7765		10. SPONSORING/MONITORING AGENCY REPORT NUMBER		
11. SUPPLEMENTARY NOTES				
12a. DISTRIBUTION/AVAILABILITY STATEMENT  Approved for Public Release IAW AFR 190-1 Distribution Unlimited BRIAN D. GAUTHIER, MSgt, USAF Chief of Administration		12b. DISTRIBUTION CODE		
13. ABSTRACT (Maximum 200 words)		<div data-bbox="1071 1173 1443 1446" data-label="Image"> </div>		
19951017 164		15. NUMBER OF PAGES 193		
		16. PRICE CODE		
17. SECURITY CLASSIFICATION OF REPORT	18. SECURITY CLASSIFICATION OF THIS PAGE	19. SECURITY CLASSIFICATION OF ABSTRACT	20. LIMITATION OF ABSTRACT	

# DETECTION OF SUMMERTIME CONVERGENCE ZONES IN CENTRAL AND EASTERN NORTH CAROLINA USING THE WSR-88D DOPPLER RADAR

Accession For	
NTIS CRA&I	<input checked="" type="checkbox"/>
DTIC TAB	<input type="checkbox"/>
Unannounced	<input type="checkbox"/>
Justification	
By	
Distribution /	
Availability Codes	
Dist	Avail and/or Special
A-1	

by

**CHARLES ANTHONY RAY**

A thesis submitted to the Graduate Faculty of  
North Carolina State University  
in partial fulfillment of the  
requirements for the Degree of  
Master of Science

**MARINE, EARTH AND ATMOSPHERIC SCIENCES**


Raleigh

1995

**APPROVED BY:**

  
 Alan J. Riordan

  
 Gerald F. Watson

  
 Steven E. Koch  
 Chairman of Advisory Committee

## ABSTRACT

RAY, CHARLES A. Detection of Summertime Convergence Zones in Central and Eastern North Carolina Using the WSR-88D Doppler Radar. (Under the direction of Dr. Steven E. Koch.)

A study of the North Carolina (NC) Planetary Boundary Layer (PBL) is conducted, using the newly commissioned National Weather Service WSR-88D Doppler Radar as well as conventional surface and GOES satellite data, to detect and to investigate the nature of convergence zones that affect the summer weather in central and eastern NC. Particular emphasis is placed on the use of the radar's "clear air mode" which is much more sensitive than the conventional non-Doppler operational radars (WSR-57 and WSR-74C) used by the National Weather Service (NWS) prior to the implementation of the WSR-88D. This sensitivity allows detection of very weak features and also provides excellent spatial resolution.

Boundaries observed include synoptic scale fronts, thunderstorm outflows, sea breezes, horizontal roll convection, thermal/moisture boundaries and boundaries that are identified as "unknown moving" and "unknown stationary." One particularly interesting "unknown stationary" boundary occurs frequently and has been labeled a "Piedmont Trough." Using the new Doppler radar, it has been determined that a significant portion of the afternoon and evening thunderstorm activity occurring in NC during the summertime is influenced by these boundaries, many of which are too weak to detect using conventional radar, and most of which are nearly impossible to find in conventional surface data alone.

It appears that some of these features may be directly related to one or a combination of the following: the local NC geology, the difference in diurnal heating experienced between the Atlantic Ocean and the NC Piedmont, or the juxtaposition of significantly different soil types in the NC Piedmont and the Coastal Plain. The relationships between the different boundaries and the local geology is investigated.

An investigation of the convective activity of all boundary categories was conducted. It was determined that thermal moisture boundaries (TMBs) and fronts were autoconvective (implies the boundary produced convection of 40 dBZ or more without interaction with other features) 100% of the time. Troughs and thunderstorm outflows were autoconvective 86% and 70% of the time respectively.

Several stability parameters were studied to determine their importance as forecasters of deep convection. As determined in other studies, only a lower bound was found, below which convection did not occur. Once this threshold was exceeded, there was no correlation between the occurrence of convection and the stability parameter.

It was found that the eastern Piedmont and the western and central Coastal Plain was a preferred location for boundaries and interactions. It is believed that the mountain range to the west and the coast to the east tend to focus the activity in this region. Sea breeze propagation into this area was a very important factor in the development and evolution of the diurnal thunderstorm cycle in NC. These sea breezes often propagated significantly further inland than was previously known. This may be related to an observed feature which has been named the Piedmont Trough.

The results of this work are compared to previous research on radar-detected convergence boundaries in Colorado. It was found that in NC, boundary interactions occur significantly more often than in CO and that those interactions tend to result in deep convection more frequently. In addition, local boundaries are found to produce convection regularly, without interaction with other features.



## **Dedication**

For the last two years of my life I have been completely immersed in my work, which has left little time for my family. As has been the case throughout my Air Force career, my wife rose to the task of raising our kids and maintaining our home. Although I recognize that this dedication can never replace the time which has been lost, it is at least a reminder of the challenges and accomplishments during this phase of our lives. This thesis is therefore dedicated to my loving wife Lisa and my two children, Dean and Dana. Thank you for the love and support you provided as I worked to attain a personal and professional goal.

## **Biography**

Charles Anthony (Tony) Ray is currently an Air Force Weather Officer assigned to Air Weather Service.

He was born in Raleigh, NC on 9 December 1959 and lived in NC throughout his childhood. Tony enlisted in the United States Air Force (USAF) on 14 August 1978. In 1986, he was selected by the Air Force Institute of Technology to attend the University of Maryland and received a Bachelors Degree in Physical Sciences with an emphasis in Meteorology. After graduation in 1988, he was selected to attend the AF Officers Training School and was commissioned as a Second Lieutenant in the AF in May 1989. Subsequent assignments included a tour as the Wing Weather Officer at Moody AFB, Georgia and Chief of Weather Contingency Plans at Yongsan Garrison in Seoul, Korea. Tony was promoted to the rank of Captain in May 1993. At the end of his tour in Korea in July of 1993, he was again selected by AFIT to attend North Carolina State University to obtain an advanced degree in Meteorology.

Upon completion of his Masters Degree, Tony will be assigned to the Operational Support Facility in Norman, Oklahoma where his expertise will be used in support of the NEXRAD program.

Charles A. Ray is married to the former Lisa Rene Rose of Rocky Mount, NC. They have two children, Dean age 7 and Dana age 4.

## **Acknowledgments**

The United States Air Force and the Air Force Institute of Technology provided this opportunity to obtain an advanced degree. Without their support, the pursuit of this goal would not have been possible.

I would also like to express my appreciation to my advisory committee, Dr. Steven E. Koch (Chairman), Dr. Allen J. Riordan, and Dr. Gerald F. Watson. Their guidance and personal interest in this work were instrumental in the successful completion of the research.

I would like to take this opportunity to acknowledge the men and women of the NWS Raleigh Office. In addition to collecting data, answering my endless questions and generally supporting my work, they taught me the differences between AF and NWS operational meteorology, and for that I am grateful. The professionalism and dedication they displayed as they worked to balance scientific and operational priorities are commendable, and I was privileged to have been a small part of their operation for a short time. The following individuals directly contributed to this research by providing operational input, collecting and/or saving data, or just generally being there when I had questions: Ruth Aiken, Margaret Baron, Joel Cline, Ed Delgado, Rod Gonski, Gail Hartfield, Ron Humble, George Lemons, Jim Merrell, Mike Moneypenny, Rick Neuherz, and Jan Price.

I would like to acknowledge Greg Dial who acted as my NWS liaison for this work. His knowledge of both theoretical and operational Meteorology enabled him to answer my "scientific questions" with an operational slant. Greg directed me to the most interesting case study in this thesis and he provided editorial support as well as an operational Meteorologist's perspective. Thanks again Greg.

I would like to personally thank Steve Harned and Kermit Keeter, the Meteorologist in Charge and the Science and Operations Officer (SOO) respectively, of the NWS Raleigh

Office. Because of their desire to support this work and the collaborative efforts between the National Weather Service and North Carolina State University, they opened their office to this researcher and provided both operational and personal support throughout the study. They ultimately made this study both possible and successful.

Work such as this is not accomplished without assistance, and I would like to thank my fellow students: Bill Bauman, Bob Rozumalski, Tom Graziano, Mike Adams, Mike Trexler, Brian Waranauskus, Chris Vandersip, Kim Kreis, Kyle Turner, Yi Jin, and Randy Allis. Each of you contributed in some way to the successful completion of this program, and I am grateful to all of you.

## TABLE OF CONTENTS

	<u>Page</u>
LIST OF TABLES .....	viii
LIST OF FIGURES .....	ix
1. INTRODUCTION .....	1
2. BACKGROUND .....	4
2.1 Doppler Radar .....	4
2.1.1 The History of Doppler Radar .....	4
2.1.2 Doppler Radar Basics .....	6
2.1.3 The WSR-88D .....	11
2.1.4 Clear Air Returns .....	16
2.1.5 Bragg Scatter .....	19
2.2 Literature Review on Boundary Detection by Radar and Satellite .....	24
2.2.1 Boundary Detection Using Doppler Radar .....	24
2.2.2 The Role of Satellite Imagery in Detecting Boundaries .....	38
3. RESEARCH METHODOLOGY .....	42
3.1 Introduction .....	42
3.2 North Carolina Geology and Summertime Climatology .....	45
3.2.1 North Carolina Geology and Topography .....	45
3.2.2 North Carolina Climatology .....	49
3.3 Data Collection and Analysis .....	52
3.3.1 Data Collection .....	52
3.3.2 Boundaries Defined .....	54
3.3.3 Data Analysis Techniques .....	60
4. GENERAL RESULTS .....	63
4.1 Types of Phenomena Identified and Contributing Factors .....	63
4.1.1 Thunderstorm Outflows .....	63
4.1.2 Sea Breezes .....	70
4.1.3 Horizontal Rolls .....	78
4.1.4 Fronts and Prefrontal Troughs .....	86
4.1.5 Thermal/Moisture Boundaries (TMBs) .....	92
4.1.6 Boundaries of Unknown Origin and Nonclassical Mesoscale Circulations (NCMCs) .....	96

4.1.6.1 Unknown Stationary (US) Boundaries .....	103
4.1.6.2 Unknown Moving (UM) Boundaries .....	105
4.1.7 Piedmont Troughs .....	107
4.2 A General Review of Boundary Statistics .....	111
5. CASE STUDIES .....	127
5.1 Case 1: 16 July 1994 .....	127
5.2 Case 2: 26 May 1994 .....	150
5.3 Case 3: 12 June 1994 .....	170
6. SUMMARY AND CONCLUDING REMARKS .....	181
6.1 Summary .....	181
6.2 Concluding Remarks .....	183
6.3 Recommendations for Future Research .....	184
7. LIST OF REFERENCES .....	187

## List of Tables

	<u>Page</u>
Table 2.1 A comparison of the WSR-88D and the WSR-57 .....	11
Table 2.2 Results of Wilson and Schreiber (1986) study .....	30
Table 4.1 NC soil characteristics .....	100

## List of Figures

	<u>Page</u>
Figure 2.1 Doppler velocity scale .....	15
Figure 2.2 Graph of reflectivity vs. structure function for a 10 cm radar .....	20
Figure 2.3 A depiction of different scattering regimes .....	26
Figure 2.4 Collision types from Wilson and Schreiber (1986) .....	31
Figure 3.1 Geological divisions of NC and the Gulf Stream .....	46
Figure 3.2 Cross section of NC .....	47
Figure 3.3 North Carolina summertime climatology .....	50
Figure 3.4 Study area .....	57
Figure 3.5 Distance from the radar vs. beam height .....	58
Figure 4.1 Radar depiction of a strong outflow boundary .....	65
Figure 4.2 Typical gust front/density current .....	66
Figure 4.3 Sea breeze circulation .....	70
Figure 4.4 Sketch of NC coastline .....	71
Figure 4.5 Sea breeze/density current speed as a function of temperature differential .....	74
Figure 4.6 Roll orientation for inflection point instability rolls .....	79
Figure 4.7 Kuettner's vorticity argument .....	80
Figure 4.8 Radar depiction (Spectrum Width) of a thunderstorm outflow moving into a horizontal convective roll field .....	84
Figure 4.9 Frontal boundary depicted in Doppler velocity .....	87
Figure 4.10 Model results from Mahfouf and Mascart (1987) .....	99
Figure 4.11 GOES visible imagery for 1701Z, 16 July 1994 .....	102
Figure 4.12 Location of Unknown Stationary boundary occurrences .....	104
Figure 4.13 Location and orientation of Piedmont Troughs .....	107



Figure 4.14	Total number of observed boundaries .....	111
Figure 4.15	Boundaries observed in combined categories (absolute numbers) .....	113
Figure 4.16	Boundaries observed in combined categories of current research (percent) .....	114
Figure 4.17	Percentage of boundaries in each category (Wilson and Schreiber, 1986) .....	114
Figure 4.18	Comparison of convective activity in Colorado and NC .....	116
Figure 4.19	Results of boundary interactions (current study) .....	118
Figure 4.20	Comparison of boundary interactions of both studies .....	119
Figure 4.21	Percent of boundaries autoconvective in NC .....	121
Figure 4.22	Depiction of movement vs. convective activity (autoconvective) .....	122
Figure 4.23	Relative importance of each data acquisition platform .....	125
Figure 4.24	Boundary detection using a combination of platforms .....	125
Figure 5.1	GSO sounding for 12Z 16 July 1994 .....	129
Figure 5.2	NWS 12Z analysis (surface pressure) .....	130
Figure 5.3	Subjective surface analysis for 12Z .....	131
Figure 5.4	Equivalent potential temperature analysis and mesoanalysis for 13Z ...	132
Figure 5.5	1354Z clear air radar imagery .....	133
Figure 5.6	Mesoscale analysis for 14Z .....	133
Figure 5.7	Mesoanalysis, radar, and satellite imagery for 16Z .....	135
Figure 5.8	Mesoanalysis, radar, and satellite imagery for 17Z .....	136
Figure 5.9	Mesoanalysis, radar, and satellite imagery for 18Z .....	137
Figure 5.10	Zoom of TMB just north of Rocky Mount (RMT) at 18Z .....	138
Figure 5.11	Mesoanalysis, radar, and satellite imagery for 19Z .....	139
Figure 5.12	Zoom of 19Z radar imagery .....	140
Figure 5.13	Mesoanalysis, radar, and satellite imagery for 20Z .....	141
Figure 5.14	Zoom of 20Z radar image .....	142

Figure 5.15	Mesoanalysis, radar, and satellite imagery for 21Z .....	143
Figure 5.16	Mesoanalysis, radar, and satellite imagery for 22Z .....	144
Figure 5.17	Synoptic-scale subjective analysis for 12Z, 26 May 1994 .....	151
Figure 5.18	Mesoanalysis and synoptic analysis for 13Z .....	152
Figure 5.19	Mesoanalysis and satellite imagery for 16Z .....	154
Figure 5.20	Mesoanalysis and satellite imagery for 18Z .....	156
Figure 5.21	Radar reflectivity and velocity at 1942Z .....	157
Figure 5.22	Radar reflectivity and velocity at 21Z .....	158
Figure 5.23	Mesoanalysis and satellite imagery for 21Z .....	159
Figure 5.24	Radar reflectivity and velocity at 22Z .....	160
Figure 5.25	12Z HAT sounding .....	162
Figure 5.26	Meteograms .....	167
Figure 5.27	Mesoscale analysis for 12Z, 12 June 1994 .....	170
Figure 5.28	Mesoanalysis, radar, and satellite imagery for 17Z .....	172
Figure 5.29	Radar wind profile at 1747Z from the Raleigh WSR-88D .....	173
Figure 5.30	Mesoanalysis, radar, and satellite imagery for 18Z .....	174
Figure 5.31	Mesoanalysis, radar, and satellite imagery for 20Z .....	175
Figure 5.32	Depiction of sea breeze in Doppler velocity .....	176
Figure 5.33	Mesoanalysis, radar, and satellite imagery for 22Z .....	177
Figure 5.34	Doppler velocity imagery at 2305Z showing sea breeze just to the east of the radome .....	178
Figure 5.35	Mesoanalysis at 23Z .....	179
Figure 5.36	Cross section through sea breeze .....	179
Figure 5.37	Depiction of sea breeze directly over radome .....	180

## 1. INTRODUCTION

Researchers are always searching for equipment and methods to help them better understand their particular area of interest and operational forecasters continuously seek better ways to support the public. With the acquisition of the new Weather Surveillance Radar (WSR) 88D in the Raleigh Office of the National Weather Service (NWS), both groups will be better able to work toward their respective goals. Both scientists and forecasters will be able to interrogate North Carolina's Planetary Boundary Layer (PBL) in ways that were not possible in the past, thereby allowing a better understanding of our atmosphere and the physics that describe it.

Initial motivation to conduct this study is provided by the need to identify, categorize, and document the different types of boundaries that routinely appear in the NC PBL. This is the first time that such a study has been undertaken in eastern NC and this study is only now made possible by the recent acquisition of the WSR-88D. As the study was initiated, the radar was just newly commissioned, and researchers and forecasters alike had no idea of just how effective the radar would be or just what the system would reveal to us about the NC PBL.

In recognition of this fact, The organization that is responsible for fielding the WSR-88D (the Operational Support Facility (OSF)) has stated that the interrogation of the PBL is its number two priority. OSF is fielding the WSR-88D throughout the country, and is therefore very interested in determining the utility of the system with respect to sampling the clear air boundary layer.

A primary interest in conducting this study is to determine the utility of the new WSR-88D radar. Case studies are examined to determine the types of boundaries that can be observed in the summertime PBL. In each case, an effort will be made to determine the effectiveness of the WSR-88D in locating and resolving the boundaries. Additionally, since

the surface station spacing is on the order of 150 km in NC, the feasibility of performing mesoscale analyses with the help of the radar and GOES 7 satellite imagery is determined.

From a scientific perspective, the study is guided in several directions. Attempts are made to locate convergence boundaries/zones, study their characteristics and ubiquity, and compare them to similar boundaries that have been identified in other locations. Each of the boundaries is categorized according to its origin, movement pattern, and the vigor with which it produces convection. To the extent possible, the vertical structure of the boundaries and their nature will be studied. An examination of the clear air capability of the WSR-88D is conducted to determine how effective the radar is in detecting weak boundaries.

It is hoped that this study will increase the understanding, nature, climatology and importance of mesoscale boundaries in NC. At the outset of this research it was believed that the increased sensitivity of the radar would reveal many surface features that "trigger" convection, and thus help to explain much convective activity which, when using older generation radars, seemed to occur randomly. To the extent possible, a limited summertime climatology study is conducted to determine the types of features that are routinely found in the NC PBL in the summertime. An attempt is made to determine the relative importance of each of the boundary types observed.

A primary objective of this research is to determine the "value added" of the new radar. The National Weather Service (NWS) and the United States Air Force (USAF) have operated conventional radar sets such as the WSR-57 and the FPS-77 in NC for years. The study will seek to determine the benefits of having a Doppler Radar in North Carolina.

Obviously the new equipment will provide data that the conventional systems were unable to provide such as Doppler Velocity and Spectrum Width. This study will examine the utility of these data fields; however, it will also compare reflectivity levels of several features to those levels that would be displayed using older radar systems. Also of interest

is the utility of some of the data fields that the 88D provides, such as precipitation totals, wind velocity profiles, etc. These are very important when considering the overall value of the new system.

Particular emphasis is placed, in this study, on determining the range limit at which the radar ceases to provide useful information about the PBL. This is one very real limitation of the new radar (or any radar) that must be considered whether research is being conducted or warnings are being issued.

As the study was conducted, particular attention was given to the weather associated with the different boundaries observed. There were several questions which needed to be addressed.

- a. Which boundaries are most likely to initiate or intensify convection?
- b. Are there any features that always or never produce convection?
- c. Do the boundaries form in situ or do they propagate into our study area?
- d. What is the relative importance of boundary mergers or intersections for producing new radar echoes?
- e. Does the ability of boundaries to trigger new convection correlate well with the thermodynamic instability or the strength of capping inversions?
- d. Are there certain "favored origination" zones in which we can expect the boundaries to form?
- e. Do propagating boundaries tend to favor one direction of movement over another?
- f. Does the Atlantic Ocean influence the inland weather to any appreciable degree?

In summary, we hope to conduct a scientific investigation of the North Carolina Planetary Boundary Layer, using the WSR-88D. We believe the information obtained will be of use to both researchers interested in NC PBL phenomena as well as operational meteorologists who must produce forecasts for the region day after day.

## **2. BACKGROUND**

This section provides the background necessary to understand the basics of Doppler radar theory. A brief discussion of the history of Doppler radar is followed by a discussion of the WSR-88D. Some emphasis is placed on understanding clear air radar returns and the Bragg Scatter phenomenon.

### **2.1 Doppler Radar**

#### **2.1.1 The History of Doppler Radar**

The word "RADAR" is actually an acronym for "RADio Detection And Ranging." As the use of radio for communication became widespread through many applications in the early 1900s, people found that radio had some interesting characteristics. For instance researchers and engineers in Germany and America found that when ships passed through radio beams aimed at a receiver on the far side of a river, the signal received would fluctuate (Rinehart, 1991).

When such demonstrations became common knowledge, it was not long before someone recognized the utility of being able to locate ships and aircraft beyond visible range. In 1935, a British organization known as the Committee for the Scientific Survey of Air Defense (CSSAD) asked Sir Robert Watson-Watt to investigate the possibility of using radar for military applications (Doviak and Zrnic, 1993). At the time, Sir Watson-Watt was working with the Meteorological Office to develop a method of providing accurate thunderstorm warnings to WWI aviators. His methods involved using a receiver sensitive to the radio signals produced by lightning. Less than five months after the request, the team of Watson-Watt and Wilkins successfully demonstrated detection and ranging of aircraft. Just a short time later, in 1936, scientists at the Naval Research Laboratory and the US Army Signal Corps conducted similar successful demonstrations.

During the early years of radar research, power production was extremely crude and generally weak. Wavelengths were long and as a result, large, bulky antennas were required. These large antennas had very poor resolution which kept scientists working to devise methods which would lead to more accurate systems. This work eventually led to the development of the magnetron.

The first magnetron was built by Randall and Booth at Birmingham University in England in Feb. 1940 (Doviak and Zrnic, 1993). It provided about 400 watts of continuous power at a wavelength of approximately 10 cm. Once this development occurred, it was only a matter of time until the shorter wavelength systems began to reveal information about the weather. Although much of the information regarding the first meteorological use of radar is cloaked in wartime secrecy, most agree that the research was conducted by Dr. J.W. Ryde during 1946. During this period, he was trying to determine if precipitation would affect the ability of a radar to resolve military targets (Doviak and Zrnic, 1993).

Radar developments continued and in the early 1940s, the first Pulsed Doppler radar was unveiled. The system, which was known as the Moving Target Indication (MTI) radar, was used to better detect moving ships and aircraft. This radar did not measure velocities but did separate moving targets from stationary clutter (Doviak and Zrnic, 1993).

During the middle to late 1940s, radar developments began to slow. The advent of the magnetron resulted in a very powerful transmitter capable of detecting targets at extreme distances; however, the receivers and processors were not powerful enough to take advantage of the large quantities of Doppler shift data which was available. It was during the 1960s and 1970s, with the advent of solid state electronics and the klystron, that radar developments again took a giant step forward and Doppler radar as we know it today became widely available (Doviak and Zrnic, 1993).

Meteorologists now routinely use very powerful, short wavelength radar systems to interrogate the atmosphere and are becoming more and more interested in sampling the “clear air.” It’s interesting that now scientists are reverting to the long wavelengths used in the 1930s and 1940s in the current development of wind profilers. However, instead of a peak power output of 400 watts, today’s wind profilers have peak power outputs on the order of 10 kW.

### 2.1.2 Doppler Radar Basics

It is difficult to discuss Doppler Radar basics without some knowledge of the important terms of the radar equation; therefore a basic derivation of the equation is appropriate. We begin with the expression

$$S = \frac{P_t}{4\pi r^2} \quad (1)$$

where  $S$  is the isotropic power density,  $P_t$  is the power transmitted by the radar unit, and  $r$  is the range from the radar. This expression gives the power incident on a spherical shell of radius  $r$ , centered on the radar. The power incident on any target is given by the expression for  $S_i$ .

$$S_i = \frac{P_t}{4\pi r^2} \cdot g \cdot f^2(\theta, \phi) \quad (2)$$

The term  $g$  is the antenna power gain along the beam axis and  $f^2(\theta, \phi)$  is the normalized power density which is a function of the antenna (Doviak and Zrnic, 1993). As previously stated, this expression gives the power incident on a target at any range, but obviously what is most important is how much of the power incident on the target is reflected back to the radar receiver. The following expression for  $S_r$  addresses this concern.

$$S_r = \frac{P_t}{(4\pi r^2)^2} \cdot g \cdot \frac{f^2(\theta, \phi)}{l^2} \cdot [A_e] \cdot [\sum \sigma_b] \quad (3)$$



Several new terms are introduced here. The  $I^2$  term is an attenuation factor and  $A_e$  is the effective collection area of the antenna. The expression which describes  $A_e$  is

$$A_e = \frac{g\lambda^2 f^2(\theta, \phi)}{4\pi} \quad (4)$$

where  $g$  and  $f^2(\theta, \phi)$  are the same as described above and  $\lambda$  is the wavelength of the radar.

With the addition of the summation term in equation (3), the concepts of backscatter and reflectivity are introduced. The backscatter cross section from a point scatterer is described by the expression for the term  $\sigma_b$

$$\sigma_b \approx \frac{\pi^5}{\lambda^4} |K|^2 D^6 \text{ (Rinehart, 1991)} \quad (5)$$

which is the Rayleigh approximation. In order for this approximation to hold, the diameter of the target ( $D$ ) should be much less than the wavelength ( $\lambda$ ) of the incident energy; if  $D \leq \lambda/16$ , then the expression is valid. Fortunately, this expression does hold for the majority of situations involving storm detection radar (5-10 cm wavelengths) and meteorological targets (with the exception of hail). It tells us that a target will backscatter proportional to the sixth power of its diameter and inversely proportional to the fourth power of the wavelength of the radar. These properties are very important when meteorologists and scientists try to determine the characteristics of the targets which they are interrogating. The  $|K|^2$  term is the dielectric factor for weather, and it ranges from 0.91 to 0.93 (Knight and Miller, 1993).

When interrogating meteorological targets, we are concerned not with single point scatterers, but with volumes of such scatterers. The expression for the backscatter of a volume of point targets is obtained by summing the diameters of the individual particles and multiplying by the volume of space occupied by the radar beam as shown in equation (6).

$$\Sigma \sigma_b = \text{volume} \times \frac{\pi^5}{\lambda^4} |K|^2 \Sigma D^6 \quad (6)$$

Substituting the expression for  $\Sigma \sigma_b$  and  $A_e$  into equation (3) gives equation (7).

$$S_r = \frac{P_t}{(4\pi r^2)^2} \cdot g \cdot \frac{f^2(\theta, \phi)}{l^2} \cdot \left[ \frac{g\lambda^2 f^2(\theta, \phi)}{4\pi} \right] \cdot [\text{volume}] \cdot \left[ \frac{\pi^5}{\lambda^4} |K|^2 \Sigma D^6 \right] \quad (7)$$

The last term in brackets is the previously mentioned reflectivity term which is denoted by the symbol  $\eta$ . The volume of space occupied by a radar beam at any distance is given by

$$\text{Volume} = \pi \frac{r^2 h \theta \phi}{8} \quad (8)$$

where  $r$  is the range,  $h$  is the pulse length, and  $\theta$  and  $\phi$  are the horizontal and vertical beam widths, respectively. Substituting this equation for the bracketed volume term and substituting  $\eta$  for the reflectivity yields equation (9).

$$S_r = \frac{P_t}{(4\pi r^2)^2} \cdot g \cdot \frac{f^2(\theta, \phi)}{l^2} \cdot \left[ \frac{g\lambda^2 f^2(\theta, \phi)}{4\pi} \right] \cdot \left[ \frac{\pi r^2 h \theta \phi}{8} \right] \cdot \eta \quad (9)$$

Recognizing that  $h$  (pulse length) is equal to the speed of light ( $c$ ) times the pulse duration, ( $\tau$ ), and assuming a circularly polarized radar beam ( $\theta \phi = \theta^2$ ) gives

$$S_r = \frac{P_t}{(4\pi r^2)^2} \cdot g \cdot \frac{f^2(\theta, \phi)}{l^2} \cdot \left[ \frac{g\lambda^2 f^2(\theta, \phi)}{4\pi} \right] \cdot \left[ \frac{\pi r^2 c \tau \theta^2}{8} \right] \cdot \eta \quad (10)$$

Now we can collect like terms in order to simplify the overall expression, which yields

$$S_r = \frac{P_t}{(4\pi r^2)^2} \cdot g^2 \cdot \frac{f^4(\theta, \phi)}{l^2} \cdot \frac{\lambda^2}{4} \left[ \frac{r^2 c \tau \theta^2}{8} \right] \cdot \eta \quad (11)$$

Now assume  $f^4(\theta, \phi)$  is approximately equal to  $\frac{1}{2 \ln 2}$  (Doviak and Zrnic, 1993)

$$S_r = \frac{P_t}{(4\pi r^2)^2} \cdot g^2 \cdot \frac{1}{2 \ln 2} \cdot \frac{\lambda^2}{4l^2} \left[ \frac{r^2 c \tau \theta^2}{8} \right] \cdot \eta \quad (12)$$

After collecting terms, this form of the radar equation results.

$$S_r = \frac{P_t}{4^3 \cdot \pi^2 \cdot r^2} \cdot g^2 \cdot \frac{1}{16 \ln 2} \cdot \frac{\lambda^2}{l^2} \cdot [c \tau \theta^2] \cdot \eta \quad (13)$$

There are a large number of constants in this equation. Obviously, numbers such as  $4^3$ ,  $16 \ln 2$ , and  $\pi^2$  are constant, but if we consider that we are usually concerned with only one calibrated radar unit that is being used for operations or research, then terms like power transmitted ( $P_t$ ), the gain ( $g^2$ ), attenuation ( $l^2$ ), beam width ( $\theta^2$ ), and wavelength ( $\lambda^2$ ) are also constant. We can collect them and call them  $C$  with the following result.

$$S_r = C \frac{\eta \tau}{r^2} \quad (14)$$

This obviously is a much simplified version of the equations above, but it allows us to focus on the important terms. The power returned to the radar is inversely proportional to the square of the distance between the target and the radar. It is proportional to the reflectivity of the target and the pulse length.

The new radar provides a wealth of information; however, there are limits which are imposed by the transmitter and receiver. For instance, the maximum unambiguous range at which the radar can provide information is given by the equation

$$r = \frac{c T_s}{2} \quad (15)$$

in which  $r$  is the range,  $c$  is the speed of light, and  $T_s$  is the Pulse Repetition Time (PRT) of the transmitter. It is sometimes easy to confuse  $T_s$  and  $\tau$ . The former is the frequency at which radar pulses are emitted and the latter is the *duration* of each pulse, which translates to a specific pulse length. It is obvious that the PRT is the only independent variable in equation 15; therefore, it uniquely describes the range. If a target lies beyond the distance

which a radar pulse can traverse twice (to the target and back to the receiver), traveling at  $c$ , then the transmitter will emit a new pulse before information from the first pulse arrives back at the receiver. This results in an ambiguous range being presented on the radar displays. Echoes which are displayed at an ambiguous range generally appear to be *elongated* along a radial.

The problem is further complicated because there are also limits to which the radar can display velocity data. This problem is described by the equation

$$v = \pm \frac{\lambda}{4T_s} \quad (16)$$

in which  $v$  is the velocity,  $\lambda$  is the wavelength of the radar, and  $T_s$  is the PRT as described above. Since generally, most radars are single-wavelength systems, again, the velocity is uniquely defined by the PRT. However, the relationship is such that the velocity is *inversely* proportional to the PRT. Therefore, as we increase the PRT in order to increase the effective range of the radar, we are *decreasing* the velocity information which can be displayed. This inverse relationship is known as the "Doppler Dilemma."

The obvious problem imposed by the Doppler Dilemma is overcome in one of several ways. Often radars are designed to emit a pulse at a long PRT, used for ranging, and a pulse at a shorter PRT, used for acquiring velocity information. In other situations, when the radar is used for one particular reason, a specific PRT can be selected which will maximize information under the specific circumstances. In some situations such as research, extreme range may not be necessary, so a PRT can be selected so as to increase velocity information the radar provides. In an operational environment, a shorter PRT can be selected which will provide better radial resolution and extended range. The WSR-88D does not allow quite the degree of flexibility described here, but it does offer some

alternatives in the form of Volume Coverage Patterns (VCP) which will be discussed in Section 2.1.3 below.

### 2.1.3 The WSR-88D

Prior to the acquisition of the WSR-88D, the radar mainstay for the National Weather Service was the WSR-57. As shown in Table 2.1, there are both similarities and differences in the two systems. For instance, both of the radars are considered to be 10 cm S-band storm detection radars. The wavelength of the WSR-57 is 10.7 cm while the wavelength of the WSR-88D is around 10 cm. The wavelength can actually vary to some degree according to the Operational Support Facility (OSF) depending on where the radar is located. Specific wavelengths are selected based on the surrounding area in such a way that there is minimal interference between the radar and other emitters.

*Table 2.1. A Comparison of the WSR-88D and the WSR-57  
(from Doviak and Zrnica and the OTB/OSF Training Manual)*

Parameters	WSR-57	WSR-88D	
		Precipitation (Mode A)	Clear Air (Mode B)
Wavelength (cm)	10.7	10	10
Pulse Width ( $\mu$ s)	4.0 (1200 m)	1.57 (471 m)	4.7 (1410 m)
Peak Power (kw)	410	1000	1000
Pulse Rep Freq (Hz)	164	320-1300	320-450
Beam Width	1.5 degrees	1 degree	1 degree
Lowest Measurable Return	+13 dBZ	+5 dBZ	-32 dBZ

Although the beam widths are similar, the new system has the narrower width of 1 degree. This slightly narrower beam provides for significantly increased azimuthal resolution. For example, at a range of 100 nm, the beam width of the WSR-57 is approximately 3.5 nm while the beam of the WSR-88D is approximately 1.7 nm. This

gives a pulse volume of about  $6.3 \text{ nm}^3$  for the older system and about  $0.6 \text{ nm}^3$  for the new one (OTB, OSF Student Guide, 1994). This leads to much better azimuthal resolution for the WSR-88D.

At this point, the similarities between the two units end and the differences become apparent. One of the most obvious differences is the peak output power. For the WSR-57 it is about 410 kW while for the WSR-88D it is about 1000 kW. The older units incorporate vacuum tube technology while the new radar is a solid state system. When the increase in power and decrease in system noise of the 88D is considered, the new system, in clear air mode, is approximately four orders of magnitude more sensitive than the older radar, as is shown in Table 2.1 under the "Lowest Measurable Return." To give the reader some idea of just how sensitive this radar is, "...a single water drop with a diameter of 6.3 mm could be detected at 20 km..." (Doviak and Zrnic, 1993).

The other major difference between the two systems is that the WSR-88D has two modes: Precipitation (Mode A) and Clear Air (Mode B). Mode B sacrifices range and a higher magnitude reflectivity display in order to provide increased sensitivity. Mode A on the other hand, while not as sensitive as Mode B, is better able to penetrate storm precipitation and provide weather data for operational meteorologists. This "decreased sensitivity" is not a problem because even when in Mode A, the radar is significantly more sensitive than the conventional reflectivity of the WSR-57. The older radar can detect signals of +13 dBZ (Alberty and Crum, 1991) and higher while the WSR-88D can display signals as weak as +5 dBZ while in Mode A. Because the it is primarily a storm detection and warning radar, the system is programmed to switch from Mode B to Mode A automatically when precipitation is detected. This is very useful for operational meteorologists; however, some problems arise when the unit is used for research since it is difficult to "coax" into clear mode and get it to remain there. More on this matter will be discussed later.

The primary differences between the two modes can be found in the pulse duration, the elevation angles scanned, and the pulse repetition time (PRT). By referring to equation 14 above, it is apparent that the returned power is proportional to the pulse duration. So the larger  $\tau$  is, the larger the amount of energy sent downrange in each pulse, and consequently the more power is returned from the scatterers. In order to get the most sensitivity from the radar (Mode B), a long pulse mode of  $4.57 \mu\text{s}$  is used which gives a pulse length of about 1410 meters. The extra power per pulse insures that even weak signals from widely spaced or poorly reflecting targets return a signal which is detectable by the receiver. However, the longer pulse length decreases the radial resolution. Therefore, for storm detection, a shorter pulse is used. In this case, the pulse duration is about  $1.5 \mu\text{s}$  which gives a pulse length of about 471 meters.

The volume coverage pattern (VCP) is one of the primary differences between the two modes. When the radar is being used in precipitation mode, operators are primarily concerned with interrogating the upper levels of the troposphere and getting the data into the system and processed quickly. Therefore, when the radar is used in Mode A, it scans elevation angles between 0.5 and 19.5 degrees and takes between 5 and 6 minutes to complete a full volume scan. Conversely, when the radar is being used in Clear Air Mode (CAM), the primary area of interest is usually the Planetary Boundary Layer (PBL) and time is not wasted scanning the higher elevations. In this mode, the radar scans only five elevation angles between 0.5 and 4.5 degrees. A full volume scan takes approximately 10 to 11 minutes. The extra time involved in a CAM scan serves both to decrease the spectrum width due to antenna rotation and to allow a higher signal to noise ratio (SNR). Both of these are primary concerns when dealing with widely spaced and/or weakly reflecting targets.

When we think of radar data in general, we usually are thinking about the reflectivity data and when we speak of Doppler radar, the first thing which comes to mind is usually the wind measurements which are available. The new WSR-88D combines both of these intuitive notions into one highly sensitive system. An additional quantity, Spectrum Width, is derived from the Doppler velocity field. According to Doviak & Zrnic, (1993), "the power spectrum of a weather signal, often referred to as the Doppler Spectrum, is a power-weighted distribution of the radial velocities of the scatterers." This simply means that when the radar samples a volume of targets, it receives information from each target regarding its reflectivity and its radial velocity. During the velocity averaging scheme, more weight is given to those targets which are more reflective (usually the larger ones due to the Rayleigh approximation). The averaged velocity is provided to the end user. However, it is important to remember that the power spectrum is composed of the radial velocities and reflectivities of each individual point target within a sampling volume.

In the conduct of this study, it was found that the Doppler velocity (hereafter referred to as velocity) and consequently the spectrum width (SW) fields were not as useful as previously presumed. The study was undertaken during one summer and the effect of the high pressure system which dominates the east coast during the summer months was underestimated. Throughout most of the study, the winds were very light and highly variable. Compounding the problem is the velocity scale on the Raleigh office WSR-88D which displays "incoming" values of 1 knot but does not display the outgoing velocities until 10 knots are reached (see Figure 2.1).



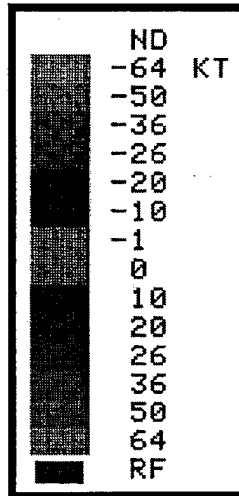


*Figure 2.1. Doppler Velocity Scale*

The result of the asymmetric scale was that we could detect incoming velocities, but observed a very broad zero line where outgoing velocities should have been indicated. When this coarse scale is combined with light, variable winds associated with the Bermuda High, it is obvious that the velocity field was not of much help in the conduct of the study. Since the SW is actually the variance of the velocity, this variance of a near zero velocity field did not provide much information. One exception to this was in the detection of thunderstorm outflows. Doppler velocity and SW generally vividly displayed these features because of the significant wind shear (speed and direction) and turbulence associated with gust fronts. Figures 5.34 and 5.36 are Doppler velocity displays in plan view and in cross section. Even in the black and white imagery, it is obvious that the majority of the flow field is shown as "zeros."

As a result of these problems, this study will primarily make use of the reflectivity field. Due to the importance of this data field in this research, considerable effort will be expended to explicitly explain the different types of reflectivity returns and their origins.

Radar reflectivity is undoubtedly the data set with which scientists, meteorologists, and laymen are most familiar since Doppler radar and the associated Doppler velocity fields are still relatively new concepts throughout most parts of the country. Reflectivity is measured using a unique set of units. We know from the derivation of the radar equation that  $\eta \propto \sum D^6$  where  $\eta$  is the “reflectivity” and  $\sum D^6$  is often called the “reflectivity factor” and given the symbol  $Z$ . Since raindrop diameters are usually measured in millimeters, and because we are interested in the total number of raindrops per unit volume, the units for the reflectivity factor are  $\text{mm}^6\text{m}^{-3}$ . Reflectivities measured in the atmosphere can range from as small as  $0.001 \text{ mm}^6\text{m}^{-3}$  to  $50,000,000 \text{ mm}^6\text{m}^{-3}$  (Rinehart, 1991). The large range of reflectivities encountered is most easily quantified by the use of a logarithmic scale for measurement. This is expressed by the equation

$$Z[\text{dBZ}] = 10 \log_{10} \left( \frac{Z}{1 \text{ mm}^6 \text{ m}^{-3}} \right) \quad (17)$$

in which dBZ stands for “decibels relative to a reflectivity of  $1 \text{ mm}^6\text{m}^{-3}$ ” (Rinehart, 1991).

#### 2.1.4 Clear Air Returns

In the past, when using conventional radar sets, reflectivity corresponded primarily to meteorological targets; however, when using the highly sensitive WSR-88D, there are other types of targets which provide returns to the radar receiver. Since they are very important to this particular study, they will be covered in some depth.

Most scientists generally agree that modern Doppler radars can sense three broad categories of targets: particulates, biological targets, and refractive index inhomogeneities. Since the category of “particulates” generally includes hydrometeors which has been discussed previously, this category will not be covered in depth at this point. The latter two categories of interest are often combined into one category called “clear air returns.”

Clear air returns have existed as long as radar has been in use. However, the lack of sensitivity and advanced interrogation techniques did not allow in-depth analysis of the returns. The echoes were often called "ghosts" or "angels" since the return could not be linked to anything tangible. Radar meteorologists often classified angels into two broad categories: (1) dot or point angels and (2) angels having substantial lateral or horizontal extent. The first category has generally been found to be birds, groups of insects, or at times, aircraft. Early radar meteorologists often detected large echoes shaped like a ring, which appeared suddenly and then disappeared just as quickly. Highly sensitive radars now allow us to track and study the rings and we have found they are flocks of birds rising from their roost. The second category has been found to be the result of elevated layers in which there are inhomogeneities in the refractive index of the atmosphere.

The category of "biological targets" usually includes both birds and insects. For the purpose of this study, we'll concentrate on insects, many of which are "weak" flyers and whose motion therefore is a function of the ambient conditions. The notion that insects could give us useful information on air motions in the absence of hydrometeors took many years to gain acceptance. However, the evidence now clearly shows that in some parts of the country, at some times of the year, not only is the scatter from insects important, it is predominant (Wilson et al., 1994). Despite this, there have only been a few studies conducted to determine the significance of insects to radar returns. In one such study (Gossard and Strauch, 1983), the researchers found approximately 1 insect per 2000 m<sup>3</sup>. Another such study was undertaken by Rinehart (1991); he found one insect for every 20 m<sup>3</sup>. Rinehart shows that by considering the equation for the volume of a radar beam at a certain range (equation 8), one can calculate the approximate reflectivity expected from the insects. He makes the assumptions that (1) the range  $r = 20$  km; (2) the pulse length  $h = 150$  m; and (3) the beam width  $\theta = 1$  degree. Using these figures, one arrives at a volume

of approximately  $1.4 \times 10^7 \text{ m}^3$ , which gives about 700,000 insects in a single pulse volume. In the study quoted by Gossard and Strauch, this would place approximately 7,000 insects in a single pulse volume. If we further assumed that the insects had a diameter of approximately 3 mm, we could use equation (6) to estimate the total reflectivity. Using the data from Rinehart's case gives approximately 15 dBZ while the data for the case quoted by Gossard and Strauch yields a reflectivity of about -4.8 dBZ. When the same computations are done using the characteristic pulse length of the WSR-88D (1410 m), and 1 insect per  $20 \text{ m}^3$ , a slightly higher reflectivity of about 16 dBZ is obtained. These levels are certainly detectable by modern Doppler radar.

Biological targets are not the only cause of clear air returns. When radar energy passes through areas in which the refractive index (RI) of the atmosphere changes significantly over distances which are small compared to the wavelength of the radar, the region containing these sharp, small-scale fluctuations can return some of the incident power back toward the radar (Rinehart, 1991). The dependence of the atmospheric RI on the "Refractivity" (N) is given by the expression

$$n = 1 + N \times 10^{-6} \quad (18)$$

N is expressed as

$$N = \left( \frac{77.6}{T} \right) \left( P + \frac{4810 P_w}{T} \right) \quad (19)$$

where T is the temperature, P is pressure in millibars, and  $P_w$  is vapor pressure in millibars. A typical value for N is about 300 which gives a typical value for n of about 1.000300. Doviak and Zrnic (1993) note that a change in the fifth or sixth significant digit is sufficient to have a measurable effect on electromagnetic wave propagation and scatter. An example is much more illustrative of just how sensitive modern Doppler radars are to refractive index fluctuations. Theory predicts that a radar will be able to differentiate between an air

mass which has a mixing ratio of 2.5 g/kg ( $P_w=4$  mb) and an air mass with a mixing ratio of 3.8 g/kg ( $P_w=6$  mb). The refractive index of the first air mass would be 1.0002733 and the second would be 1.0002815.

### 2.1.5 Bragg Scatter

The process in which the energy is reflected from RI fluctuations is called Bragg scatter, and requires several conditions to be met.

(1) The turbulent eddies must be on the order of one half the wavelength of the radar. This is about 5 cm for the WSR-88D.

(2) The eddies must lie within the inertial subrange. This is the range of eddies in which energy is neither created nor dissipated, but is simply transferred from the larger, energy-containing eddies to the smaller, energy-dissipating eddies.

(3) The mixing must occur in such a way that air parcels having relatively higher temperature and moisture content are brought into close proximity to parcels having relatively lower temperature and moisture content.

The relationship between Bragg scattering and radar reflectivity is given by the expression

$$\eta = 0.38 C_n^2 \lambda^{-1/3} \quad (20)$$

where, as before,  $\eta$  is reflectivity,  $\lambda$  is the radar wavelength, and  $C_n^2$  is a quantity called the "structure function." Figure 2.2 is a graphical representation of this relationship for a 10 cm radar.

In order to compare the reflectivities from Bragg Scatter to those from the Rayleigh scatter with which we are more familiar, we must use the empirical relationship

$$dBZ = 10 \times \left[ \log_{10} C_n^2 + \log_{10} \lambda^{11/3} + 15.13 \right] \quad (21)$$

in which the symbols are the same as previously identified (Ralph, 1994).

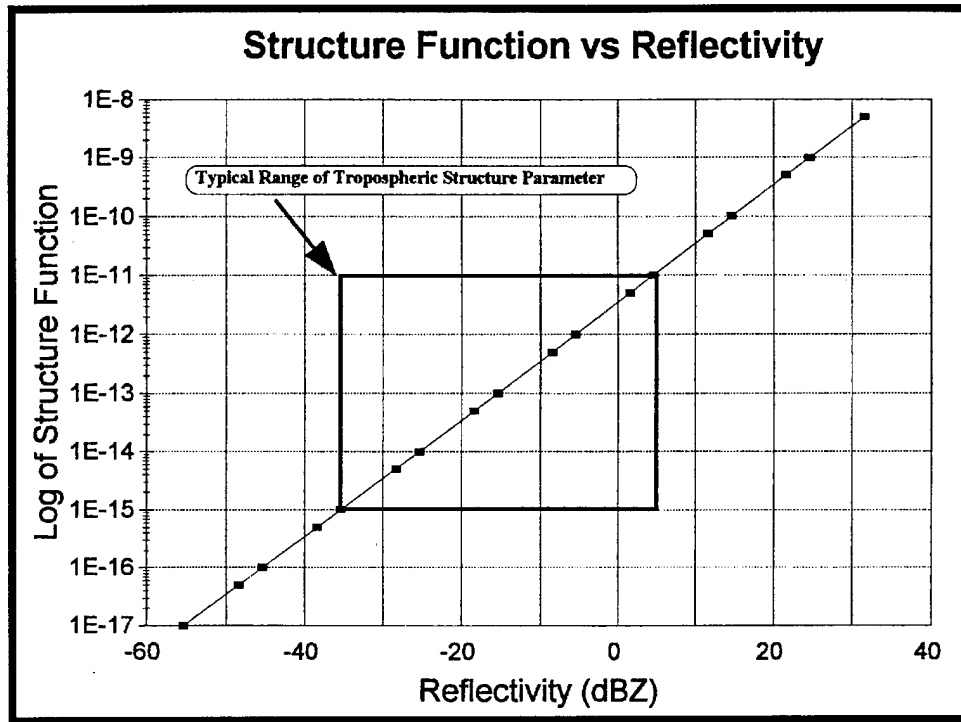


Figure 2.2. Graph of reflectivity vs. structure function for a 10 cm radar

The structure function is essentially a measure of the mean-square fluctuations of the refractive index, as a function of distance (Battan, 1959). Contributions to it come primarily from variations in moisture, temperature, and to a lesser degree, pressure. For instance, the contribution through temperature variation is described by

$$C_T^2 = 2.68 \left( \frac{g}{T} \right)^{-2/3} \times \left( \frac{z}{w' \theta'_s} \right)^{-4/3} \quad (\text{Stull, 1993}) \quad (22)$$

where  $(w' \theta'_s)_s$  is the surface heat flux and  $z$  is the height of the mixed layer. Similar equations exist for the variations of the structure function due to moisture and pressure. It is obvious that when equation 20 is combined with known radar reflectivity and equation 22, then information can be retrieved concerning the surface heat flux, moisture flux, and the surface energy budget in general.

There is some disagreement among researchers as to the value of  $C_n^2$  in different layers of the atmosphere; however, all do agree that the parameter is highly variable. Rabin and Doviak (1989) found that at any specific location, the structure function in the lower atmosphere would increase proportionally with the surface heat flux. Battan (1959) found  $C_n^2$  to range between  $10^{-16}$  to  $10^{-14}$  throughout the atmosphere. Doviak & Zmic (1993) indicate that the  $C_n^2$  ranges from  $6 \times 10^{-17} \text{ m}^{-2/3}$  for weak turbulence to  $3 \times 10^{-12} \text{ m}^{-2/3}$  for strong turbulence, with an average of about  $5 \times 10^{-13} \text{ m}^{-2/3}$ .

There has been a significant amount of emphasis placed on understanding the specific scattering mechanisms. This is because different types of boundaries scatter differently, and in order to determine the origin of the boundary, we must understand what the reflectivity field is telling us.

There are several reasons why the origin of radar returns is important. For example, if a meteorologist is interested in sampling the environmental wind in a clear air regime, then he must be reasonably certain that his return is from passive tracers, and not "strong flyers," for obvious reasons. Konrad (1970) notes that "an understanding of just what the radar "sees" is important to the interpretation of the radar returns and patterns ...". For the purposes of this study, efforts will be made to use the theory upon which both kinds of returns (Bragg scatter and Rayleigh scatter) are based in order to draw conclusions regarding the probable origin of the boundaries in question. Unfortunately, if researchers have only a single wavelength radar producing circularly polarized beams, echo origin often cannot be determined unequivocally (Wilson et al., 1994). Since the WSR-88D falls into this category, throughout this study, emphasis will be placed on the signal strength of the return, its elevation above the ground, and the distance at which it was located in an attempt to determine the specific scattering mechanism. The use of satellite imagery and mesoscale analysis will be maximized as the origin and significance of each boundary is investigated.

Several studies have been conducted which address the problem of determining echo origin using conventional, storm detection radar. Wilson et al. (1994) used multiple wavelength, polarization diversity radars to determine the origin of echoes of interest. Although the specific techniques used are beyond the scope of this study, the results are extremely pertinent. The team found that in the southeastern US, the majority of clear air scatterers *within* the mixed layer was insects. In fact, they note that the depth to which they found particulate scattering to dominate was a good indicator of the depth of the mixed layer. This is to be expected because the highest concentration of the insects is near the ground. The turbulent mixing which occurs in the convective boundary layer (CBL) effectively erases the thermal and moisture variations which result in Bragg scattering and also serves to disperse weak flying insects from the lower levels up to the inversion height. The exception to the above statement occurs in the vicinity of vigorously growing cumulus clouds where temperature and moisture fluctuations are most pronounced at the outer edges or "skin" of the parcel (Konrad, 1970). Although generally,  $C_n^2$  decreases with height as noted by Gossard and Strauch (1983), Doviak and Zrnic (1993) note that during vigorous convection, it may increase an order of magnitude.

Generally, when Wilson et al. (1994) detected echoes above the mixed layer by using multiple wavelengths and polarization diversity, they found that the echoes were from Bragg scatter and not due to insects. They also found that they could observe Bragg scatter above the mixed layer at distances beyond 30-40 km using the S band (10 cm) radar. Konrad (1970) also found that the 10 cm radar was especially adept at detecting refractivity fluctuations in the CBL.

Wilson and Mueller (1993) quote investigators (i.e., Gossard, 1990) who indicate that returns from insects would range from about -10dBZ<sub>e</sub> to 20 dBZ<sub>e</sub>. They also noted that at 10 cm wavelengths, Bragg scattering returns would generally be less than or equal to



-25 dBZ<sub>e</sub>. However Gossard notes that in the vicinity of strong density currents, the structure function could be greater than  $10^{-12} \text{ m}^{-2/3}$ . This would give a reflectivity of approximately -5 dBZ. Knight and Miller (1993) found that at 5 cm wavelengths, they obtained reflectivities between -10 and -20 dBZ<sub>e</sub> from cumulus clouds which just become visible to radar. From a 10 cm radar, such as the WSR-88D, these reflectivities would be on the order of -8 and -17 dBZ<sub>e</sub> respectively. There is a slight decrease in reflectivities due to the weak inverse dependence of reflectivity on wavelength (see equation 20). Although these are weak returns, they would be detectable on the 88D operating in the clear air mode.

Thus, given these findings, it is anticipated that convergence boundaries/zones seen in the strongly heated, weakly sheared summertime PBL are due principally to insect congregations. The exception would be where density current-like structures occur, such as along thunderstorm outflow boundaries and the sea breeze, as there the high turbulence levels and refractive index gradients promote the importance of the Bragg scattering mechanism.

## **2.2 Literature Review on Boundary Detection by Radar and Satellite**

During the past 10 years, there has been an incredible amount of research which utilized Doppler radar, much of which was related to the detection of boundaries in the PBL. More recently, the research has made use of the radar to sense the optically clear PBL in search of precursors to thunderstorm formation. Within limits, the Doppler radar is well suited for this task.

### **2.2.1 Boundary Detection Using Doppler Radar**

As long ago as 1970, researchers such as Thomas Konrad were using high power, narrow beam radars to detect irregularities in the atmospheric refractive index. He was specifically interested in the process of “turbulent mixing” in the convective boundary layer (CBL). Since his work involved “clear air sensing” he realized the importance of completely understanding exactly what it was that the radar was “seeing.”

In his work, Konrad divided the atmosphere into essentially three different regimes. The lowest layer which was highly unstable was called the “superadiabatic” layer. The next layer above it is called the “slightly stable” layer while the uppermost layer in the CBL is called the “subcloud” layer. He found that as the heated air parcels accelerated upward and penetrated into the slightly stable layer, they were positively buoyant and continued to rise. The potential temperature increases slightly in this region and the moisture decreases slightly. In the subcloud layer, the lapse rate is more stable and the moisture decreases at a higher rate. Therefore as a thermal penetrates this region, the temperature and moisture fluxes between the warm, moist thermal and the cool, dry environment air are enhanced.

As Konrad conducted this study, he had three radars at his disposal: an X-Band (3 cm), an S-Band (10 cm), and a UHF radar. As he interrogated the CBL, Konrad found that the convective cells appeared as “doughnut” shapes or rings on the Plan Position

Indicator (PPI). His explanation of this feature involves a description of convective dynamics as well as clear air radar reflectivity. Thermals consist of warm, moist air rising through a relatively cooler, dryer environment. The mixing which takes place at the edges of the cells through entrainment processes causes Bragg scatter which is discussed in Section 2.2. This results in relatively higher reflectivity occurring at the cell edges. As the radar beam penetrates to the center of the cell, where there is only warm moist air, little if any energy is reflected back to the radar. As the beam exits the cell, the entrainment of cool, dry air at the edge of the cell results in Bragg scattering, and again, the radar detects an area of relatively higher reflectivity. These are the "rings" which Konrad (1970) observed. These features were most easily detected using the S Band (10 cm) radar.

Konrad found that under a specific set of wind conditions as discussed by Kuettner (1971), the thermals tended to be aligned in rows. This was the topic of a more recent study by Christian and Wakimoto (1989). They were specifically interested in the relationship between the radar observed clear air reflectivity maxima and the visible cumulus clouds which often appeared above them. This particular study was conducted in Colorado and the team had access to three radars: the National Center for Atmospheric Research (NCAR) CP-2 (10 cm), CP-3 (5 cm), and CP-4 (5 cm). Additionally they had access to a PROFS (Program for Regional Observing and Forecasting Service) mesoscale network and a photographic network. They found that the cloud bases seemed to be just above the inversion capping a well-mixed PBL. They believed that the clouds cap vertical extensions of the BL, which because of roll circulation and convection, protrude into the stable layer (Christian and Wakimoto, 1989). They found that the reflectivity maxima tended to be aligned with the mean wind, and that the clouds tended to be directly over the reflectivity maxima. Although not all of the radar reflectivities were associated visible clouds, the echoes greater than 12 dBZ did have clouds directly over them.

Once this relationship was established, the team was interested in determining what was causing the clear air reflectivity maxima in the lower and upper levels. The cloud layer reflectivity was especially interesting because fair weather cumulus are difficult to detect with 10 cm radars. The reflectivities would be between -15 to -30 dBZ (Gossard and Strauch, 1983). They speculated that in the well-mixed boundary layer, the reflectivity was from particulate (Rayleigh) scatter while above the mixed layer, it was from Bragg scatter. The recent work of Knight and Miller (1993) and Wilson et al. (1992) substantiate this using multi-wavelength, polarization diversity radar. It therefore appears that the lower level reflectivities detected by Christian and Wakimoto resulted from convergence of Rayleigh scatterers (primarily insects) produced by counter-rotating vortices. In the upper levels, the higher reflectivities were caused by Bragg scatter resulting from the thermals rising in the relatively cooler, drier environmental air as noted by Konrad (1970). Figure 2.3 is a simplistic depiction of the two scattering regimes.

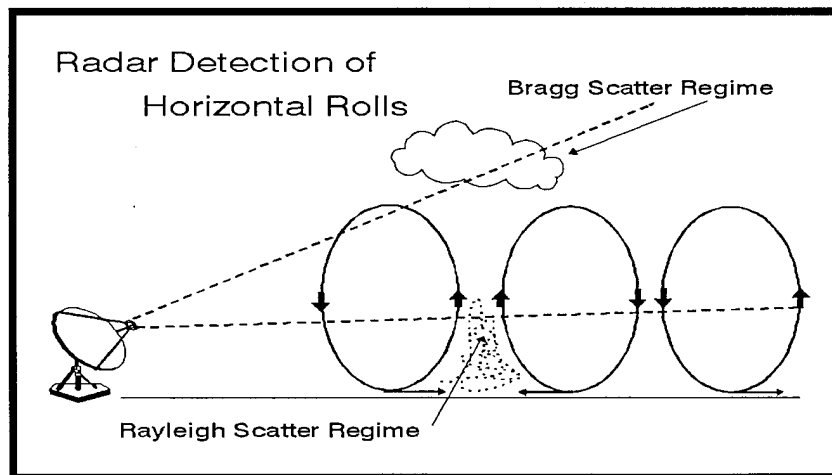


*Figure 2.3. A depiction of different scattering regimes*

Wilson et al. (1994) examined the origin of clear air echoes so that estimates could be made of the accuracy of Doppler derived wind fields. They realized that if Doppler-

measured winds were the result of strong flying insects (those which could fly against the wind) then the measurements were not useful to researchers or forecasters. Data used in this study were taken from four regions: Florida, Colorado, Kansas, and the tropical Pacific Ocean. Radars used were S-Band (10.7 cm), X-Band (3.2 cm), C-Band (5.5 cm), and the MIT (Massachusetts Institute of Technology, 5.4 cm) radar aboard the ship *Vickers*. Differential reflectivity ( $Z_{DR}$ ) was used in order to determine the eccentricity of the scatterers. The relationship for  $Z_{DR}$  is given by

$$Z_{DR} = 10 \log \left( \frac{Z_h}{Z_v} \right) (dB) \quad (23)$$

in which  $Z_h$  and  $Z_v$  refer to the horizontally and vertically polarized beams. Using this technique, a volume of scatterers is sampled using horizontally polarized radar waves, then resampled using vertically polarized waves, and their respective reflectivities compared using equation 23. If the targets are approximately circular (such as cloud droplets) then the resulting reflectivities would be about the same and  $Z_{DR}$  would be about zero. However, as the length-to-width ratio of the scatterers exceeds 1, horizontally polarized reflectivities would become exceedingly higher than reflectivities from vertically polarized waves. Equation 23 tells us that  $Z_{DR}$  would become increasingly larger. This would be the expected result if the scatterers were insects. The use of this methodology in the study indicated that the majority of the scatterers within the mixed layer were indeed insects.

As shown by the above research, the Doppler radar is very useful in providing information about the optically clear boundary layer. It is equally impressive at providing information about the horizontally nonhomogeneous boundary layer in which there are discontinuities of moisture, temperature, and scatterers. Numerous studies have been conducted of these discontinuities or "boundaries." For example, Rabin and Doviak (1982) used a Doppler radar to study the pre-thunderstorm environment in the optically

clear boundary layer. They realized that in order to successfully forecast thunderstorm formation, more information was needed than could be provided by hourly reporting stations separated by distances up to 200 km. They found that the Doppler radar at Norman, Oklahoma could provide high resolution information about the optically clear boundary layer within 120 km (75 mi), particularly surface convergence in the Doppler velocity field and/or low level reflectivity when it detected a convergence boundary. They also noticed that lines of cumulus clouds tended to be located near the boundary, but usually they were offset from the boundary by some distance. They account for this displacement by noting that as the air parcels were lifted to the convective condensation level (about 2 km), they were also being transported by the wind.

Wilson and Schreiber (1986) studied the relative importance of radar detected convergence lines in the initiation of thunderstorms in the vicinity of Denver, Colorado. The diverse topography around the Denver area played a significant role in initial and subsequent thunderstorm formation. Storms in the area usually formed in the Rocky Mountains in the early morning and over the ridge lines in early afternoon. This formation was generally attributed to upslope, confluent flow. In the afternoon and early evening, after the upslope flow had reversed, the thunderstorms tended to propagate down to the plains. This study utilized the two NCAR CP-2 and CP-4 Doppler radars as well as a PROFS and a PAMS (Portable Automated Mesonet) mesonet. The PROFS mesonet has a spacing of about 25 km while the PAMS network is spaced at about 8 km. In addition to the instrumentation, the team had observers in chase cars which were directed by the radar operators. Although both radars were capable of observing the winds in the optically clear air, they found that sometimes the atmospheric conditions or the orientation of the boundaries resulted in the radar detecting the feature only in one of the data fields (reflectivity or velocity). In general, they found that reflectivity provided the most useful information with reference to boundary location. Returns in the reflectivity and velocity

fields tended to be relatively weak in May and then increase through the growing season, into August. Wilson and Schreiber suggest that the clear air reflectivity was due to both insects and seeds. Both of these scatterers would tend to increase throughout the growing season, and then decrease drastically as the weather turns colder. The use of the dual polarization CP-2 radar allowed them to test the theory. Their conclusions were based on the same arguments presented earlier by Christian and Wakimoto (1989).

The primary objective of this study was to determine the importance of radar-observed boundary layer convergence lines in the initiation of thunderstorms in the Colorado Plains. The team defined a "boundary" to be a "radar signature of a thin line of enhanced reflectivity and/or a line of apparent convergent flow in Doppler velocity." The line had to be 1-3 km wide, greater than 10 km long, and persist for longer than 15 minutes. The features had to be within about 50 km of the radar in order to be included in the study. The researchers found several basic boundary types: mountain outflows (gust fronts from orogenic thunderstorms); gust fronts (non-orogenic); synoptic fronts (associated with a front appearing in surface data); the Denver Convergence Line (a topographically induced feature which results in convergence in an area just east of Denver, under synoptic scale southerly flow); unknown stationary (of unknown origin but possibly related to differential heating, moisture, or cloud cover); and unknown moving (some of which may have been due to gravity waves). Wilson and Schreiber believed that all of the above boundaries were the result of convergent flow, but *they could not prove this in every case*. The exception to the above definition was horizontal convective rolls. These rolls are convergent features, but they occur *within* and not *between* air masses.

Table 2.2 summarizes some of their findings. It includes the boundary types, the number and percent of total that each category comprises, and the percent which initiated thunderstorms.

Table 2.2. Results of Wilson and Schreiber (1986) Study

Boundary Type	Number (percent)	Percent initiating storms
Gust front	54 (33)	61
Mountain outflow	14 (8)	71
Synoptic front	12 (7)	58
Denver convergence line	11 (7)	82
Unknown (stationary)	31 (19)	48
Unknown (moving)	44 (27)	68
Total	166 (100)	63

Of particular interest, is that 79% of the boundaries identified and recorded were either unknown or a result of thunderstorm outflows. To put these figures into perspective, one should realize that Wilson and Schreiber studied *only days in which they believed there would be thunderstorms*. Therefore it should not be surprising that thunderstorm outflows comprised a large percentage (33%) of their data. Furthermore, they explicitly state that the origin of 46% of their boundaries could not be identified, even *with* the use of two mesonets. The point here is not to downplay the significance of the research. Indeed, the work is extremely important. It is simply to emphasize both the importance of thunderstorms in the initiation of new convection, and the very subtle nature of some of the features which exist within the PBL.

Other important results describe the proximity of new convection relative to the boundaries, and the types of collisions which occurred as a result of moving boundaries. They found that storms tended to form between 0 to 20 km behind moving boundaries, within 15 km of stationary boundaries, and within 5 km of colliding boundaries. In their discussion of merging boundaries, they divided their cases into three types: mergers (one boundary catching another), collisions (two boundaries propagating into one another from



opposite directions) and intersections (collisions at acute angles, generally greater than 30 degrees). Figure 2.4 is a graphical illustration of the boundary types.

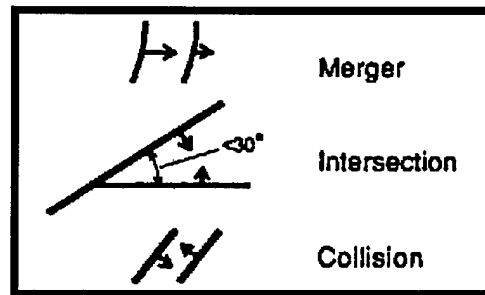


*Figure 2.4. Collision types from Wilson and Schreiber (1986)*

Wilson and Schreiber found that 84% of boundary collisions increased the intensity of existing convection or produced new convection. They found that 63% of mergers and 64% of intersections produced new convection. These statistics make a significant statement concerning the importance of boundaries in the PBL. They underscore the necessity of using Doppler radar to locate and identify such features and to nowcast the near term evolution of the resulting convection. It was determined that previously unseen boundary layer features were probably the triggers of seemingly random or “air mass” thunderstorms.

Schreiber (1986) conducted studies of two cases which involved stationary convergence boundaries of unknown origin in Colorado. In both cases, since the first thunderstorms of the day were triggered by the boundaries, it was speculated that the increased convergence resulted in enhanced vertical velocities which enabled air parcels to reach the convective condensation level (CCL). She states that apparently convection initiation along such boundaries is the rule, rather than the exception in Colorado. Fankhauser and Rodi (1989) also studied the kinematic and thermodynamic structure of radar-detectable clear-air boundary-layer convergence zones. The study was conducted as

a part of the Convection Initiation and Downburst Experiment (CINDE) near Denver's Stapleton Airport in the summer of 1987. The availability of the NCAR King Air aircraft enabled researchers to acquire information on how the boundaries varied with height, instead of depending solely on Doppler radar data as had previous studies. They showed that a quasi-stationary boundary of about 5 dBZ was produced by the confluence of cool, moist air from the northwest with warmer, drier air from the southeast. On each penetration, the instruments vividly recorded the boundary. The feature contained a wind shift that did not occur in the maximum radar reflectivity band, but rather on the eastern edge of the band. It was in this same location, that the largest mixing ratio gradient was found to occur. The aircraft also flew a vertical stair-stepped pattern in order to obtain samples of the entire boundary layer. They found that some of the cool, moist parcels had been transported to the top of the boundary layer and were depicted by two "spikes" in the mixing ratio at about 4.2 km (top of the PBL). They note that when clouds formed, their bases were located at this same level. It is obvious from these results that this particular boundary represented a convergence zone in which the magnitude of the vertical velocity generated was sufficient to lift parcels to the top of the PBL. This would support the contention by Wilson and Schreiber (1986) and Rabin and Doviak (1982) that boundaries such as this provide enough lift to initiate convection.

Eilts et al. (1991) continued research in this field on the east coast of Florida. Thunderstorm forecasting in this area is of great interest for two reasons. First, space shuttle operations are conducted at Kennedy Space Center (KSC) routinely and thunderstorms will always negatively impact those operations. The second reason is that during the summer, thunderstorms are reported at KSC during more than one half of the days. These two factors work together to make thunderstorm nowcasting a very important issue along the east coast of Florida.

The Eilts study sought to determine if there were signatures in the radar reflectivity or velocity fields which may be of help in nowcasting thunderstorms with 10 to 30 minutes of lead time. Within this time window, they were obviously looking for methods which would both help forecast movement of existing cells as well as help determine exactly where and when new cells would form. The primary radar used in this research was a 5 cm system placed about 65 miles west of KSC that scanned a 100 degree sector to the east. This allowed adequate coverage of the east coast sea breeze, which is responsible for initiating the majority of thunderstorms in the area.

Since the sea breeze is of primary interest to their study, the researchers describe two typical scenarios. They note that when the boundary layer synoptic flow is on-shore, the sea breeze tends to form earlier, is relatively weaker, and moves a significant distance inland over time. But if the prevailing boundary layer flow is off-shore, then the sea breeze forms later, is stronger, and does not propagate as far inland. The sea breeze obviously provides the convergence necessary for thunderstorm initiation and generally could be predicted with some success. But the goal of this study was to precisely predict the location of new convection with 10 to 30 minutes of lead time. Even though data is provided by the 29 instrumented towers which cover 1600 km<sup>2</sup> in the vicinity of KSC, more site specific information was found to be needed. The radar could locate convergence boundaries (a sea breeze in this case), but the mesonet data was *too coarse* to be of use in forecasting individual cells.

In general, it was found that any type of "kink" or "bulge" along a convergence boundary was a fairly good predictor of convection and that such an area should be watched for indications of increasing echo aloft. Once the echo aloft reached about 10 dBZ, there was about 13 minutes until the first lightning strike. The results from this study

indicate that given strong low level convergence, an unstable atmosphere, and radar echo aloft, thunderstorms should be forecastable with 10-30 minutes of lead time.

With the importance of radar detected convergence boundaries now common knowledge, much more emphasis has been placed on determining the exact location of convection initiation. One possible way to do this is to locate possible convergence boundary intersections or mergers. Wilson et al. (1992) realized the value of a technique which would allow forecasters to nowcast thunderstorms accurately. They studied the interaction between a convergence boundary and one of the most common PBL features: the horizontal convective roll. This research drew on data obtained during CINDE, which included several Doppler radars, a mesonet, mobile upper air soundings, wind profilers, research aircraft, and three photography sites. The boundary of interest in the case study presented here is the Denver Convergence Line (DCL). As previously discussed, this is a boundary layer feature which is topographically induced under synoptic-scale southerly flow. On the day of interest, a boundary moved into the Denver area from the east and collided with a previously established DCL about 1500Z. Cloud formation gradually increased until after about 1630Z when radar detected echoes of about 40 dBZ<sub>e</sub>. By 1730, a very strong line of 60 dBZ<sub>e</sub> cells had formed and spawned three nonsupercell tornadoes (Wilson et al., 1992). The primary interest of the research team was to determine the character of the low level forcing which produced these features.

The kinematics of the convergence line was studied in some detail. By flying two research aircraft over the boundary at levels ranging from 400 to 900 m AGL, they found that the boundary, which was clearly convergent at the lower levels, became divergent at upper levels. The flights also vividly displayed the conditions on either side of the boundary which included a wind shift, a weak increase in virtual potential temperature, and an increase in mixing ratio from 8 g/kg to 10 g/kg. Soundings obtained near the boundary showed that for tens of kilometers on either side the feature, the atmosphere was stable to

convection; however, in the vicinity of the boundary, the mixed layer was significantly deeper, the mixing ratio higher, and the air mass was potentially unstable. From this research, the following conclusions were reached:

(1) The DCL boundary was modified as a moving boundary collided with it. The resulting convergence zone was about 3-4 km wide and had a sharp moisture gradient.

(2) Storms did not form in the earlier part of the day because the vertical wind shear was unfavorable. As the adverse shear became more favorable, the updraft became more erect, and deeper convection resulted.

(3) Boundary layer mesocyclones were found to be common at the intersection of a boundary and a horizontal roll. These features were fairly long lived (about 2 hours) and tended to increase the surface convergence and vorticity to the point that storm initiation was likely. These studies showed that although the radar could provide some guidance as to the general location of thunderstorm initiation, they could not provide the precise location or time of formation. More "fine scale" information was needed, both horizontally and vertically.

Mueller et al. (1993) used a mesonet with 10-15 km spacing and 1 minute averaged data as well as eight sounding stations located within 25,000 km<sup>2</sup> to determine if higher resolution information could increase the skill of meteorologists forecasting thunderstorm initiation. CINDE (discussed above) data and NCAR CP3 Doppler radar data were employed. To estimate the latent instability of the atmosphere, the Lifted Index (LI), the modified LI (MLI), the forecast MLI (FMLI), and the estimated MLI (EMLI) were computed. This study showed that several mechanisms must work in unison to generate thunderstorms; when one element adversely affects deep convection, then the storms may not form. For instance, a "trigger" is generally needed in the lower levels to lift parcels to their level of free convection (LFC). The strength of the resulting convection is a function of the buoyancy of the environmental air or the Convective Available Potential Energy

(CAPE) parameter. According to Mueller et al. (1993), if all of these parameters are adequately known, then forecasters should be able to precisely forecast thunderstorm initiation.

The investigators first looked at proximity soundings and the parameters which could be derived from them. Wilson and Schreiber (1986) had estimated that a boundary modifies the atmosphere within 10 km of its location; therefore, only proximity soundings within 10 km of a stationary boundary were used in this study. They found that when MLI was  $< -1$ , storms occurred 60% of the time versus 10% of the time when the MLI was  $> 1$ . When they considered the negative area, they found that when there was more than  $120 \text{ J kg}^{-1}$  of negative energy, cells did not form. They tended to form 77% of the time when there was  $40 \text{ J kg}^{-1}$  or less of negative energy. When they computed the EMLI values using mesonet data and assuming a well mixed boundary layer, they found only that positive EMLI values helped forecast where thunderstorms *would not* form. The negative EMLI values did not provide information concerning if or when thunderstorms would form. Thus potential instability was a necessary but not sufficient condition for thunderstorm formation. When the team considered the wind profiles derived from the proximity soundings, they found that there were simply too many variables which were not considered to state unequivocally whether or not the wind profile played a significant role in storm formation. They therefore conclude that due to the cost and logistical problems inherent in deploying proximity soundings, they were of marginal use.

The Denver, Colorado area is considered a weakly forced environment in the summertime. The afternoon soundings are typically neutral with a well-mixed boundary layer from the surface to about 2-3 km AGL. Winds aloft are generally light and from the west (Mueller et al, 1993). Due to the quiescent conditions, the researchers hypothesized that variations in the boundary layer are the critical factor in determining when and where

thunderstorms occur. Therefore, an investigation of differences in the horizontal homogeneity of the boundary layer was appropriate. Mueller et al. (1993) assembled data from soundings and computed statistics regarding the variation in moisture, temperature, and lifted indices. They found typical ranges of mixing ratio of only 1-3 g kg<sup>-1</sup> and potential temperature of 1-2 °C (10°C in thunderstorm outflows). They note that three common features responsible for these variations are mesoscale air masses, stationary boundaries, and horizontal rolls. They acknowledge that stationary boundaries and horizontal rolls actually occur *within* an air mass. In order to test their observational results, they conducted a computer simulation which would model the parameters which they deemed important. They found that by varying the speed of propagation of the density current and the vertical profile, they could control whether or not thunderstorms formed. They then tested the thermodynamic dependence of the model by using a control "base state" which was known to produce thunderstorms. The simulation showed that variations on the order of 3°C and 1 g kg<sup>-1</sup> of moisture had a large influence on the formation of deep convection. The overall results of this study are extremely important to research and operational meteorologists everywhere. They found that thunderstorm initiation is governed by factors which are not measurable with a surface mesonet. These factors include, for example, vertical shear of the horizontal wind, negative CAPE, and moisture depth. They also found that storm formation was sensitive to spatial and temporal variations in the thermodynamic field on a much smaller scale than was resolvable in mesonets.

Wilson and Mueller (1993) studied the accuracy of 30-minute thunderstorm nowcasts conducted in the Denver area. Their results are applicable to situations in which there is weak, synoptic-scale forcing and thunderstorms are typically short lived. Although the researchers had access to numerous data collection platforms, emphasis was placed on

tools which operational forecasters could easily access such as Doppler radar data, satellite imagery, and visual observations. They discovered that due to their limitations, satellite data was of limited utility because it was only available every half hour and it was often poorly navigated. Extrapolation techniques useful for nowcasting were developed, but will not be covered here. What is pertinent to the current research are the general findings.

These findings are actually updated data compiled from the research of Wilson and Schreiber (1986). They found that stationary boundaries initiated thunderstorms about 60% of the time and the storm location was within 10 km of the boundary. Moving boundaries initiated storms 65% of the time and the storms formed between 0 - 15 km behind the boundary, 10 to 40 minutes after passage. When boundaries collided (see above discussion for definition of colliding boundaries), storms formed 63% of the time, within 0 - 5 km of the collision. It took between 15 to 30 minutes for the storms to form. When intersecting boundaries were considered, storms formed 54% of the time. The formation tended to occur within 5 km of the intersection point and between 15-30 minutes after the intersection occurred.

In summary, the researchers noted that by utilizing Doppler radar to detect convergence boundaries forecasters could generally predict the vicinity of thunderstorm formation. However, the exact "placement and timing" was much more difficult. Some reasons they provided for these problems were that 1) we have a basic deficiency in our knowledge concerning the details of thunderstorm initiation and evolution and 2) we need more detailed observations of thermodynamics in the boundary layer.

### **2.2.2 The Role of Satellite Imagery in Detecting Boundaries**

"The mesoscale evolution of deep convection is one of the most challenging problems in meteorology today," (Purdom, 1976). This statement is just as true today as it was when it was stated 19 years ago. The advances made over this period of time include the addition of the Doppler radar and higher resolution GOES (Geostationary Operational



Environmental Satellite) to the meteorological instrument suite. However, the evidence presented by previous authors (Wilson and Schreiber, 1986; Eilts, 1991; Wilson and Mueller, 1993) would indicate that the more sensitive and specialized the equipment becomes, the more researchers and forecasters realize the deficiencies in our knowledge base. Therefore, research in the field continues.

The ability of radar to detect subtle or clear air boundaries is receiving much attention now primarily because of the deployment of the new WSR-88D. However, clearly satellite imagery had revealed the existence of mesoscale boundaries in the planetary boundary layer many years ago. Purdom (1973) discussed the work by Fujita (1963) concerning the mesohigh. He was able to show, by using rapid scan GOES data, that the leading edge of Fujita's mesohigh was often visible in satellite imagery as an "arc cloud." The feature he saw was a group of clouds shaped like an arc, moving away from the center of the high. He showed that the intersection of this line with another "arc cloud" was often the focus of intense or severe convective development. Purdom (1976) and Scofield and Purdom (1986) later showed that other features such as sea breezes, dry lines, areas of convective cloud mergers, lake breezes, boundaries resulting from differential cloud cover, and areas of organized convective development were readily apparent using high resolution, 1 km satellite imagery. Purdom points out that when all of the above features are considered, there is little if any randomness associated with thunderstorm development.

Probably the most studied of the terrain-induced features is the sea breeze. Purdom (1976) maintained that GOES imagery is one of the most useful tools in the study of this feature simply because of the scale on which sea breezes occur. Satellite imagery can display a feature over a very large area which may lead to a better understanding of the forcing mechanisms. For example, the study of such imagery showed that the curvature of the coastline either increases or decreases the convective activity, by increasing or decreasing convergence along the sea breeze boundary. When the coastline is convex

toward the body of water, convergence will be increased; when the curvature is concave, convergence is decreased. The sea breeze type of phenomena is not unique to coastlines. Differential heating, which causes the sea breeze, can also lead to lake and river breezes. The resultant lake or river breeze is much more dependent on the low level flow patterns, but evidence of these features is very common in GOES imagery. Whenever any of these features interact with another, the likelihood of deep convection is increased (Purdom, 1976).

One question which was often raised concerned the sporadic nature of the initiation of convection along Purdom's arc clouds. Purdom (1979) paid particular attention to those areas of an arc cloud which *did not* result in convection. He found that an arc cloud moving into a field of cumulus was actually merging with or intersecting an area which was already convectively unstable. His explanation involved both dynamic and thermodynamic arguments. He stated that research had shown that cumulus clouds act to moisten and destabilize the boundary layer as well increase the height of the capping inversion. This makes the cumulus fields much more unstable to deep convection. Also associated with cumulus fields, one will typically find increased vertical velocities ( $>1 \text{ ms}^{-1}$  beneath deep trade cumulus). He noted that the area behind the arc was generally cloud-free and attributed this to the rain cooled air and to the subsidence associated with the mesoscale high pressure system. This cooler, denser air spreads out beneath the thunderstorm and undercuts the moist, warm air of the environment, thereby lifting it. If the parcels are lifted high enough, condensation occurs, clouds form, and the outflow becomes visible in the satellite imagery. Therefore, an arc cloud moving into a region which has already been destabilized somewhat by existing cumulus, would likely produce deep convection. When the arc moved into a clear air zone, the inherent stability of the air suppresses deep convection to the point that it is unlikely to occur.

Purdum and Marcus (1982) conducted an extensive study of convection in the southeastern US to test this conclusion. They studied over 9850 convective storms during June, July, and August 1979 from 1800-0000Z (noon to 6 pm local time). They found that thunderstorm outflow boundaries, seen through satellite imagery as arc clouds, often propagated for 100 miles or more beyond their location of origin before initiating new convection.

The investigators used half hourly, 1 km GOES data and classified storm generation mechanisms into four categories: (1) "mergers" (development on an arc cloud as it moved into a cumulus region); (2) "intersections" (development where two arc clouds came into contact); (3) "local forcing" (development which was obviously not due to the merger or intersection phenomena); and (4) "indeterminable."

Other conclusions drawn from Purdom's work over the years are that: (1) Arc cloud lines are almost never detected by *conventional* (pre-WSR-88D) radar, indeed thunderstorm evolution that appears as random on radar is seen to be very well ordered when viewed with geostationary satellite data. (2) Thunderstorm outflow boundaries may maintain their identity as arc clouds for several hours after the convection which produced them has dissipated and can cause deep convection to develop along it well over 100 miles from its point of generation. (3) Deep convective development along an outflow boundary is a selective process - it only occurs where the arc cloud merges with a cumulus region or intersects another boundary, whereas when the arc moves into clear skies, no deep convection develops, and (4) as the convective regime evolves on a given day, and much of the cumulus field dies away, the majority of the thunderstorms are confined to boundary intersection points. The results of Purdom's work and his conclusions will be carefully considered later in the current research.

### **3. RESEARCH METHODOLOGY**

#### **3.1 Introduction**

This study is necessarily very broad-based since this is the first time that work of this type has been undertaken in North Carolina. Similar studies have been conducted in Colorado and Florida. However, Colorado lacks the typical summertime moisture found in NC and Florida lacks the diverse topography of NC. These factors combine to make this study interesting from both the research and operational perspectives.

At the most basic level, we wanted to determine the “value-added” of the new WSR-88D over the older radar system. We did this by interrogating the boundary layer in search of convergence boundaries/zones which would help to focus the forcing for both existing and future convection. Once a feature was located, attempts were made to identify it. Those efforts and results were then documented.

Since there has been no similar work conducted in NC with which the present research could be compared, there were many scientific questions which we wanted to address. We wanted to know how the abundant moisture and diverse topography would influence boundary formation and movement. Would the characteristics of these features be different from those encountered in drier, flatter regions? What are the origins of the boundaries? Are the features predictable in their formation and movement? Are there certain regions in NC which seem to initiate certain types of boundaries? Just how important are different types of boundaries in the diurnal evolution of NC thunderstorms? Finally, how do the statistics of the current study compare with those in the Wilson & Schreiber study (1986) in terms of the relative importance of various kinds of boundaries and of boundary interactions for producing new convective cells.

Operational concerns focus primarily on the formation and movement of the features, and how they affect the weather. As previously discussed, accurately forecasting

initial thunderstorm formation has been and continues to be one of the most elusive goals of operational forecasters. This study seeks to point out preferred boundary origination regions and document the boundary formation and movement.

Emphasis is placed on determining if there are any predictors or precursors to boundary formation which forecasters could use in their nowcasts. It is recognized that there are many variables which influenced the outcome of each individual case, such as upper level forcing mechanisms, convective available potential energy, and the thermodynamic characteristics of each individual feature. Therefore another goal is to study all of the available data to determine if there is a data field which can be used to enhance forecast accuracy. It is hoped that forecasters can use the science and techniques described in this study, in conjunction with standard data sets such as soundings, surface data, satellite imagery, and Doppler radar data, to better understand their local area and the features it contains.

Peripheral benefits of this research include a display of just how effective collaborative efforts can be when researchers and operational forecasters thoroughly understand each others needs and carefully lay out their goals, assumptions, and expectations. Other benefits include a thorough testing of the new radar on very weak features. The boundaries observed in this study were carefully interrogated using all of the tools the radar had to offer. In general, the features were studied in the Doppler velocity, reflectivity, and spectrum width fields at all available scan levels. Derived products of the WSR-88D, such as the Storm Relative Motion Map, the Velocity Azimuth Display, and the Storm and Cumulative Precipitation Total were also used when it was expected that their application would prove beneficial. The research vividly shows which modes and products were most useful for interrogating the extremely subtle features which were encountered.

The purpose of this section is primarily to familiarize the reader with the local geology and climatology in order to better understand the possible importance of these

factors on the preferred location and types of boundaries in NC. It will also provide introductory comments and information regarding the conduct of the study and the data collection methods/platforms used.

## **3.2 North Carolina Geology and Summertime Climatology**

### **3.2.1 North Carolina Geology and Topography**

North Carolina has a very diverse range of topographic features ranging from the Appalachian Mountains in the extreme western portion of the state to the coastline along the Atlantic Ocean to the east. Included in this discussion of topography will be the Gulf Stream. Although not actually a “topographic” feature, the surface of the extremely warm current acts to modify the weather throughout the state, so a discussion of meteorological features as they relate to local topography would be remiss if the Gulf Stream was not considered.

From the westernmost tip of North Carolina to the coastline, the total distance is approximately 837 km (520 miles). The elevation varies from 2037 m (6684 feet) to sea level over this distance. The western wall of the Gulf Stream lies between 30 and 100 km (19 and 62 miles) offshore (Keeter et al., 1995). Figure 3.1 is a schematic which shows the geological divisions in NC as well as the proximity of the Gulf Stream.

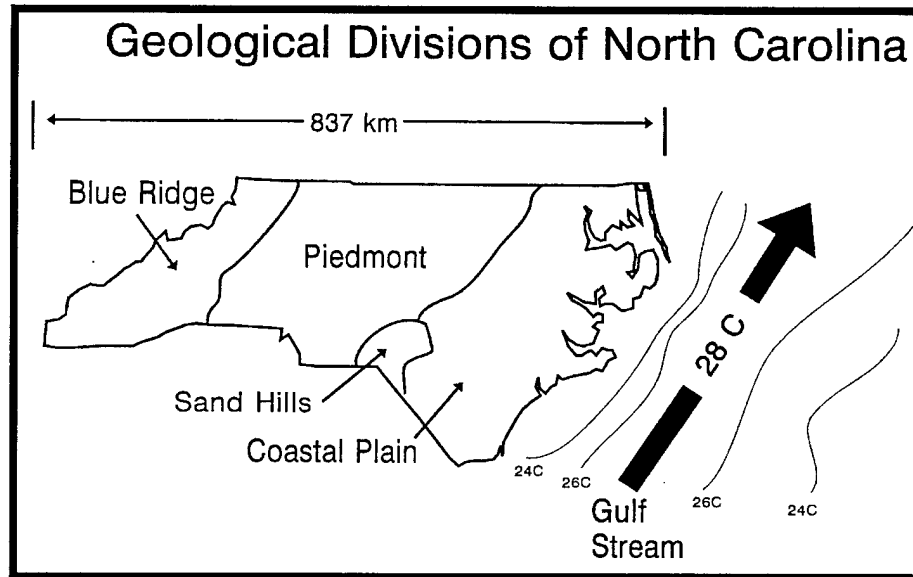


*Figure 3.1. Geological divisions of NC and the Gulf Stream.*

The manner in which the land surface varies from the mountains to the coastline is not at all homogeneous. The terrain is divided into three distinct regions: the Blue Ridge, the Piedmont, and the Atlantic Coastal Plain as shown in Figure 3.1. The division of the state into these regions is based on the different soil types which occur in each specific region.

The Blue Ridge is the western land region and has the highest elevations in the state. It is approximately 190 km (118 mi) across, from west to east (note that this varies greatly depending upon the specific locations measurements are made). The region is generally comprised of dissected, rugged mountains with steep slopes and narrow valleys. Local relief is from several hundred feet to a few thousand feet from valley floor to ridge crest (Daniels et al., 1984). The highest mountains and steepest ridges are generally composed of rock with an extremely shallow layer of soil which is unsuitable for farming or pasture land. The less steep mountains with gentler slopes are often forested or used for



pasture land while the very fertile valleys and coves are used for agriculture (Tant et al., 1990).

The North Carolina Piedmont begins at the foothills of the Appalachian Mountains at an elevation of about 457 meters (1500 ft) above mean sea level (MSL). Moving eastward, the terrain becomes flatter and the local relief decreases. Through a distance of about 255 km (158 mi), the terrain drops to about 91 meters (300 ft). The Piedmont is a region of gently rolling terrain, with narrow stream valleys where local relief is generally in tens of feet but does range in some places to hundreds of feet. Land use is primarily by farms and industrial concerns. The soils in this area are primarily firm, acidic, and clayey. On its eastern edge, the Piedmont is bounded by the NC Fall Line also known as Coat's Scarp. The scarp separates the rockier, hilly Piedmont from the lowlands of NC.

Geologists believe that Coat's Scarp as well as several other scarps throughout the coastal plain (see Figure 3.2) are "high water marks" denoting the inland progression of the Atlantic Ocean millions of years ago (Daniels et al., 1984). From Raleigh to Morehead City (135 nm), the terrain drops from about 91 meters (300 ft) to sea level.

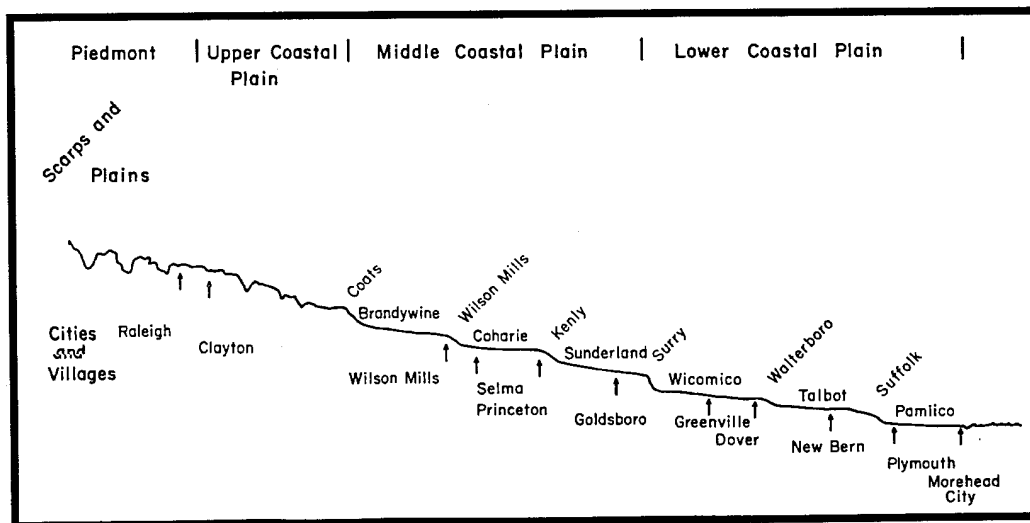


Figure 3.2. Cross section of NC.

The upland portion of the Coastal Plain (nearest to the Piedmont) is gently sloping with a seaward gradient of about 0.1 to 0.3 m per km. The soils are generally a sandy clay loam mixture and are underlain by about 30 m of fluvial and marine sediments. They are of approximately Pleistocene to Pliocene age (2 to 5 million years) (Daniels et al., 1984). Eolian (wind blown) sand formations are also common in the Coastal Plain and are probably the remnants of sand dunes.

The region of the Coastal Plain which is known as the "Sand Hills" is located in the southern portion of the state where the NC/SC boundary intersects Coats Scarp. It is named due to the extremely high sand content of its soil. Geologists have found evidence of both Tertiary (2 to 60 million years old) to Holocene (less than 1 million years old) Eolian sands and Cretaceous (65 to 140 million years old) to Tertiary fluvial and marine sediments (Daniels et al., 1984)

The lower Coastal Plain ranges from Surry Scarp (see Figure 3.2) to the coast. Generally the soils are sedimentary in nature and of early to late Pleistocene in age. The majority of the land is low, level marshland, covered by trees and water. The soils in this region are generally classified as a mixture of clay and loam and sand and loam. This is a region of gentle slopes which are dissected by rivers and local relief is generally in tens of feet.

The entire Coastal Plain region as shown in Figure 3.2 is generally very flat and it is not believed that this gentle relief produces any significant "upslope" flow. For instance, considering that from Raleigh to Morehead City (a distance of about 217 km) the local relief is about 91 meters. With a  $5 \text{ ms}^{-1}$  flow upslope, vertical velocities of only about  $0.2 \text{ cm s}^{-1}$  would be induced. It is believed that this is negligible.

Although the land mass of North Carolina ends at the coast, the surface which the planetary boundary layer "feels" continues out into the ocean. As previously mentioned, the western wall of the Gulf Stream lies between 30 and 100 km off of the NC shoreline.

It is approximately 100 km wide and moves from south to north, transporting water which has a temperature generally above 20 °C (68° F), even in the winter time. (Keeter et al., 1995). The temperature of the waters which lie between the shore and the current vary greatly with the seasons, with the strongest contrast between the current and these waters occurring in the winter.

### **3.2.2 North Carolina Climatology**

The climatology of North Carolina has been the subject of numerous studies. Keeter et al. (1995) studied the effects of North Carolina topography on wintertime weather patterns with emphasis on coastal cyclogenesis, coastal frontogenesis, cold-air damming, "Piedmont fronts," and coastal flooding. Numerous authors have studied the problems of cold air damming along the Appalachian Mountain chain and coastal frontogenesis. Businger et al. (1991) studied the Piedmont Front and Cione et al. (1993) studied the effects of the Gulf Stream on winter cyclones. Riordan (1990) examined the mesoscale features of a coastal front during the GALE (Generation of Atlantic Lows Experiment). In each of these works, the topography of North Carolina (to include the Gulf Stream) was a primary consideration.

The above studies concentrated on wintertime weather, but there has also been some interest in warm season phenomena. For example, Vescio et al. (1993) studied a severe weather incident which occurred along a thermal/moisture boundary (TMB) in the eastern part of the state during the summertime. The summertime weather in NC is dominated by the Bermuda High which is a semi-permanent system that moves with the seasons. During late spring, summer, and early fall, the high pressure center is generally located off of the southeastern coast of the US. The clockwise rotating winds around the center bring warm, humid air from the Atlantic Ocean and Gulf Stream into North and South Carolina. The subsidence inversion associated with the high pressure system tends

to disconnect the lower portion of the atmosphere from the free atmosphere, resulting in low wind speeds and relatively high temperatures. In the central portion of the state, summer temperatures average near 32° C with dewpoints often between 21 and 23 °C. The weak south or southeasterly winds from the Bermuda High often dominate the weather in the eastern and central portion of the state. As such, one would expect that there may be some type of discontinuity located where the maritime tropical air from the high pressure meets the relatively cooler and drier continental air from north and west or the highly modified warm, moist air flowing from the Gulf of Mexico. Figure 3.3 is a subjective representation indicating how some TMBs may form in NC during the summertime.

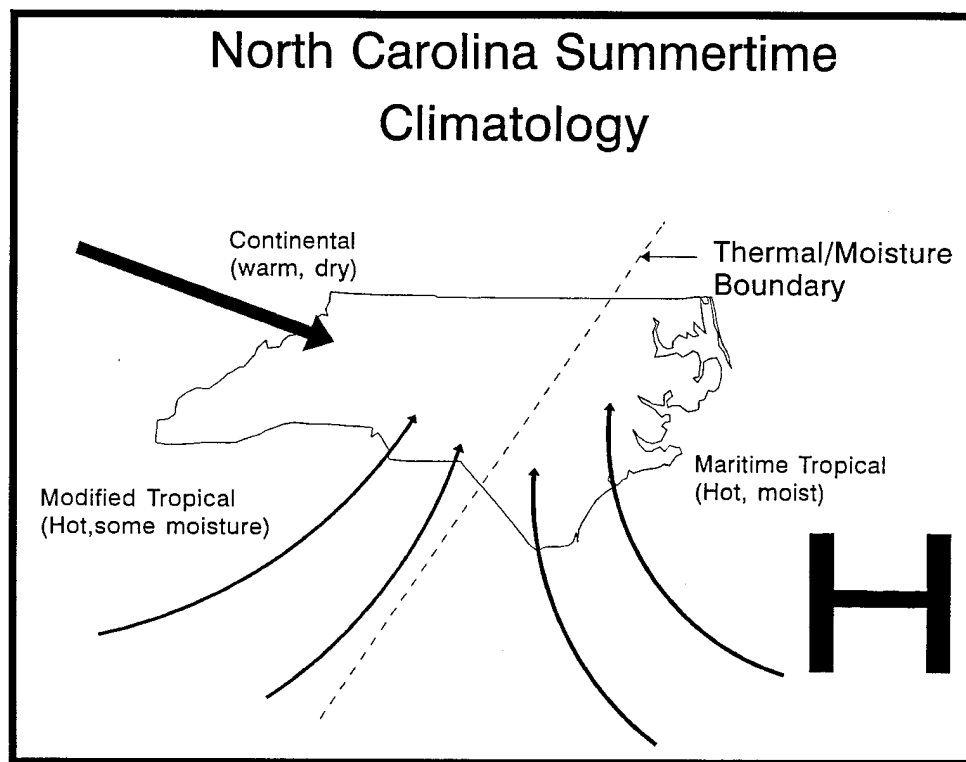


*Figure 3.3. North Carolina summertime climatology.*

Generally, the diurnal pattern of thunderstorms follows a very definite cycle in the eastern portion of the state. The first thunderstorms to form on a typical, convectively unstable day are generally near the coast and are associated with the sea breeze. The feature usually becomes active between 11 am and 1 pm local time, but can vary significantly depending on the prevailing synoptic conditions. One other area which was found in this research to rival the coastline for the "first thunderstorm of the day" is the area in the southeastern part of the state which is known as the "Sand Hills" (see Figure 3.1). The storms preferentially form in this region due to differential heating and possibly due to differences in the surrounding soil types. There will be further discussion of this area and the thunderstorms it generates later in this thesis.

Generally, once the thunderstorms form, the outflows or gust fronts they generate act to produce more thunderstorms, often many miles from the parent cell. This is the convective scale interaction which Purdom (1976) speaks of; the gust fronts which are often visible in the visible satellite imagery are the "arc clouds".

Not all thunderstorms form along the sea breeze boundary, however. There are times when very weak, unseen boundaries seem to dominate thunderstorm initiation and evolution. These weak features are the topic of this study.

### **3.3 Data Collection and Analysis**

Data for this research were collected from May 1994 through September 1994. This period was chosen because the primary interest was warm season boundaries. There was no emphasis placed on collecting data during "thunderstorm days" or those days which were expected to be very convective. Instead, data were collected whenever a boundary was observed. As previously discussed, this method of collecting data supports the number two priority of the Operational Support Facility, which is to generally explore the planetary boundary layer using the WSR-88D and identify features indigenous to our area.

#### **3.3.1 Data Collection**

Since there was not a team dedicated to insuring data availability, and because we were using real-time conventional data sets, there were several problems encountered in our data collection efforts. In fact it seems that each data acquisition platform to which we had access failed during some part of the data collection phase.

Probably the most reliable piece of equipment was the WSR-88D. The radar was out of commission for about 14 days throughout the whole period that data were collected. Once it received a direct lightning strike during a data collection event and on another occasion there were problems with the power supply. Sporadic problems occurred with the Level IV archive recorder which were quickly resolved by NWS staff members. There were other times when the radar was taken "down" for routine maintenance. The periods selected for these scheduled down times are usually early in the morning before convective activity begins. Unfortunately, this is the pre-convective environment in which we were most interested. However, it is recognized that the routine preventative maintenance is necessary to insure the proper functioning of the system, and that the older, conventional radar sets also required such maintenance. This type of downtime was not unforeseen and

for the most part, the impact was limited. This is simply a part of the equation which must be considered when using an operational radar which is commissioned for storm detection.

It was recognized from the outset that satellite imagery would be vital to this research. Unfortunately, this study was conducted when GOES-8 was put into orbit and being checked out. The University of Wisconsin Space Science and Engineering Center provided McIDAS (Man-Computer Interactive Data Analysis System) satellite imagery for this study, but was unable to meet customer requests during a significant portion of the summer. This detracted from our ability to do in-depth studies on some of the cases.

The third and final data set we used were various forms of surface charts. North Carolina State University has a meteorological data ingest system which acquires data from Unidata. These data were used in the objective and subjective analysis schemes applied in this research. Unfortunately, during the summer of 1994, there were problems with data ingest and archive as a new data ingesting software program was installed in order to facilitate the use of a new mesoscale model. The new software had significant problems in the early stages of installation, resulting in huge data ingest problems for approximately one month.

The problems encountered have been explained here primarily to show the differences between data collection efforts using real data and experimental data. For the most part, when experiments are conceived, there are numerous redundancies incorporated because it is known that some equipment will experience failure. Additionally, there are personnel dedicated to managing the equipment whose primary duty is data collection. In an operational setting, there are personnel who are responsible for equipment maintenance, but their primary responsibilities are to operational concerns. The primary job is to issue quality forecasts and protect the public. This is vividly illustrated when the situation with the McIDAS satellite data is considered. Support to research concerns was delayed while

personnel worked on commissioning GOES-8. This is not meant as criticism but is merely pointed out as a fact of life in operational meteorology.

This series of data collection problems resulted in many cases in which the data were incomplete. Therefore some improvisation was necessary. For instance, when McIDAS satellite imagery was not available, imagery from the local NWS office was used. There were also situations in which needed radar data were not available. For example, in several cases it was found that data were missing from disk or that archive files had been corrupted. This caused problems when specific hours of radar data were needed to characterize the convection in a specific area. The improvisation used in these situations involved the use of satellite and surface data. For instance, if the radar imagery necessary for determining whether a cell had grown into a thunderstorm was missing, satellite data was used. If satellite imagery revealed a well developed anvil with the cell of interest, it obviously was a thunderstorm. Also an observing station reporting thunderstorms in the area of concern would lead a reasonable person to the same conclusion: the cell is indeed a thunderstorm. It is recognized and acknowledged that this is not as objective as merely looking at radar data and noting 40 dBZ cells, but then again, this was not a field experiment and we did not have access to numerous redundancies in data sets. We made use of the data available and used sound meteorological reasoning. In short, we simply made the best use of the data which we had.

### **3.3.2 Boundaries Defined**

Prior to beginning a discussion which focuses on the data gathered in this study, it is appropriate to define our work area and explicitly define the term "boundary". It is also necessary to discuss the circumstances under which each of the data acquisition platforms which are being used (radar, satellite, surface charts) will and will not provide useful information on the boundaries.



In the radar data set, a boundary is a linear area of relatively higher reflectivity. No minimum length is set because of the large number of variables which affect the reflectivity field. In the velocity field, a boundary is defined as a linear zone of convergence in the lower levels or a zone of divergence in the upper levels (above the planetary boundary layer). Again, no physical length has been designated. This is different from most other boundary studies which usually set some length in order for a feature to be recognized as a boundary. It is not believed that the physical "length" of a feature defines whether the feature is truly a boundary or not. It is expected that the radar-related variables are more important in determining whether and how much of a feature is seen than the actual physical length of the feature itself. For example, a significant number of cases in this study show features which increase and decrease in length and "detectability" due to factors such as diurnal heating, distance from the radar, and the clear air reflectivity of the atmosphere immediately surrounding the feature. This is especially important since we are studying features at distances beyond those normally used. We do recognize that a boundary must persist for some specified length of time in order to modify the local environment and also to facilitate study. Therefore, a feature must exist for at least one hour prior to being considered to be a boundary in this study. The one exception to this rule is when thunderstorm outflows interact with other boundaries within the one hour time frame. When studying thunderstorm initiation from colliding boundaries, cells must reach a radar reflectivity of at least 40 dBZ in order to be considered a thunderstorm. In the absence of the required radar imagery, the determination will be made by using satellite or surface data as discussed above.

The conditions which must be met to detect a feature in the radar fields are fairly complicated. When a feature is located close to the radar so that the beam is still within the mixed layer (generally within 50 nm), convergence must be sufficient to cause an increase in reflectivity. This increase in reflectivity is due to an increase of Rayleigh scatterers as a

result of the local convergence. Wilson and Schreiber (1986), Eilts et al. (1991), Gossard and Strauch (1983) and Knight and Miller (1993) indicate that these "scatterers" are generally insects in the lower portion of the atmosphere. Knight and Miller noted that when insects are caught in the convergent updraft and are lifted to higher, cooler levels, they fold their wings and "fall out" which also leads to an increase of the scatterers in the lower levels. They note that the continuity equation does not apply to insects. When a measurable synoptic scale wind is present, the Doppler velocity field is very useful in detecting the convergence signature of boundaries.

At some distance away from the radar (beyond 50 nm) the beam exits the daytime mixed layer and enters the free atmosphere. For the radar to detect a boundary in the reflectivity field at this distance, there must be a thermal plume or cloud present in which the updraft temperature and dewpoint are significantly different from the ambient environment. Under the correct conditions, the radar can detect clear air echo via the Bragg scatter mechanism as discussed in Section 2.1.5. At these distances and heights, the environmental winds are generally stronger than those located at the surface so that it is sometimes possible to observe velocity returns which indicate divergence aloft, with associated convergence implied at the surface. Note that if convergence is not taking place or if there is no convective line produced (clear air thermals or clouds) then the radar probably will not be able to detect the feature.

In the satellite imagery, a boundary is considered to be a cloud line or a zone of differential low cloud cover which persists for an hour. In order for the satellite to detect a boundary, two conditions must be met. First, a cloud must form by some mechanism, and second, the atmosphere between the feature and the satellite sensor must be optically clear.

In order for a surface chart to depict a boundary, it must be detectable by analyzing one of the standard station plot fields such as pressure, temperature, and dewpoint. It must also persist for one hour or more. While surface charts are disadvantaged by having very

coarse data points, a careful mesoanalysis readily shows pressure, temperature, and dewpoint features and trends. Charts have the advantage of allowing the analyst to visualize the winds and directly observe extremely weak convergence.

With consideration for our operational concerns, the definitions used for our boundaries and the distances at which they were studied in this work are significantly different from those stipulated in most purely research oriented studies. For instance, the study area used in this research is effectively the range of the radar which is approximately 120 nm (200 km). The radar was regularly used to study the formation and movement of the NC sea breeze along the coastline which is 90-120 miles away. Figure 3.4 is a radar-generated depiction of NC which shows the radar site and the coastline. The range rings represent distances of 30 nm. Figure 3.5 shows graphically the elevation of the radar beam at different distances from the radome, in the absence of anomalous propagation.

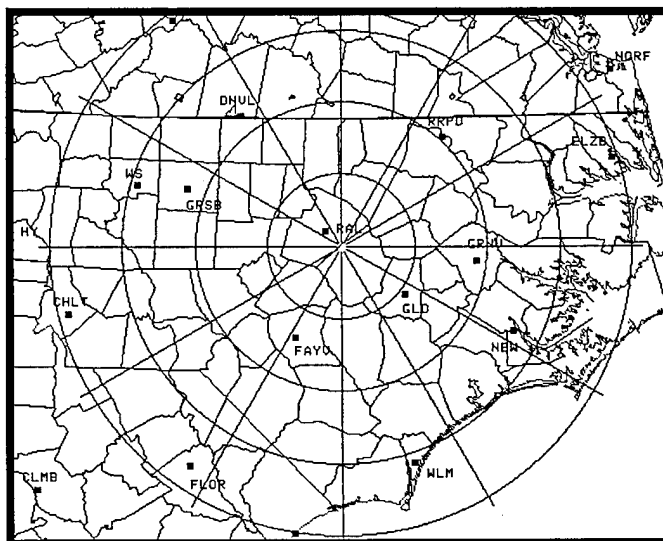


*Figure 3.4. Study Area. Range rings are in 30 nm increments.*

From studying both figures, it is obvious that as far away as the NC coast, the radar beam is more than 10,000 ft above the ground. Therefore, the radar reflectivity returns are not

due to surface convergence, but are a product of surface convergence: cumulus congestus and cumulonimbus clouds.

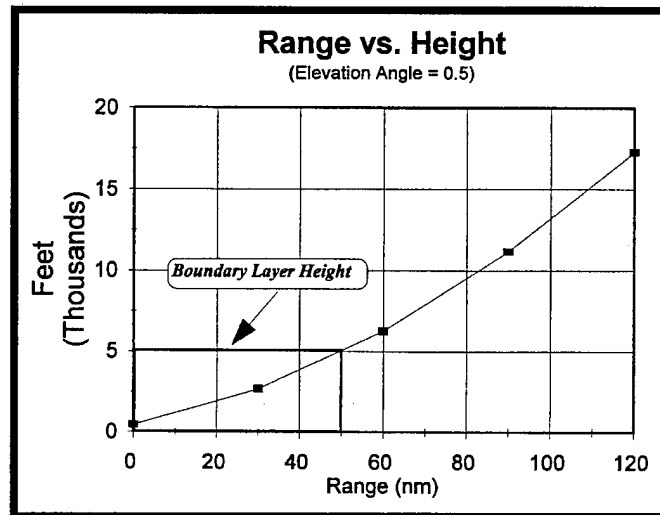


Figure 3.5. Distance from radar vs. beam height.

At such large distances, the radar return is due to Bragg scatter as the radar beam penetrates the warm clouds and rapidly rising thermals as discussed by Christian and Wakimoto (1989) and Gossard and Strauch (1983).

As previously mentioned, the distances at which boundaries were studied in this research are well beyond those used in the work of Wilson and Schreiber (1986) and Eilts et al. (1991). However, their studies were motivated primarily by research concerns which happened to have an operational application. The present research is first and foremost driven by operational concerns. We wanted to see and use the same data to which a meteorologist working at the WSR-88D radar console would have access. We did not have access to an aircraft (Fankhauser and Rodi, 1989) or rapid scan satellite imagery (Purdom, 1976; 1979) or a mesonet (Wilson and Schreiber, 1986). Researchers and forecasters in this area must learn to glean the maximum amount of information from the

data which they have at hand. Since they must forecast for a region which is much larger than the 30 or 40 nm circle which most researchers study, we wanted to maximize the range at which we gathered information and studied features so that the results would be beneficial to the operators. We recognize that we may be sacrificing some scientific "exactness" so that we may better understand the general convective patterns and features which are important in forecasting the weather in central and eastern NC. It is left to future researchers interested in this work to fine tune the methods and data gathering techniques which are described here.

This is not to say that there were no limitations imposed on the ranges at which we observed features. For instance, with increasing range, the radar returns become increasingly weaker, as predicted by the radar equation (equation 14). When one considers that many of the subtle features we studied were very weak, even when located close to the radar, it is obvious that the radar probably will not provide much useful information if the feature is located 80 miles (120 km) away. But realistically, the operational forecasters would not be able to observe the feature at that distance either and they would not be able to use it to make forecasts. Therefore, the constraints we are working with are very real; they are imposed by nature, the limitations of our technology, and by the laws of physics. Most importantly, they are the types of constraints imposed on weather forecasters at the NWS Raleigh office every day.

As the range increases, two other factors must be considered. The first problem concerns resolution of the radar and beam filling considerations. As previously discussed in the radar section, the beam continually broadens as it propagates away from the radar. Therefore, less energy impacts targets at larger distances and the returns are weaker. Also, as the radar beam propagates, it becomes increasingly higher above ground level. If one considers that convergence boundaries and other features which are of interest in this work are confined solely to the planetary boundary layer, and the assumption is made that the

PBL is about 1.5 km deep (5000 ft), then the radar beam is only interrogating the PBL within the first 50 nm or so. Beyond that distance, the beam has risen above the mixed layer and into the free atmosphere (see Figure 3.5). It is important that this range-height relationship be held constantly in mind. Whenever a feature is observed on the radar, it is NEVER at the surface. Also, if the beam is pointing west, the terrain below it is rising slightly and if it is pointing east, the terrain is dropping away from it. The elevation changes within the 120 nm study area are relatively small compared to the rate at which the beam increases, so they will be ignored in this study. For example, from the location of the radar site to the Atlantic coast, the terrain drops between 300-400 ft. However, in the same distance, the radar beam rises approximately 16,500 ft.

### **3.3.3 Data Analysis Techniques**

Data were collected on 27 cases. A cursory examination was conducted of each potential case to determine if sufficient data was available to warrant further analysis. Several cases were discarded due to operational constraints and because of missing data. We retained 23 cases from which all of the data was gathered. Three of the cases will be analyzed in some detail in order to identify the features of interest and the weather associated with them.

In addition to radar data and satellite imagery, each of the cases was examined using 1 mb subjective, hourly pressure analysis. In addition to these standard data sets, we also used the GEMPAK Barnes objective analysis method (Koch et al., 1983) to study temperature and moisture parameters in an attempt to further isolate specific boundaries and features and determine the origin of the features. Several non-standard surface analyses were used to analyze the more puzzling features. The techniques used will be discussed in detail below in the discussion of the types of boundaries identified.

Once all of the data had been initially analyzed, and the boundaries of interest identified, the data was compiled. The boundaries were categorized and several stability

indices were computed using the SHARP Skew-T analysis program of the NWS (Hart and Korotky, 1991). Morning soundings were modified to reflect the environment in which the features were observed. In order to insure objectivity, SHARP was used to compute the average mixing ratio of the lowest 150 mb. This "averaged" parcel was then lifted to obtain the indices of interest. The indices utilized were the Lifted Index, the Showalter Index, Total Totals, Convective Available Potential Energy, the K Index, and the Sweat Index. The days were categorized based on the stability and it was noted whether each boundary was identifiable using satellite imagery, radar data, or surface data.

In making the determination of whether a feature was "identifiable" in the different data sets, it should be noted that this too was approached from the standpoint of an operational forecaster who was actually looking for a feature. For example, if a boundary which was previously unseen or unnoticed on radar could be detected by first locating it on satellite and then looking back at the radar, then that feature was "identifiable" in radar imagery. However, a thermal/moisture boundary which is only discernible using subjectively or objectively analyzed  $\theta_e$  fields on a surface chart would not be "identifiable" on a surface chart. This is considered a "non-standard data set" which would not routinely be used by forecasters.

Statistics were computed which we hope will help show the relative importance of each type of boundary in producing convection. The radar data was analyzed to determine if the boundary was associated with convective cells of 40 dBZ or more. In the event that radar data was not available for the period of concern, other methods, which were described above were used to differentiate between thunderstorms and other clouds. Note that the determination of whether a boundary was convective did not have as a requisite that convection was associated by collisions, but instead was based solely on whether the feature produced convection alone (hereafter referred to as autoconvection).

Attempts were made to identify all cases of interacting boundaries and the effect the interaction had on the convection. The cases were divided into the categories labeled collisions, mergers, and intersections. The definitions which follow are essentially those used by Wilson and Schreiber (1986). "Collisions" occur when two boundaries which are moving in opposite directions meet with an angle of incidence of 30 degrees or less. "Mergers" occur when a moving boundary overtakes another boundary, moving in the same direction, or when the moving boundary meets a stationary boundary. Intersections occur when boundaries meet with an angle of incidence of greater than 30°. Figure 2.4 is a graphical depiction of each of these interactions.

Section 3.3 has provided the reader with some idea of the study area and the definitions which were used in the current research. Some of the differences between this study and that of Wilson and Schreiber (1986) were covered as well. The next few sections will document the different types of features observed in this research and some statistics will be presented. These statistics are often based on a limited number of samples and it is not expected that they are statistically significant in the strictest sense. However, it is believed that they give some indication as to the types and relative frequency of occurrence of boundaries which occur in the NC PBL.



## **4. GENERAL RESULTS**

For the 23 total cases for which data were gathered from May - September 1994, 95 boundaries were identified. Section 4.1 will discuss the different types of boundaries observed and draw comparisons to the work of other authors regarding these features. Section 4.2 is a general discussion of the overall statistical results of this work. The relative utility of the different data acquisition platforms as well as the importance of collisions in this area will be considered. Finally, the results will be more closely compared to the results obtained in the Wilson and Schreiber (1986) study.

### **4.1 Types of Phenomena Identified and Contributing Factors**

During the course of this study, a total of ten different types of boundaries were identified: sea breezes, thunderstorm outflows, prefrontal troughs, fronts, troughs, horizontal rolls, thermal/moisture boundaries (TMBs), unknown stationary, and unknown moving. One boundary which was initially labeled as "unknown stationary" occurred so frequently that it was placed in a separate category referred to as the "Piedmont Trough (PT)." Further explanation will be provided on this unique feature below.

#### **4.1.1 Thunderstorm Outflows**

Thunderstorm outflows or "gust fronts" are probably one of the most prevalent and most studied summertime boundary layer features. There are numerous reasons for this interest, one of which is the danger they present to aviation. Aircraft which are taking off or landing are greatly affected by thunderstorm outflows and numerous incidents have been attributed to them (Klinge and Smith, 1987). A second reason for the keen interest in the features is that gust fronts are known to be prolific producers of thunderstorms. Indeed, Purdom and Marcus (1982) argued that Convective Scale Interaction (CSI) was responsible for over 73% of all new convection which formed in the southeastern United States during summertime afternoons and evenings. Wilson and Schreiber (1986) found that

thunderstorm outflows comprised 33% of all of the boundaries they encountered during their study. Other researchers such as Eilts et al. (1991), Mueller and Carbone (1987) and Weaver and Nelson (1982) recognized that these features are extremely important in determining where new convection will occur, in agreement with Purdom (1976). It is no wonder that these features are given so much attention.

Obviously as implied by its name, thunderstorm outflows are produced by thunderstorms. There is general agreement that two mechanisms are responsible for this downrush of relatively cool, dry air. The first mechanism, precipitation drag, is considered to be the weakest contributor (Weaver and Nelson, 1982). The primary contributor to the downdraft is evaporational cooling which results from the entrainment of dry, mid-tropospheric air. As the drier air evaporates the precipitation, a bubble of relatively cooler, denser air is pulled to the surface by gravity. As the dome of cooler air approaches the surface, it spreads out radially due to conservation of horizontal momentum (Goff, 1976). The cool, dense air undercuts the warm, moist PBL air and lifts it. If the surface air is moist enough, a roll cloud (also commonly known as an arcus cloud or a shelf cloud) may form. If the vertical velocities generated are substantial and a sufficiently deep layer is affected (Koch et al., 1991) the surface parcels may be lifted to their level of free convection and a new thunderstorm may form. The foregoing is essentially a description of the CSI process. Figure 4.1 is a radar depiction of a strong thunderstorm outflow moving toward the radar site. The CSI process is evident as the outflow produces showers (echoes behind the boundary).

There have been numerous studies concerning gust fronts and their characteristics. In a study of 20 outflows, Goff (1976) found that they could produce vertical velocities from 2 to 6  $\text{ms}^{-1}$  and that they propagated at an average speed of 10  $\text{ms}^{-1}$ . Figure 4.2 is a depiction of a typical gust front. Klinge and Smith (1987) studied nine different gust front cases in Colorado and found that the maximum depth was 4.2 km and the shallowest

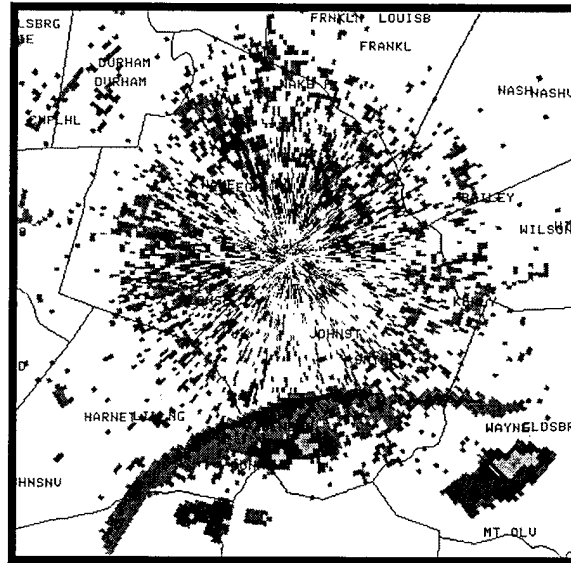


*Figure 4.1. Radar depiction of a strong outflow boundary. The feature is moving from the southeast, toward the radar, generating showers as it moves.*

was 300 m. The average depth for all nine of the cases was 2.6 km. The researchers determined the depth by using the Doppler radar. They located the point most distant from the radar at which they could identify the gust front. The radar then provides the altitude of the point indicated by the cursor. Mueller and Carbone (1987) found that the depth of the outflow could range from several hundred meters to over 2 km and that they could sustain themselves for several hours and travel tens of kilometers. They note that “in equilibrium, density currents usually maintain a constant propagation speed. The horizontal hydrostatic pressure gradient force that drives the density current toward warmer, less dense air is balanced by drag due to both surface friction and momentum mixing in the turbulent wake.”

As alluded to above, thunderstorm outflows are often described as density currents, which are generally considered to be “the stable parallel gravity flow of one fluid relative to another that results from small differences in their densities,” (Goff, 1976). Koch et al. (1995) found that some cold fronts display a leading microstructure of a density current.

Goff compared cold fronts, thunderstorm outflows, and sea breezes and noted that cold fronts are deeper, longer lived, and of greater horizontal extent than the other features. He

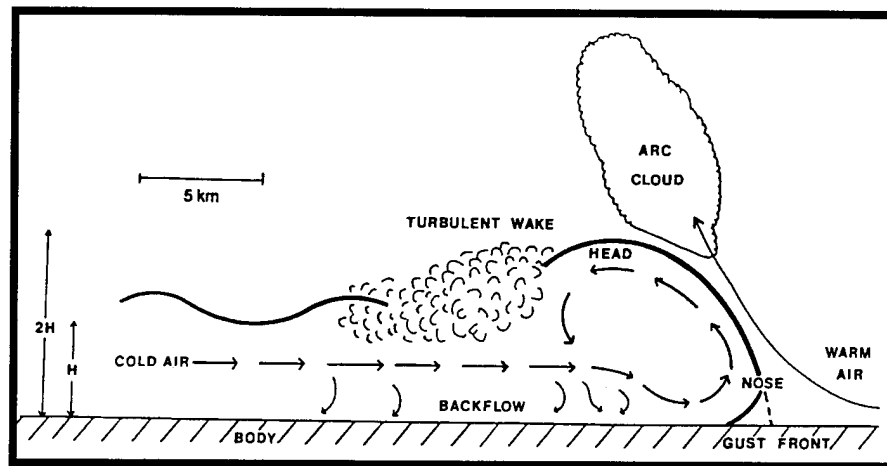


Figure 4.2. Typical gust front/density current (Houze, 1993).

points out that a sea breeze, which is driven only by density differences caused by diurnal heating, has no links to upper level dynamics as do gust fronts and cold fronts. As such, the analogy between gust fronts and density currents is often questioned.

Wakimoto (1982) acknowledges that there is still some discussion on whether the gust front is actually a density current. He addresses this question by dividing the evolution of a gust front into four stages: formative, early mature, late mature, and dissipating.

The formative stage is characterized by heavy precipitation which produces strong reflectivity returns. The gust front is directly below the thunderstorm and is beginning to spread out. Its depth is greater than 1 km and it is traveling at between 10 to 20  $\text{ms}^{-1}$ .

The early mature stage begins as the gust front pushes an “envelope” of precipitation well ahead of the advancing storm. Convergence between the down draft and the environmental air produces vertical motion which lifts or “curls” the rain curtain. Wakimoto calls this a “precipitation roll.” The gust front at is from 1 to 2 km deep and it is

propagating between 10 to 30  $\text{ms}^{-1}\text{m}$  (Wakimoto, 1982). The radar reflectivity is provided by the precipitation roll and is generally on the order of 15 dBZ.

The late mature stage begins as the precipitation roll is completely curled back into the gust front and a horizontal vorticity maximum exists along the leading edge of what was formerly the precipitation roll. The depth of the gust front has decreased to between 0.5 and 1 km and the speed is now between 10 to 25  $\text{ms}^{-1}$ . The radar reflectivity at this stage is provided by a composite of dust, insects, and the precipitation roll.

In the dissipating stage, the gust front is completely cut off from the parent thunderstorm. The depth is now less than 0.5 km and the speed is between 5 to 15  $\text{ms}^{-1}$ . At this point, all precipitation in the roll has evaporated and the remaining reflectivity is provided by dust, insects and possibly thermal discontinuity.

Wakimoto maintains that in the late mature and dissipating stages, the thunderstorm outflow is most like a density current. He found that the vertical transfer of momentum which was provided by the down draft, in no way contributes to the propagation speed in these latter stages. Once the outflow is cut off from the supply of cool, downward flowing air, its propagation (speed and distance) depends only on the density differences between the gust front and the environmental air. He notes that the outflow can travel tens of kilometers in this manner.

In order that the current study would not be dominated by gust front outflow boundaries, data was not collected solely to record gust fronts. Once another feature of interest had been located and data collection initiated however, gust fronts were recorded. Because of the external control imposed, there were only 25 outflows included in the research data base; however, this is still the largest category of boundary encountered. This is strong evidence as to the importance of this boundary category in the NC PBL.

When the results of this research are compared to the thunderstorm outflow statistics presented above, there are absolutely no surprises. It was found that the average

depth of the thunderstorm outflows studied in this work was 1.9 km. The minimum depth was 1.4 km and the maximum depth was 2.7 km. The average speed of the features was  $7.8 \text{ ms}^{-1}$ . The maximum speed observed was  $9.8 \text{ ms}^{-1}$  and the minimum was  $6.3 \text{ ms}^{-1}$ . Depths of individual features were obtained by placing the radar cursor on the outflow at the *most distant point from the radar* at which the feature could be observed. At this point, the beam is penetrating the very top of the boundary. Speeds were obtained by using consecutive radar images.

Purdom (1976) noted that gust fronts were very capable thunderstorm initiation mechanisms. In the current research, 72% of the features were autoconvective (they produced thunderstorms without colliding with other boundaries). It should be noted that many of the outflows encountered interacted with other features within just a few minutes of becoming visible in the radar and/or satellite imagery. There was not time for them to produce convection independent of other features. Outflow boundaries were involved in a total of 26 collisions, mergers, or intersections with other boundaries. In 100% of these cases, existing convection intensified or new convection developed!

When forecasting the weather in the vicinity of a thunderstorm production mechanism as productive as outflow boundaries, it is very important to be able to recognize these features quickly and accurately. Therefore, this study made note of the number of outflows which were visible or recognizable in each of the data acquisition platforms. Of the 25 cases, 96% were detectable by radar and 76% were detectable by satellite. Conversely, only 8% were identifiable in surface charts. One would not intuitively expect that such transient features would be revealed in data fields which are as temporally and spatially coarse as surface charts. However, there were cases in which the thunderstorm outflows resulted in strong wind shifts and temperature and dewpoint discontinuities which

persisted for hours. In these situations, the surface charts did provide information to forecasters concerning the features.

As predicted by Purdom (1976) and Purdom and Marcus (1982), thunderstorm outflows are responsible for the majority of convective initiation in this area during the summertime, and they are generally visible in the satellite imagery. In the cases in which the satellite imagery was not helpful, there was a significant amount of anvil "blow off" which obscured the ground. There was only one situation in which the radar did not provide useful information on a thunderstorm outflow. This feature was first identified in the satellite imagery, was located more than 162 km (100 nm) from the radar, and the radar beam was overshooting it (beam height is approximately 13,000 ft (3.9 km) at that distance.

When the work of Purdom (1976) and Purdom and Marcus (1982) was conducted, Doppler radars were generally only located in research laboratories and the average weather forecaster had no knowledge of their capabilities. However, the new systems are now being deployed over the entire nation. Once in place, they can and will provide a mesoscale resolution which cannot be matched by any conventional satellite system currently in use. Moreover, the temporal resolution of the storm detection Doppler radar is significantly better than that afforded by the satellite acquisition system. As this is written, GOES-8 imagery is just becoming available (in real time) to forecasters around the US. It provides excellent 1 km resolution in the visible wavelengths and updated images every half hour. At the time the images are received, however, they are between 15 minutes and 30 minutes old. In contrast, the Doppler radar can provide high resolution imagery every six minutes, within a range of 120 nm. The intent here is not to downplay the importance of satellite imagery, but to point out that each data acquisition platform has its strengths. When the two systems are used together, they provide a forecaster with detailed information about what is happening from hundreds of kilometers away to just a few kilometers distant.

#### 4.1.2 Sea Breezes

As expected, sea breezes comprised a significant portion of this research. Out of a total of 95 boundaries, 19 (20%) were sea breezes. This is the second largest category studied.

As a result of their ubiquitous nature, sea breezes, like thunderstorm outflows are very well studied phenomena and as such, are fairly well understood. It is generally agreed that sea breezes can be characterized as density currents. They form when, through diurnal heating, the land becomes hotter than the surface of the ocean, resulting in less dense air over land and more dense air over the water. The denser air then begins to move toward the less dense air, and the circulation is initiated (Figure 4.3).

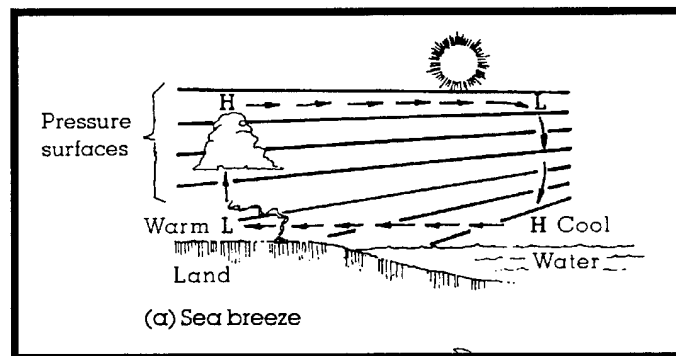
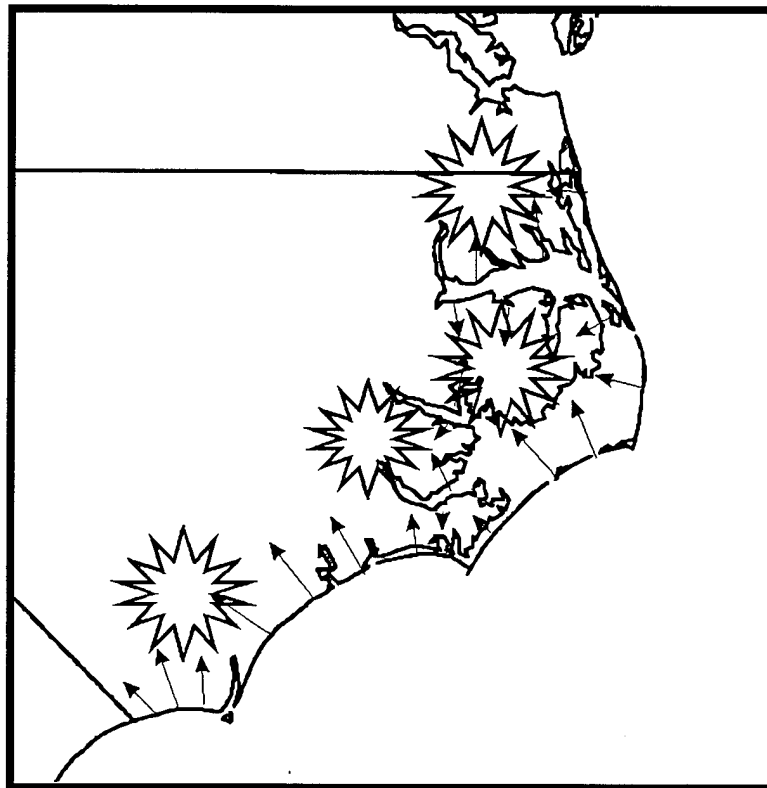


Figure 4.3. Sea breeze circulation (Ahrens, 1985)

Since sea breezes can be found in some form on nearly every coastline, they have been studied by many researchers using different methods (Purdom (1976), Eilts (1991), Zhong and Takle (1992), and Wakimoto and Atkins (1994)). Purdom (1976) noted that local terrain and the curvature of the coastline play an important role in influencing the initiation, intensity, and propagation of sea breezes. For example, where the coastline is convex toward the water, there is an enhancement of convergence and convection.



Conversely, where the coastline is concave toward the water, there is divergence and the sea breeze front is less intense. Figure 4.4 is a sketch of the NC coastline which provides indications of locations where convergence and divergence would most likely occur based purely on the shape of the coastline.



*Figure 4.4. Sketch of NC coastline with arrows indicating the influence of the coastline shape on the movement of the sea breeze. Stars indicate zones of relatively higher convergence associated with the coastline shape.*

Also note mesoscale flows induced by the sounds/inland waterways. These features tend to greatly increase convergence as the sea breeze passes their locations and are often the sites of convective initiation early in the day. The stars indicate areas where greatest convergence occurs and where thunderstorms are most likely to form first. It should be

noted that the environmental wind direction and speed is very important in determining when and where the sea breeze will initiate convection.

Eilts et al. (1991) conducted a study of the sea breeze as it relates to the initiation of convection in the vicinity of Kennedy Space Center (KSC) in Florida. They found that when the low level flow is on-shore, then the sea breeze is established early and propagates a significant distance inland; however, under these circumstances, the feature is not very strong. In contrast, when the low level flow is off-shore, the sea breeze does not begin until late in the day and it moves little, if at all. Under these circumstances, the feature is much more intense and results in stronger convection. These concepts have been corroborated by other researchers since 1991, including Wakimoto and Atkins (1994). They noted, in support of Purdom (1976), that once the sea breeze initiated the first few thunderstorms, then the remaining storms are generally initiated by the gust fronts from the initial convective activity.

In a basic but important observational study, Zhong and Takle (1992) noted that the sea breeze circulation in its entirety is not symmetric, but extends offshore for a distance which is about twice the distance it extends onshore. As the boundary moves inland, the temperatures tend to drop, the dewpoints rise, and the winds become "on-shore." They indicated that these "characteristics" tend to weaken as the boundary penetrates further inland.

Observations by Wakimoto and Atkins (1994) showed that the sea breeze is not a uniform entity, as previously assumed, but that it has clefts and inflection points along the frontal edge as found by Meuller and Carbone (1987) in a thunderstorm outflow. Wakimoto and Atkins maintain that these structures, which have been observed in laboratory produced density currents, are not produced or maintained by the same mechanisms. They also note that there are no preferred regions of relatively higher convective activity along the sea breeze front, except at those locations intersected by

horizontal rolls. This fits Purdom's (1976) contention that one of the situations in which an otherwise inactive boundary may initiate convection is when it enters a convective cloud field.

As indicated previously, there have also been a significant number of modeling studies which concentrate on sea breezes. Modelers have attempted to reproduce such features as the initiation of the circulation, the maximum propagation distance and speed, and the observed vertical velocities. Studies by several researchers (Mahfouf et al., 1987; Sha et al. 1991; and Zhong and Takle, 1992) found that models produced sea breezes which propagated at an average of  $8 \text{ ms}^{-1}$  and generated  $11 \text{ cm s}^{-1}$  positive vertical velocities. The features were generally on the order of 1 km deep and that the depth of the following flow was generally about half that of the head (see Figure 4.2). Most of the models also produced a maximum inland propagation distance of between 50 and 90 km.

Mahfouf et al. and other researchers (Ookouchi et al., 1984; Sha et al., 1991) found that sea breezes (and other surface-based thermally direct circulations) initially move at a moderate pace in the morning, slow down in the early afternoon, and then speed up significantly around sunset. There has been some observational evidence to support this. The primary explanation for this interesting development was that during the day, the balance of forces was between the horizontal pressure gradient force generated by the differences in density, and the dissipation due to friction and turbulent mixing. As the sun sets, the turbulent mixing decreases significantly and therefore surface propagation speeds increase. In an attempt to better understand the phenomenon, Ookouchi et al. (1984) studied the observed differences between the temperature of the ocean and the land and derived an empirical relationship which gives some indication of the intensity of the expected circulation. Their relationship was

$$U_{\max} = 0.20\Delta\bar{T}_{\max} + 1.9(\text{ms}^{-1}) \quad (24)$$

in which  $\Delta\bar{T}_{\max}$  is the average maximum temperature difference between the ocean and various locations inland. They compared their results to another derived relationship

$$V_{SB}^2 \approx 1.5\Delta\bar{T}_{LS} \quad (\text{Biggs and Graves, 1962}) \quad (25)$$

in which the terms have the same meaning as the above. Figure 4.5 is a graph depicting the results of both of the equations given the same temperature differences.

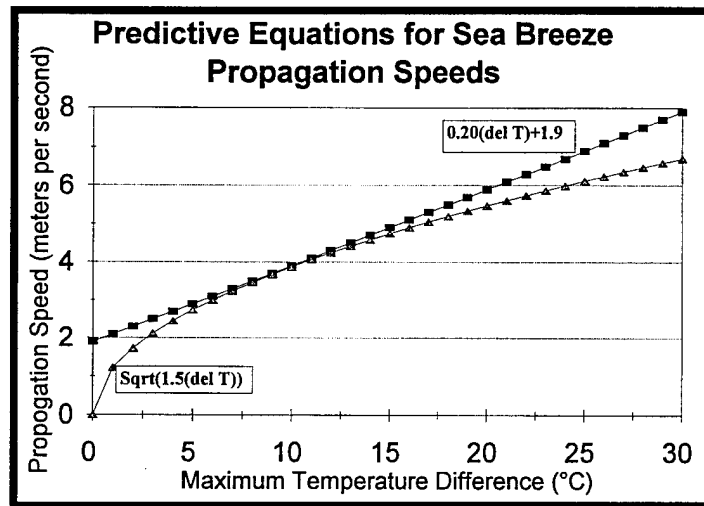


Figure 4.5. Sea breeze/density current speed as a function of temperature differential.

With the work of previous researchers as background, the sea breezes observed in the current research can be considered. A detailed case study of one interesting sea breeze event has been included in Section 5.3. In general, the sea breezes were very convectively active, as would be expected. About 74% of the features were autoconvective and 26% were not. Of this 26% (5 cases) two of the boundaries eventually interacted with other features and resulted in increased convection. In all, sea breezes were involved in 16 collisions. Of these 16 collisions, 88% resulted in new convection while 12% resulted in no noticeable change.

Three cases were examined in order that the depths of North Carolina sea breezes could be compared to the depths observed by other authors. It was found that the depths of the sea breezes were 1.1, 1.3, and 1.4 km. These depths were obtained as the density current moved close enough to the radar for the beam to penetrate the top (generally within 80 km (50 nm) of the radome). In each case this occurred after 7 p.m. local time. This compared favorably with other researchers who found that the depths of sea breezes generally were on the order of 1 km.

The speed of propagation and the inland penetration distance were studied as well. Seven cases were studied to determine the speed of propagation of NC sea breezes. The maximum speed was found to be  $5.4 \text{ ms}^{-1}$  and the minimum was  $2.7 \text{ ms}^{-1}$ . The average for all of the cases was  $3.7 \text{ ms}^{-1}$ . Researchers also found a large variation in the propagation speeds, and these appear to be fairly typical. Attempts were made to acquire the necessary ocean temperatures so that the  $\Delta T$  could be compared to the speed of the motion, but time constraints were prohibitive. However, the 19Z temperatures at Cape Hatteras and Wilmington were compared to temperatures inland at Raleigh, Fayetteville, Greensboro, and Goldsboro. The maximum  $\Delta T$  (calculated difference between highest inland temperature and lowest coastal temperature, with the sea breeze located between them) ranged from  $1^\circ\text{C}$  to  $10^\circ\text{C}$  with an average of about  $4^\circ\text{C}$ . Sea breezes were observed to occur at both the maximum and minimum temperature differences. For the average propagation speed ( $3.7 \text{ ms}^{-1}$ ), the average temperature difference predicted by both equations (Figure 4.5) was about  $9^\circ\text{C}$ . This temperature difference is higher than that observed. There are several reasons for this. First, the coastal temperatures were assumed to be representative of the ocean surface temperature. This is a poor assumption at best since the land can be expected to modify the ocean temperatures. Another possible explanation for the observed high propagation speeds (compared to  $\Delta T$ ) is related to the

time of day the speeds were measured. Since the radar was used measure the speed, the features were inland quite some distance and the measurement was taken late in the event (they were within 50 nm of the radar). As previously discussed, the PBL appears to become decoupled from the rest of the atmosphere late in the day, resulting in an increase in speed of density currents. Therefore, the speed measurement, while correct, may represent a high bias due to the time of the day it was measured.

When the maximum penetration distance was studied, the features were not considered to be sea breezes if their propagation was obviously aided by thunderstorm outflows. It appeared that the inland penetration distance depended upon several factors to include the environmental flow, the convective activity in the Sand Hills and Coastal Plain regions, and the maximum temperatures in the interior of the state. Six cases were evaluated for total penetration distance. It was found that the largest distance was 193 km (based on radar observations) and the smallest was 35 km (based on satellite imagery). The average of the six cases was 114 km. The interesting point of this is that sea breezes do seem to travel quite some distance inland, definitely beyond the distances generally expected.

In the study of sea breezes, there was more variance in the performance of each of the data acquisition platforms than was seen in the study of thunderstorm outflows. For example, only 73% of the cases were directly detectable by the radar. It should be noted that in order for the radar to be given credit for detecting the feature, the boundary (actual density current) must be visible in the radar imagery, and not the convection which was produced. For example, the radar is capable of observing any thunderstorm which is initiated along the coastline. However, the beam would be well above the sea breeze at that point. Therefore, generally the radar detected only those boundaries which came within about 50 nm of the radar. In contrast, the satellite detected 100% of the boundaries on which data was collected during the period. It should be noted, that the satellite imagery

was not available until after the majority of data collection had been conducted. The surface data revealed sea breezes 88% of the time. They were considered “detected” when the surface winds turned on shore. Note that the satellite provided 30 min resolution while surface data was hourly.

Satellite imagery was studied to determine the approximate times that the sea breeze becomes established on the NC coastline (note that hourly data was used). Eleven cases were studied and it was found that in five of these, the circulation becomes visible as a cloud line at about 1600 UTC. The breeze became visible at 1700 UTC in three of the cases. Therefore, about 73% of the time, the breeze becomes apparent in satellite imagery in the mid to early afternoon. In just three cases, the circulation became visible prior to 1600 UTC. Twice, it was visible at 1500 UTC and once it was visible at 1400 UTC. Note that in these cases, the circulation was very weak and difficult to track inland. The synoptic flow was onshore. These characteristics are predicted of an “early sea breeze” by Eilts et al. (1991) and Wakimoto and Atkins (1994).

#### 4.1.3 Horizontal Rolls

When compared to thunderstorm outflows and sea breezes, horizontal rolls are not true boundaries in the most precise sense. They obviously do not separate different air masses but actually occur within a single air mass. However, the convergence they provide at the surface and the significant modification they induce in the boundary layer necessitate their inclusion in a study of important boundary layer features. The fact that they are routinely detectable by Doppler radar further supports the contention that they should be considered in this study. For these reasons, the horizontal convective roll will be considered a "boundary" just as any other feature in this research. It is left to the reader to remember that the definition is not being applied in its strictest sense.

Horizontal rolls are generally thought to be interesting but innocuous atmospheric features, which for the most part occur in fair weather. This is true, but researchers such as Wakimoto and Atkins (1994) and Wilson and Schreiber (1986) have made note of these features as they influence deep convection. Purdom (1976) also linked the existence of horizontal rolls to the increased likelihood of deep convection when a boundary enters the roll field. The discussion below will describe the dynamics of horizontal rolls and some of the early work in the field will be covered. The results of this research will then be discussed as it relates to the theory and observations.

Brown (1980) cited common examples of linear features in geophysical flows, such as cloud streets. These features have been studied exhaustively for decades. The existence of cloud bands in the earth's atmosphere is the result of the atmosphere's attempt to reorganize in order that flow conditions may be maintained. This reorganizational process is generally manifested in some kind of instability process, such as convection. There are many, many different kinds of instability. However, for the purposes of this study, only two processes which are often observed in the atmosphere and which result in horizontal



rolls will be discussed. The first is "Inflection Point Instability" and the second to be considered is "Thermal Instability."

Inflection Point Instability (IPI) has been investigated by numerous researchers but the results from the work of Brown (1972 and 1980) are probably the most illuminating. Brown (1972) studied high Reynolds Number ( $Re$ ) flows (large inertia/small viscosity) which have an inflection point in the wind profile. This is the natural configuration of the atmosphere since the  $Re$  is often larger than  $3 \times 10^7$  (Stull, 1993) and the vertical wind profile often contains an inflection point. Under these conditions, Brown states that the horizontal rolls which form will tend to be oriented perpendicular to the wind shear vector. Figure 4.6 is provided as illustration.

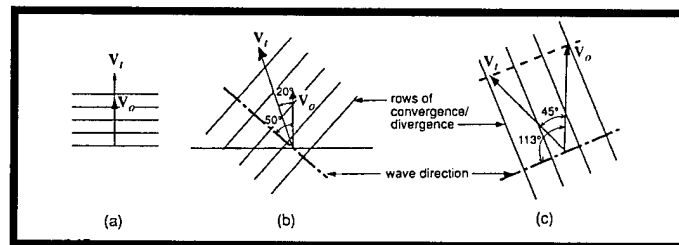


*Figure 4.6. Roll orientation for Inflection Instability Rolls. (After Brown, 1980)*

In Figure 4.6,  $V_o$  represents the wind vector in a lower level while  $V_i$  represents the wind vector in an upper level. Figure 4.6 (a) depicts a situation in which there is no directional shear, only speed shear. Under these circumstances, Brown maintains that horizontal rolls would tend to form perpendicular to the wind shear vector. This situation would result in Kelvin-Helmholtz waves if the density stratification were stable. Figure 4.6 (b) shows the situation if there is some turning in the wind with height as well as some increase in wind speed. If the wind shear vector is drawn from the tip of  $V_i$  to the tip of  $V_o$ , then it is obvious that the horizontal rolls are again perpendicular to the wind shear vector.

Figure 4.6 (c) depicts the situation when there is only directional shear. The wind shear vector is drawn as a dashed line and it is shown that the horizontal rolls are again perpendicular to the wind shear vector.

The second kind of instability to be considered in this work is the Thermal Instability (TI) mode. Kuettner (1971) studied the convective rolls which formed under unstable stratification (positive density profile) and which had a curvature in the wind profile on the order of  $10^{-5} \text{ m}^{-1}\text{s}^{-1}$ . He found that generally convective rolls formed along the “mean wind” of the convective layer. He argued that the curvature in the wind profile worked to suppress the perpendicular convective rolls. Figure 4.7 is a classic figure from the work of Kuettner (1971) which depict the important points of this argument.

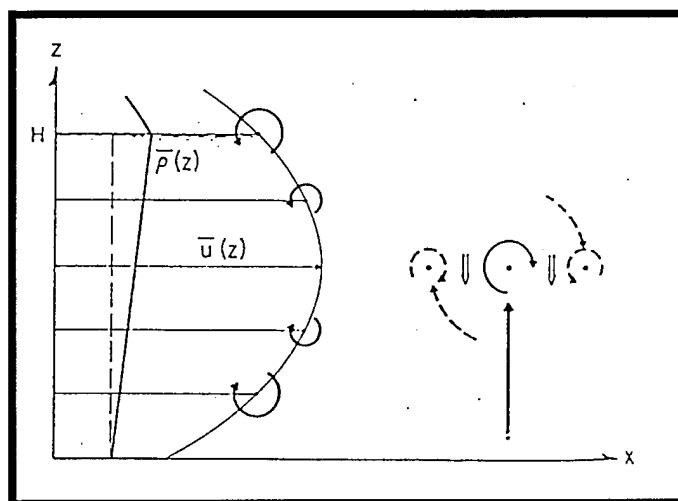


Figure 4.7. Kuettner's vorticity argument (After Kuettner, 1971)

Kuettner maintains that in a convective mixed layer, the winds are zero at the surface and increase quickly to a maximum at about halfway up through the layer. Therefore, the maximum vorticity is located near the surface. As convective thermals lift these vorticity maxima, the vortices find themselves in an environment in which their rotation tends to move lower vorticity parcels downward and higher vorticity parcels

upward. This results in a net downward acceleration which tends to "push" the vorticity maxima back to the original level. Note that if the vorticity maxima had been allowed to rise to the convective condensation level, then the cloud roll which formed would have been perpendicular to the mean wind. So the vorticity acts to preferentially suppress the perpendicular modes while allowing the parallel or longitudinal modes to grow. These cloud bands which form parallel to the mean wind in the boundary layer are essentially "Kuettner's Cloud Streets."

It should be noted however, that very seldom does the atmosphere support only one mode or the other. As noted by Brown (1980), the environmental flow often has an inflection point in the wind profile and there are often some atmospheric layers which are unstably stratified. Therefore, rolls which are observed are sometimes the result of a combination of mechanisms. Brown (1980) noted that when there is no shear at all, then convective activity is manifested in the form of Rayleigh-Bernard cells. In the convective boundary layer with only weak speed shear, rolls will tend to be longitudinal in nature. If there is an inflection point in the wind profile, which is often the case, then the rolls will form at some angle to the left of the mean wind. This angle has usually been observed to be between 0 and 20 degrees.

Since these features are frequently observed, it is no wonder that there have been numerous observational studies conducted. LeMone (1973) compared the results from a field experiment in which the structure and energetics of horizontal rolls were studied and compared to theory. The rolls were found to occur in moderately strong winds and since, in the PBL,  $Re > 500$ , it was concluded that the instability type was Inflection Point Instability. In general, LeMone's observations agreed with the theory as set forth by other researchers, with horizontal wavelengths and width-to-depth ratios falling within those predicted by Kuettner (1971). The roll axes tended to lie between 10 and 20 degrees to the left of the wind at the base of the inversion. LeMone notes that this is in support of

Brown's (1972) hypothesis which states that IPI rolls should be located at about 18 degrees left of the wind, under neutral stratification. Because of the evidence, LeMone concluded that these rolls were the result of the inflection point instability mechanism, caused by wind shear.

Christian and Wakimoto (1989) studied horizontal rolls in the atmosphere using powerful Doppler radars and compared their findings to those proposed by theory. All of their measurements were taken of horizontal convective rolls in the "clear air." Throughout the study, high pressure dominated the synoptic situation and was responsible for a deep stable layer. In general, they found that the boundary layer was well mixed by afternoon; the winds were strongest at the surface and decreased upward to the top of the boundary layer, where they were weakest. At the top of the inversion, the winds began to increase again. The average wind speed was found to be about  $4.4 \text{ ms}^{-1}$ ; while for most other studies, the winds in the lower levels were between 6 and  $20 \text{ ms}^{-1}$ . Radar showed the horizontal rolls as echo bands oriented in the direction of the mean boundary layer wind. The research team believed that the lower portions of the radar echoes were formed by particulates (Rayleigh scatter) and that the upper echoes were the result of refractive index fluctuations (Bragg scatter) (see Figure 2.3). They support this assumption by noting that the 5 cm radar used could not detect any echo aloft, while the 10 cm radar did. Radar theory suggests that the longer wavelength radar units are more suited to studying refractive index fluctuations (consider wind profilers). The cloud streets were aligned directly over the updraft/convergence zones as depicted on the radar. However, the clouds were only observed over the strongest low level echoes (greater than 8 dBZ). The clouds actually formed in the stable layer and it was deduced that they capped a boundary layer intrusion into that layer, as a result of the vertical velocities generated by the convective rolls. Note that the radar echoes do not represent clouds since clouds (with no precipitation) are difficult to detect using 10 cm radars.

Other researchers have studied horizontal rolls with an emphasis on how they affect deep convection. Wilson and Schreiber (1986) regularly observed horizontal rolls in the Colorado boundary layer. They noted that the features appeared as “long, thin lines of enhanced reflectivity that remain almost stationary for a few hours.” In agreement with Kuettner (1971) and LeMone (1973), they note that the features were generally oriented along the mean wind of the boundary layer. They frequently saw small cumulus clouds associated with the rolls but indicate they were seldom observed to initiate storms by themselves.

Wilson et al. (1992) studied the interaction of convective rolls with other boundary layer features. In agreement with the work of Christian and Wakimoto (1989) they found that the radar fine line reflectivity was due to a convergence of scatterers (insects) resulting from the helical circulation of the rolls (see Figure 2.3). They also observed that relatively strong areas of rotation (misocyclones) along a convergence boundary were often located at points at which the convergence boundary was intersected by horizontal convective rolls. It was suggested that the juxtaposition of the local convergence due to the convergence boundary and the updraft and deeper moisture due to the horizontal convective rolls resulted in favorable dynamics for the initiation of the misocyclone. In turn, these misocyclones were often the focus for strong thunderstorms and in one case, a weak tornado was induced.

Wakimoto and Atkins (1994) studied the relationship between horizontal rolls and the Florida sea breeze as they related to thunderstorm formation. They found that the along frontal variations in the (sea breeze) structure appeared to be controlled by the horizontal rolls, with the intersection regions being the preferred zones for deep convection. Even when the sea breeze gently merged with rolls which were oriented parallel to it, cloud development tended to occur only in those areas in which the two features met. For the purposes of this research, this would be a “merger.”

In North Carolina, we found in the WSR-88D imagery that horizontal rolls often appear around noon and they tend to persist until the late evening. They generally cover large areas of NC from the eastern Piedmont to the coast. This area, known as the Coastal Plain, is usually the most convectively active region in the state. Therefore, sea breezes and thunderstorm generated outflows often propagate into the region occupied by the rolls (see Figure 4.8).

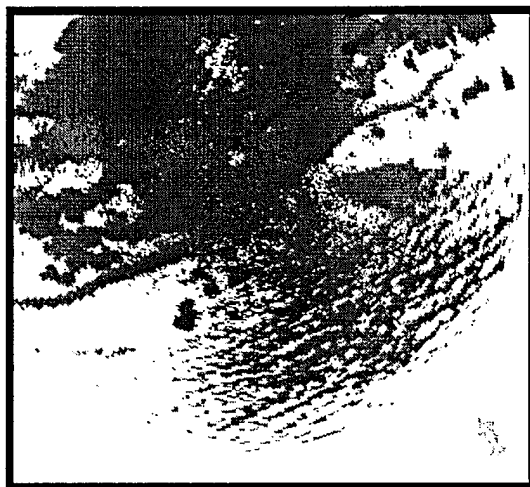


*Figure 4.8. Radar depiction (Spectrum Width) of a thunderstorm outflow moving into a horizontal convective roll field.*

We also found that horizontal rolls comprised approximately 8% of the 95 boundaries studied, and that the radar revealed these features 100% of the time (as did the satellite imagery). As expected, the surface data was of no help in identifying these small scale features. When considering the relative utility of the data acquisition platforms for detecting horizontal rolls, it should be noted that it is not necessary for clouds to be present in order for the rolls to be present. The existence of the clouds simply implies that the rolls have generated the appropriate amount of vertical velocity required for the parcels to reach their convective condensation level. The work of Christian and Wakimoto (1989) documented cases in which the Doppler radar revealed "clear air" rolls. In the study of

several of the cases in this research, the rolls located in close proximity to the radar were observed in Doppler reflectivity fields prior to the occurrence of condensation. Condensation occurred a short time later, making the features visible in the satellite imagery. It should also be noted that the preferred region of formation of horizontal convective rolls in North Carolina is approximately 60 miles (nearly 100 km) southeast of the radar. At this distance, the radar beam is above the lower level convergent zone (see Figure 2.3) and is apparently detecting the refractive index inhomogeneities due to the rising thermals, as noted by Christian and Wakimoto.

Horizontal rolls were involved in 10% of all of the collisions studied; they were not generally autoconvective. Only three of the cases (38%) produced 40 dBZ showers without interaction with some other feature. Even then, the showers produced were very small and dissipated quickly. There were five situations in which rolls interacted with other features, initiating new convection or increasing existing convection 80% of the time.

#### 4.1.4 Fronts and Prefrontal Troughs

There are various ways of “defining” a frontal boundary. At the most basic level, a front simply separates two different air masses. However, this simple definition in no way addresses the spectrum of intensities of different types of fronts at different times of the year. For example, some authors consider the wind shift line to be the frontal boundary while others search for the intense temperature gradient. Even these definitions are subject to scrutiny for wind shift lines often occur in advance of a front, as in the case of pre-frontal troughs (PFTs). Often the intense temperature gradient is not so intense and the primary difference between the air masses can be found in the moisture field.

The ambiguity involved in identifying frontal systems was addressed in recent work of Sanders and Doswell (1995). They had a “panel of experts” conduct synoptic scale analysis of a frontal system in the midwest. The result of the experiment was that there were significant disagreements in the placement of the boundaries. In essence, frontal (or boundary) placement is very subjective. The determination of whether a boundary is indeed a front is based on two conditions for this work. First, the feature must have temporal and spatial continuity on the synoptic scale. In other words, the National Weather Service must have been able to track the feature for more than one diurnal cycle and it must be large enough to be depicted on a synoptic surface analysis. The second condition which must be met is that it must have some upper level support and not be strictly a surface based feature. For example, surface features which have some (weak) jet support aloft or vorticity maxima associated with them will be considered to be “fronts.” Features which do not meet both the scale and upper level support criteria are called Thermal/Moisture Boundaries (TMBs) in this study and will be discussed in Section 4.1.5.

Doppler weather radar is well suited to detect cold fronts. Wilson and Schreiber (1986) found that frontal boundaries could be detected in all three Doppler radar fields. They described the fronts as “multiple parallel convergence lines.” Even those which are



not precipitating will usually be detectable in reflectivity, velocity, and spectrum width. Figure 4.9 is a frontal boundary located just to the west of the radome, as depicted by the Doppler velocity field. The front was producing precipitation in Virginia and West Virginia, but due to an influx of dry air, there was no precipitation in North Carolina. Even the black and white imagery shown here vividly shows the boundary.

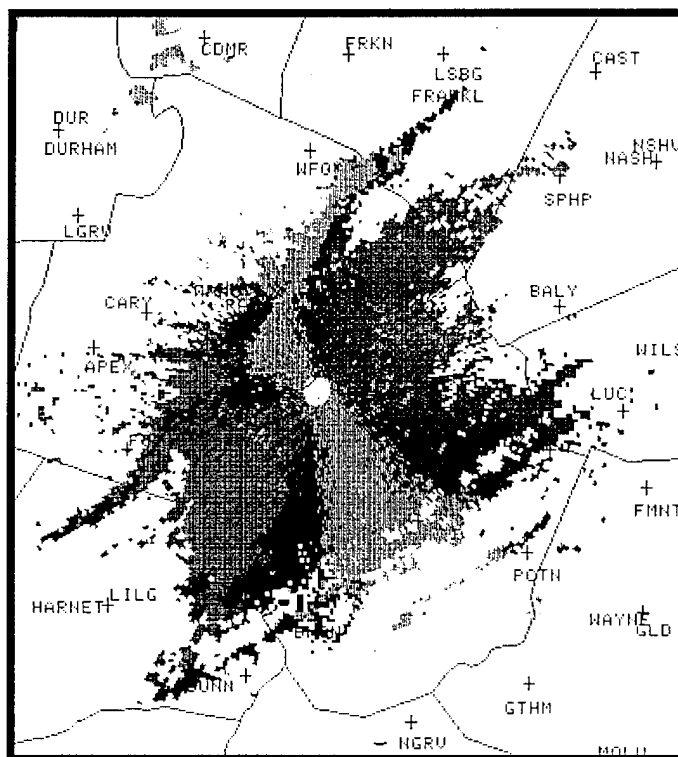


*Figure 4.9. Frontal boundary depicted in Doppler velocity. The boundary as seen here is not producing precipitation. Note horizontal rolls ahead of the front.*

Summertime frontal passages in North Carolina are typically very weak and the upper level forcing requirements necessary for inclusion in this study were seldom met. Even so, the extremely high convective available potential energy (CAPE) and the mesoscale interactions with terrain and other boundaries in North Carolina combine to

make the events very interesting. One of the appealing aspects of frontal passages in NC is that they are often associated with a prefrontal trough (PFT). The PFT is often responsible for the most significant portion of the weather. An examination of PFTs and the mechanisms which likely produce them will be discussed as each type of frontal situation is discussed below.

A typical summertime frontal passage scenario occurs as a north to south oriented frontal boundary enters the western portion of NC. If the air behind the front is truly cooler and more dense than the air in the interior of the state, the eastward progression is often retarded by the mountains (low Froude number flow). At times, the trough (and upper level support) associated with the surface front appears to "outrun" the air mass discontinuity and may propagate into the interior of the state. It is along this PFT that strong thunderstorms often develop during the summertime. By the time the cooler air reaches the interior of the state, the hot, subtropical air mass has been modified by rainfall and evaporational cooling to the point that there is very little difference between the two air masses and no further precipitation develops. However, if there is significant upper level support (significantly cooler air, vorticity, or divergence) associated with the surface feature, as the front moves over and around the mountains and into the surface trough, explosive regeneration may occur leading to locally severe weather.

The tracking of frontal boundaries as they move through the mountains is often a difficult proposition in NC. The advance of cold (cooler) dense air is usually retarded at the western side of the Appalachians. At some point in time, forecasters in NC observe a discontinuous "jump" in the frontal location, as it appears to cross the mountains.

This phenomenon was observed as mesoanalysis was conducted on one case in this study. The boundary was tracked using a surface (isotherm) that appeared to represent the leading edge of the cooler air. As expected, the forward movement of the boundary appeared to end at the western side of the mountains. However, it was noticed that during

the day, the temperatures significantly increased in the Piedmont and Coastal Plain, eventually forming a “pocket” of warm air in the region. The western edge of the “warm pocket” was characterized by a relatively tight temperature gradient on the *eastern* side of the mountains. If an analyst were not aware of the effects of the diurnal heating, he/she may be tempted to analyze the front on the eastern side of the mountains. This diurnal heating effect is believed to be at least partially responsible for the “discontinuous jump” often observed with frontal systems crossing the Appalachians. This was only observed in one case and as such, the process deserves significantly more study prior to conclusions being reached.

Another typical summertime frontal passage is actually an ambiguous event which may or not be called a “front.” An eastward moving extratropical cyclone, near the border of the United States and Canada, is often accompanied by a generally west to east oriented surface frontal feature. If the high pressure area behind the front is strong enough, the east-west boundary may move into the interior of the US and across the Virginia/North Carolina border. By this point, the feature is very weak, upper level dynamics are minimal at best, and the feature is rarely recognizable as a front at the point of its southernmost progression. The surface front is depicted on synoptic charts well to the north, possibly through West Virginia or Pennsylvania associated with the tightest thermal gradient and beneath the upper level support. However, there is often a weak but noticeable wind shift associated with the boundary much further to the south and some drier air is often brought southward. For the purposes of this study, this feature would be called a thermal/moisture boundary or TMB. It is mentioned here primarily to point out that the difference between a TMB and synoptic front may often appear to be one of degree, but the real criterion is whether any upper level dynamics can be found to support a frontal analysis. A case study will be presented later in this work which details just such an occurrence.

As mentioned earlier, PFTs are often responsible for a significant portion of the weather associated with fronts. They occur fairly regularly in North Carolina. For example, of the five frontal events studied, three of them had associated PFTs. Since the summertime situation is not very dynamic, there is some interest as to the mechanisms which act to produce PFTs. Unfortunately there is not a significant amount of literature devoted to this very important feature.

Bluestein (1993) indicates that the "trough associated with a frontal zone moves from a region where surface pressures are rising to a region where the surface pressures are falling." Therefore, any mechanism which may serve to lower surface pressures in advance of the front may work to induce a PFT. One method by which a PFT may form has been addressed above. The pressure trough and associated upper level dynamics "outrun" the cooler, denser air of the frontal boundary, which is held against the western side of the mountains. The upper level divergence serves to lower the surface pressure ahead of the feature. Another mechanism by which the PFT may form is the mountain lee trough. There has been a significant amount of work devoted to studying this particular feature; however, during this study, with no evident synoptic forcing, the upper level flow was generally approximately parallel to the mountains. Even during the few times that there was a weak westerly component to the winds, the entire flow field was generally of 5 kts or less. It is not believed that lee troughing was a significant contributor to the features observed during this study. This is not to say that the mountains play no part in the formation of PFTs. Actually, it is believed that there are several mechanisms which work in unison to produce them. One other possibility is that the intense heating which occurs in the NC Piedmont/Coastal Plain is partly responsible for the feature. It will be shown later that this interior region of NC is often responsible for producing a "Piedmont Trough," resulting from differential sensible heating.

In this study, a total five fronts and three PFTs were studied. All of the fronts were autoconvective. Of the five cases, three of the fronts were detectable in the satellite imagery. In one case, data was unavailable and in one case, the actual frontal boundary was obscured by thunderstorm debris produced by the PFT. Four of the five frontal boundaries were detectable in both radar imagery (reflectivity and velocity) and surface data. The radar did not detect one feature due to the distance at which it was studied and the surface data was unavailable for one case. It should be noted that these features in general were well resolved by all three data acquisition platforms. Again, even though data were missing from one platform or obscured on the other, the use of all three in a detailed mesoscale analysis unfailingly provided the information which forecasters required in order to produce their products.

Like the fronts, all of the PFTs were autoconvective. They were all visible in the radar imagery and in the surface data but one was not detectable in the satellite imagery. In this case, the feature was producing thunderstorms, but they were oriented so that a forecaster probably would not recognize they were being produced by the PFT.

Of the 51 collisions observed, fronts were involved in six and PFTs were involved in four. The frontal collisions resulted in intensification of existing convection or initiated new convection 83% of the time. The one situation in which convection was diminished is extremely interesting involves an "unknown moving" boundary. This case will be addressed in a case study later in this research. Of the four collisions in which PFTs were involved, convective activity was increased 100% of the time.

#### **4.1.5 Thermal/Moisture Boundaries (TMBs)**

There are numerous types of frontal boundaries and similar features which occur in North Carolina. Generally, the most studied are cold season phenomena whose origins can be traced to the existence of the warm Gulf Stream current to the east and the Appalachian Mountains to the west. In his study of the NC Coastal Front, Riordan (1990) examined the reintensification of a dissipating synoptic scale frontal boundary as it interacted with the warm waters of the Gulf Stream. Businger et al. (1991) studied the development and movement of the Piedmont Front and an associated severe weather event. Keeter et al. (1995) examined the contribution of North Carolina topography to the occurrence of both “wedge fronts” and thermal moisture boundaries.

Although the features described above are primarily cold season phenomena, there is no reason to expect that the Gulf Stream or the Appalachian Mountains play no role in the formation of mesoscale boundaries and circulation patterns in North Carolina in the summertime. Indeed, the new radar depicts several new or poorly understood features which can probably be associated with exactly the features studied above, with an associated decrease in upper level dynamics and an increase in moisture due to the summertime synoptic scale flow. For the purposes of this research, these features will be called thermal/moisture boundaries (TMBs) or, if no determination can be made as to the characteristics or origin of the feature, “Unknown Stationary” (US) boundaries. While the US boundaries will be discussed later, the TMB is the topic of this section.

The term thermal/moisture boundary is a descriptive name for the features. In summer, they are essentially discontinuities in the temperature and/or moisture fields, which may or may not be accompanied by a very weak wind shift, resulting in little or no detectable convergence at the surface. Obviously, this description could also apply to a front because a front is just a TMB...with upper level dynamics.

In North Carolina, TMBs originate in one of several ways. The most easily understood would be the example used in Section 4.1.4 in which a surface frontal boundary essentially "outruns" its upper level support. It tends to propagate southward and eastward as a density current primarily due to the horizontal pressure gradient force induced by the relatively high pressure behind and lowering pressures ahead due to differential heating (Koch et al, 1995). Features of this type are generally detectable in the surface data, sometimes in radar imagery, and rarely in satellite imagery until convection begins. Other ways in which TMBs may originate are associated with the Appalachian Mountain barrier and the "Cold Air Damming" and "Cold Air Pooling" as discussed by Hartfield (1995).

It is unfortunate that TMBs are difficult to detect in the radar and satellite data because they can be the focus for severe weather. In 1980, Maddox et al. conducted a study of tornadic thunderstorm interactions with thermal boundaries. The authors point out, in agreement with Purdom (1976), that shallow baroclinic zones, such as those produced by old thunderstorm outflows and dissipating frontal boundaries (implying no upper level support) are favored locations for severe storms. He notes that these are areas in which moisture convergence and vorticity are maximized. He found that within a hot, moist, unstable air mass, warm air advection and surface friction cause winds to veer and increase with height. In a cool, moist air mass, the cold (cool) air advection and surface friction combine to cause a wind profile which has a maximum speed near the surface and veers little or backs with height. The "spatial distribution of these wind profiles help maximize moisture, convergence, and vorticity into a narrow mixing zone" (Maddox et al., 1980) which is favorable for the development of severe thunderstorms.

Korotky (1990) documented the influence of a TMB in the formation of a severe tornado which traveled over 84 miles (including north Raleigh, NC) in a two hour period, killing four people, injuring 157, and leaving almost 1000 homeless. He noted that the

TMB was the result of the juxtaposition of rain-cooled air in western North Carolina with the more unstable air to the east. He maintains that the interaction of these surface features with strong middle and upper tropospheric dynamics was directly responsible for the tornadic event.

Vescio et al. (1993) studied another severe weather event in NC which occurred, in part, due to a TMB in the eastern part of the state. They note that "the eastern half of North Carolina is a favorable location for quasi-stationary thermal/moisture boundaries;" the features are often topographically induced; and the characteristics of each feature tend to vary significantly. Similar to the case studied by Korotky (1990), this TMB was actually a dissipating synoptic scale frontal boundary. High pressure was present over the mountains and foothills of NC which the authors indicate was maintained by cloudiness and rain. An outflow boundary which extended from Georgia, appeared to intersect the TMB in central North Carolina. They acknowledge that some clearing in the eastern part of the state allowed greater instability to build in that area. The current research will indicate that diurnal heating in the area known as the Coastal Plain (Figure 3.1) often results in a weak pressure trough which will hereafter be referred to as the Piedmont Trough (PT). This feature will be examined in detail in Section 4.1.7.

With the significant importance of TMBs firmly established, consideration can be placed on determining the types of TMBs which occur in NC, the specific features observed in the current research, and the convective activity associated with them. The TMBs discussed in the cases above were the result of old synoptic scale fronts and occurred in transitional weather periods in which there were some upper level dynamics present to the west. However, the boundaries themselves appeared to exist without the presence of upper level support, indicating that they were surface based phenomena.

There were a total of four TMBs observed during this study; the most interesting of these is studied in detail in Section 5.1. In general, these features are fairly difficult to



locate using any of the three data acquisition platforms, especially in the coarse surface data. The satellite detected all four of them after the initial convection began. The radar detected three of the four boundaries. Only two of the features were readily identifiable in the conventional surface data (pressure, temperature, dewpoint). As the features were investigated, it was found that air parcels on either side were only different by a degree or two in the temperature and dewpoint fields. As such, they were generally undetectable when conducting a standard temperature or dewpoint analysis. However, by utilizing the surface  $\theta_e$  field, which combines the small differences in both temperature and dewpoint, much more information could be extracted from the coarse surface data set.

As previously mentioned, all of the TMBs encountered were convectively active. They were all autoconvective and although they comprised only about 4% of the total number of boundaries observed, they were involved in 25% of all of the boundary interactions observed. In each of these interactions, new convection was initiated or existing convection increased in intensity.

#### **4.1.6 Boundaries of Unknown Origin and Nonclassical Mesoscale Circulations (NCMCs)**

When this research was initiated, it was known that there would be some circumstances under which we would not be able to identify some of the features which we could detect. This was expected due to the spatial and temporal coarseness of the surface data set at our disposal. Even with PROFS and PAMS mesonets, two Doppler radars and half hourly GOES 7 data, Wilson and Schreiber (1986) could not identify all of the boundaries in their study. In fact, they found that 46% percent of all of their boundaries were "Unknown Stationary" or "Unknown Moving." If the mesonets at their disposal, with resolutions of 25 and 8 km respectively, could not resolve the features they encountered, then it would be unrealistic to believe that our 150 to 200 km station spacing could resolve all of our features.

There is currently a significant amount of attention being given to understanding the microphysics of the planetary boundary layer and the forcings which result from surface heterogeneities and differential heating. It is believed that the Unknown Stationary (US) boundaries as well as some of the better understood features encountered in this research are the result of these "Nonclassical Mesoscale Circulations." Numerous authors agree that NCMCs are capable of producing boundaries and have conducted numerical and observational studies which support their views.

McCumber and Pielke (1981) found that soil moisture was the most important surface parameter which must be modeled. Their study of moist soil, which was allowed to dry, showed that the thermal conductivity could vary several orders of magnitude from wet soil to dry soil. They note that higher moisture content results in the use of some of the incoming solar radiation to evaporate the moisture. This energy is expended in latent heating, leaving less energy available to heat the soil (sensible heating). They also found

that the total energy flux in dry soil was about three times that in moist soil and concluded that soil moisture was the most important parameter by a large margin.

Zhang and Anthes (1982) conducted sensitivity studies to determine the relative sensitivity of the planetary boundary layer to different surface variables. They specifically studied soil thermal capacity, albedo, roughness length, and moisture availability. Their findings indicate that the most important factors, in order of most important to least important were: moisture availability, roughness length, albedo, and thermal capacity. They found that the PBL was only sensitive to changes in roughness length of an order of magnitude or more. When they decreased the albedo in their model runs, more incoming radiation was absorbed, which increased ground temperature as expected. But this increase was not as dramatic as the temperature increase found to result from low moisture availability.

Ookouchi et al. (1984) indicated that circulations induced by moisture discontinuities were strong enough to play an important part in the local cumulus convection and air quality. For example, they found that the intensity of a sea breeze tended to decrease as soil moisture increased. Their experiments revealed that NCMCs had many characteristics in common with sea breezes. For example, the equations presented for sea breeze intensity as it relates to the temperature differential appeared to be applicable to NCMCs as well. Also like sea breezes, they noted that the flow due to NCMCs tended to respond to Coriolis forcing. After a sufficient amount of time, flow from the east is converted to flow from the south by the Coriolis force. At some point, westward flow ceases and a low level wind maximum flowing from south to north remained. The researchers also observed the "decoupling" of the flow in the late evening and an increase in horizontal velocity of the flow, just as observed in sea breeze circulations.

The work of Ookouchi et al. (1984) makes one marvel at the intricate natural feedback mechanism of the sea breeze and inland sea breeze mechanisms. On the hottest,

driest of days, when there is a deficit of surface moisture, the Bowen ratio is very large (large sensible heat flux compared to latent heat flux) and the sea breeze is relatively stronger and more likely to penetrate greater distances inland, producing showers as it moves. On days when there is ample soil moisture or clouds, resulting in locally cooler temperatures, the Bowen ratio is much smaller, the resulting sea breeze will be relatively weaker, penetrate less far inland, and produce fewer showers.

Segal et al. (1986) also studied NCMCs but their emphasis was on those circulations which originated due to differential cloud cover. Under control conditions consisting of moist soil and a weak capping inversion, differential cloud cover was introduced into a numerical model. They found that the resulting soil temperature could vary as much as 7°C. When this temperature difference is used in the graph shown as Figure 4.5, the resulting circulation would be expected to attain a speed of approximately 4 ms<sup>-1</sup>.

In another modeling study, Benjamin and Carlson (1986) found that lee troughs deepened by four to five millibars when diurnal surface heating was added to model runs. They note that this is observed in nature along the southern California coast where the diurnal heating routinely produces a heat low. This particular mechanism may also be at work along the Atlantic Coastal Plain; it will be discussed in some detail in Section 4.1.7 of this study.

Koch et al. (1995) studied the effects of cloud cover on frontogenesis, vertical velocity, and frontal structure. They found that differential heating across the frontal boundary significantly increased the intensity of the front, deepened the PBL ahead of the boundary, and produced a deep frontal updraft. They note that the same mechanism is relevant to *any kind* of boundary across which there are differences in cloud cover.

Mahfouf and Mascart (1987) went beyond “moisture availability” and considered soil texture in their model. They maintain that it should be considered because moisture availability and plant uptake of the moisture is actually a function of the soil texture. Specifically, they studied the NCMC initiated between zones comprised of sand and clay. They found that if the model was initiated with equal moisture distribution over both zones, there were extremely high latent heat fluxes observed over the sand as compared to clay. Figure 4.10 depicts the latent and sensible heating observed in their model.

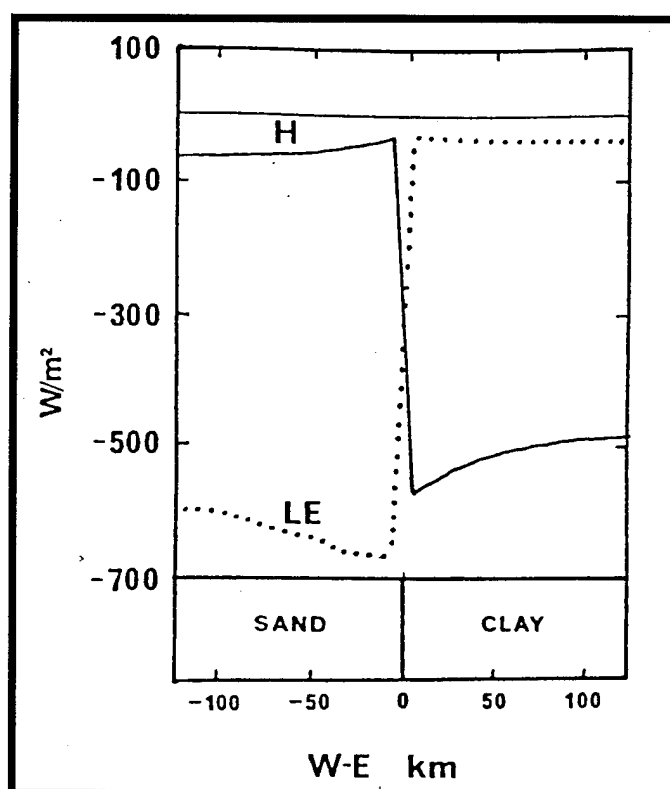


Figure 4.10. Model results from Mahfouf and Mascart (1987). Negative numbers indicate positive flux.

They maintain that this is a direct result of the sand having a higher level of “moisture availability” than does the clay. They note that the primary difference between clay and sand is the “granulometry.” Sand grains are generally from 2mm to 50  $\mu\text{m}$  in size while

clay grains are less than 2  $\mu\text{m}$ . This results in much higher hydraulic conductivity for sand than for clay. As shown in Table 4.1, the hydraulic conductivity for sand is two orders of magnitude greater than for clay.

*Table 4.1. NC Soil characteristics. Extracted from Mahfouf et al. (1987) and McCumber and Pielke (1981).*

Soil Type	Porosity ( $\eta_s$ )	Hydraulic Conductivity ( $K\eta_s$ ) ( $\times 10^{-6} \text{ m s}^{-1}$ )	Dry Volumetric Heat Capacity ( $\times 10^6 \text{ Jm}^{-3}\text{K}^{-1}$ )
Sand	.395	176	1.463
Loamy Sand	.410	156	1.404
Loam	.451	7.0	1.212
Sandy Clay	.426	2.2	N/A
Clay	.482	1.3	1.089

Due to higher permeability, the moisture in the sand is released much more readily. Mahfouf et al. (1987) note that the resulting differences in the sensible heat flux are capable of producing thermally direct, mesoscale circulations with speeds greater than  $8 \text{ ms}^{-1}$  and upward vertical velocities greater than  $15 \text{ cm s}^{-1}$  over the clay soils.

This study is of extreme interest to local meteorologists because the modeled scenario is naturally occurring in central and eastern North Carolina. As discussed in the section on NC Geology, the Piedmont is composed primarily of clays and the Coastal Plain is composed primarily of sand, sandy loam, and some sandy clay. The characteristics for each of these soils is shown in Table 4.1. If central and eastern NC were to receive approximately equal amounts of rainfall and cloud cover, then according to the modeling studies of Mahfouf et al. (1987), there would be significantly more latent heating occurring in the Coastal Plain than the Piedmont. This would result in surface temperatures which were slightly higher in the Piedmont than in the Coastal Plain. McCumber and Pielke (1981) found that sand quickly released its moisture load to evaporation due to its high level of hydraulic conductivity. Once the surface moisture had been depleted, "...the attendant reduction in latent heat flux was accompanied by a stronger sensible heat flux that

promoted deeper turbulent transfer in the atmosphere.” It is believed that once the moisture in the Coastal Plain has evaporated, the temperature differential would reverse and the Coastal Plain would have a higher sensible heat flux since the Piedmont still retained some of the moisture. Although nature is rarely as perfect as computer simulations, Figure 4.11 is a satellite image showing what is believed to be evidence of differential heating due to geological and vegetation differences between the Piedmont and the Coastal Plain. The geological feature known as Coat’s Scarp, which divides the region is approximately defined in the cloud patterns and is approximately located between the two arrows.

Segal and Avissar (1988) agree with the foregoing authors in their contention that “common daytime circulations such as sea breezes...are directly related, in their intensities, to the magnitude and the horizontal distribution of the surface sensible heat fluxes.” They quote authors from different parts of the world who regularly observe differences of 1-4 °C between irrigated crops and dry, bare ground. The magnitude of these differences are significant for two reasons. First, Wilson and Meuller (1993) found that temperature differences on the order of 2-3 °C were often responsible for the initiation of convection. By using the equations of Ookouchi et al (1984) and Figure 4.5, a horizontal wind of 2 to 3  $\text{ms}^{-1}$  would be expected to result from those temperature differences.

Pielke et al. (1993) maintain that *any* surface heterogeneity that “results in spatial variations in sensible heat flux can generate mesoscale circulations.” They used GOES satellite imagery to map albedo for a region of the midwest which had diverse topography. The differences in the albedo were due to soil and rock variability, and to other variables such as vegetation cover. When the temperatures derived from the albedo differences were



*Figure 4.11. GOES visible imagery for 1701Z, 16 July 1994. This image depicts the differences in the cumulus cloud field between the Piedmont and the Coastal Plain. The geological change between the two regions occurs approximately between the two arrows.*



input into their model, they found that circulations of  $5\text{-}10\text{ ms}^{-1}$  were produced. They note that “the mesoscale albedo variations are an important contribution to surface fluxes of heat and moisture, and to the development of thermally forced mesoscale circulations, particularly during the summer.”

These findings may seem to contradict those of Zhang and Anthes (1982) in which it was determined that albedo had very little affect on surface fluxes. It appears that this may true when there is moisture available, but when moisture is not considered to be a variable, then the findings of Pielke et al. (1993) would appear to be applicable.

Out of a total of 95 boundaries, there were 21 (22%) which could not be identified with some degree of certainty. There were 16 (17%) which were classified as “Unknown Stationary (US)” and 5 (5%) which were classified as “Unknown Moving (UM)”. It became obvious near the end of the data collection period, that some of the US features were occurring in approximately the same location with a high degree of frequency. When the data was tabulated, it was found that of the 16 US boundaries on which data was collected, 13 of them were located in roughly the same area and had approximately the same characteristics. Since this comprised a significant portion of the data base (about 14%) it was felt that the boundaries should be grouped together into one category and studied as a whole. As previously mentioned, these features will be referred to as Piedmont Troughs (PTs) and will be discussed in Section 4.1.7.

#### **4.1.6.1 Unknown Stationary (US) Boundaries**

With the exclusion of the PTs, only 3 boundaries remain in the “Unknown Stationary” category; each of them will be examined separately. Figure 4.12 shows each of the US boundaries. Due to the subtle nature of these features, a radar image is not used here.

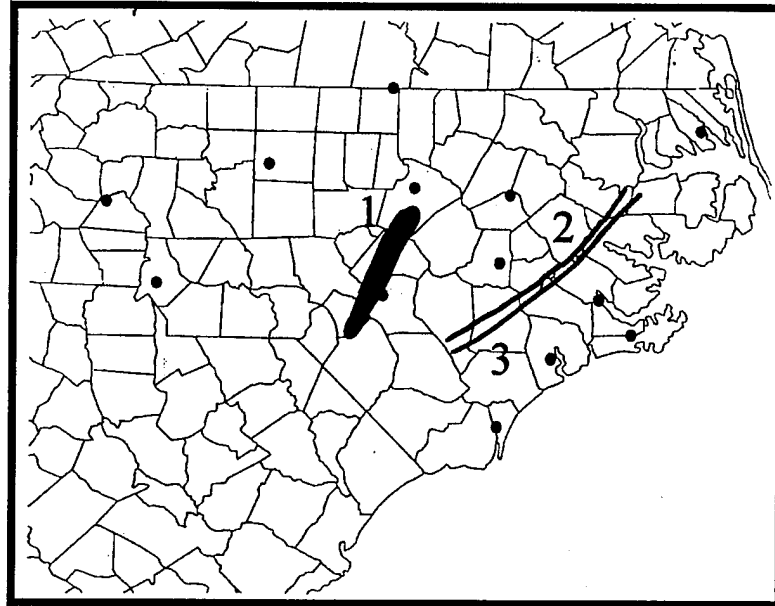


*Figure 4.12. Location of Unknown Stationary Boundary occurrences.  
Dots illustrate locations of surface reporting sites.*

Boundary #1 was detected on radar on 12 August, located just a few miles west of the radar site and south of RDU. The feature was very broad (about 7 nm wide) with a reflectivity of about 15 dBZ. It was detectable in the radar reflectivity field from about 15 nm to a distance of about 60 nm. This implies that the feature ranged in depth from about 1500 feet to at least 6100 ft. The boundary was not visible in satellite or surface data, it was not autoconvective and no difference could be detected in the temperature or moisture fields on either side of the feature. Dots in Figure 4.12 indicate locations of reporting stations.

The other two features in this category can be discussed together since it is felt that they are essentially the same type of feature. One was present on 15 Jul 94 and the other was present in about the same location on 16 Jul 94, under similar synoptic flows. These are boundaries numbers 2 and 3 in Figure 4.12.

These features initially appear to be sea breezes, however, they were detected by radar early in the morning prior to the initiation of the sea breeze. They were stationary

throughout the time that they are visible in the imagery. They both are visible in the satellite imagery but not in the surface data. It is felt that these features may be zones of very weak convergence due to both horizontal roll convection and enhanced by differential heating. The area to the east of the boundaries is known as the "Tidewater Area" and is composed of very moist soils, wetlands, swamps, and the intercoastal waterway of NC. West of the features is the Coastal Plain, which has been discussed previously as it pertains to NCMCs. This zone would be a preferred region for enhanced convergence due to differential heating.

The 15 July boundary was not autoconvective, and it did not interact with any other boundaries. However, the 16 July boundary was autoconvective. It also was involved in a merger with an inland propagating sea breeze later in the day, resulting in deep convection at the point of the merger. This feature is further discussed in detail in a case study included in Section 5.1 of this work.

#### **4.1.6.2 Unknown Moving (UM) Boundaries**

As with the US boundaries, there were only a few UM boundaries, the most interesting of which will be presented in Section 5.2. Out of the 95 features included in this study, only 5 (5%) were categorized as "Unknown Moving." This is compared to the Wilson and Schreiber (1986) study in which they found that 44 (27%) of their features were categorized as UM. As a whole, the features were not very convectively active. Only 1 feature was autoconvective. There were only two occasions in which UM boundaries interacted with other features. In one, the convection was actually decreased. This interesting boundary that approached the radar site from the coastal area was associated with very dry air. It was the only feature in the study which actually decreased convection when it interacted with other boundaries. This very interesting feature will be studied in depth in Section 5.2. The other interaction resulted in an increase of convection.

Of the four remaining boundaries, two appear to be trapped gravity waves which were not resolved at the surface. One of the remaining features appeared to be a dry "surge" behind a synoptic scale front. The radar depicted a very broad area of slightly increased reflectivity moving quickly to the south. The feature was not visible in satellite imagery until later in the day when the convective temperature was reached. At that time, the front edge of the boundary, by then located well to the south of the radar, was clearly outlined in fair weather cumulus. It is believed that relatively higher reflectivity detected by the radar was due to Bragg scatter resulting from instability associated with the cooler, drier air above the surface layer which was quickly warming due to solar insolation. There were large gaps in the temporal continuity of the surface data on this day and as a result, we were unable to unequivocally explain the feature. The remaining feature appears to be a thunderstorm outflow moving inland from the eastern coast, initiating thunderstorms as it moved. However, due to data acquisition problems encountered with the radar during this event, this feature too was impossible to positively identify. The satellite imagery was not helpful in this case because the event occurred at night and the IR resolution is very coarse.

#### 4.1.7 Piedmont Troughs (PTs)

As previously discussed all of the PTs were initially categorized as US. In general, they were very convectively active features which occurred during a significant portion of the days which were studied (13 days out of 23). Since they only readily show up in a 1 millibar surface pressure analysis, they were not detected (explained) until detailed analysis of each of the cases was undertaken. Once the features were identified, they accounted for a significant amount of convection which was previously unaccounted for. Figure 4.13 depicts the location and orientation of each of the surface features.

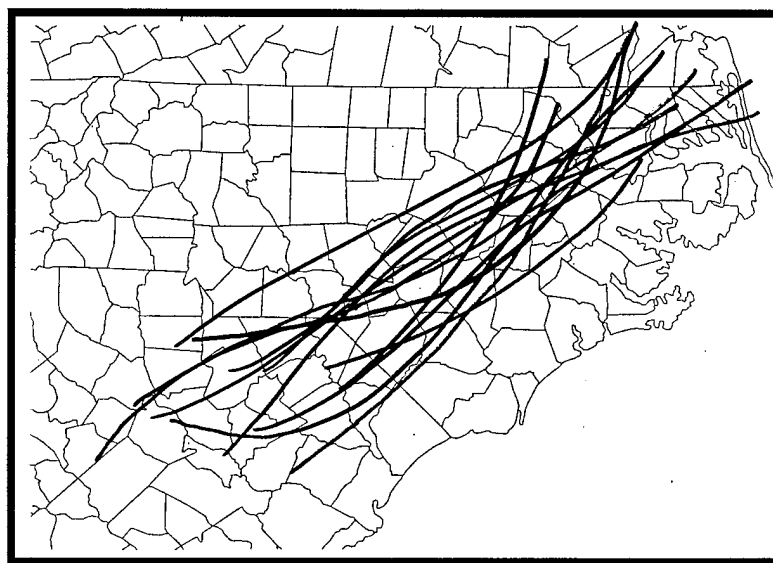


*Figure 4.13. Location and orientation of Piedmont Troughs. Each line represents the axis of lower pressure.*

Each of the thirteen convergence zones identified are drawn on Figure 4.13 with each dark line representing the approximate axis of the trough. It is evident that the features tend to align approximately across the zone in which the Piedmont joins the Coastal Plain.

The most pressing question concerning the PT involves the origin of the feature. After studying each case numerous times, it is believed that the feature originates in situ. It

appears to be a pressure trough which results from the intense heating of the Coastal Plain and eastern Piedmont. When one considers the frequency with which sea breezes are observed along the NC coast, then one would intuitively expect that just such a feature as this (heat low phenomenon) would exist. After all, the sea breeze is driven by density variations resulting from differential heating. If there were not enough differential heating to result in reduced density at the surface in the Coastal Plain, then we would not observe the sea breeze with the frequency which we have.

Several authors whose work has been previously discussed, found results that would support this hypothesis. For instance, the work McCumber and Pielke (1981) and Mahfouf et al. (1987) leads one to speculate that increased sensible heating may occur in the Coastal Plain region, due in part to the difference in soil types found in the Piedmont and the CP. Benjamin and Carlson (1986) studied the effects of surface heating and topography on regional severe storms. He found that lee side troughs tended to deepen by 1 to 3 mb when the effects of diurnal heating were introduced into the model.

There are numerous different types of pressure troughs which occur in the NC summertime boundary layer, including lee troughs and prefrontal troughs. However, in this study, a feature was only identified as a PT if it displayed a notable deepening due to what was believed to be diurnal heating, like a heat low. If there were other obvious mechanisms present which could account for the feature, then it was not considered to be a PT.

Although there were no boundaries identified as lee troughs in this study, primarily due to the poor vertical resolution of the data, it is possible that some trough features in this study were at least partially the result of weak lee troughing. In most of the cases encountered in this study, the winds had only a very weak westerly component, if any. Due to the Bermuda High, low and middle level flows were usually very weak and approximately parallel to the Appalachian Mountains. During the few events in which

fronts propagated into the study area, winds aloft were often significant, and troughs identified were considered to be prefrontal and not "lee side." In actuality, it is probably impossible to differentiate between the two under these conditions, given the coarse data we have at our disposal.

The Piedmont Troughs were extremely active and played a significant role in the diurnal convection cycle in the coastal plain region. For instance, every one of the features was autoconvective. They were involved in a total of 20 interactions with other boundaries, which resulted in increased convection 100% of the time. Therefore, the feature is of significant interest to forecasters and researchers alike.

The radar only detected PTs 42% of the time. These were instances in which the features were well established and convergence was especially strong or when the line was producing convection (dry or moist) that the radar could detect via the Bragg scatter mechanism. The satellite imagery depicted the feature 67% of the time. There were no cases in which both the radar and the satellite were unable to provide some information on the features. The PT is one feature in which a detailed mesoanalysis of the surface charts was most helpful. The surface charts revealed the weak trough 100% of the time. It should be noted that a standard pressure analysis was accomplished using 1 mb isopleths. This feature was not usually detectable in a regional, 4 mb surface analysis.

In summary, the PT is an interesting feature for several reasons. First, it was not something which we expected to find. However, sea breeze theory and modeling studies by the quoted authors tend to support that the feature is probably very real and probably exists far more often than our coarse data set can resolve. What is also interesting about the PT is that it is a very subtle feature which can easily be overlooked by forecasters not sensitive to mesoscale processes. The fact that this hard-to-detect feature is a prolific producer of thunderstorms makes it a primary concern when nowcasting thunderstorms. Whether the boundary is a result of lee troughing or diurnal heating, or a combination of

both is really not at issue at this point. What is important is to recognize that the features are important mechanisms which initiate thunderstorms in our area and that they are very difficult to detect in radar and satellite imagery.



## 4.2 A General Review of Boundary Statistics

This section will compare the statistics obtained in this study to those obtained in the study of Wilson and Schreiber (1986). The topics of boundary interactions, convective activity, and data acquisition platforms will be discussed as well.

Figure 4.14 is a detailed look at all ten categories of boundaries which were included in this study.

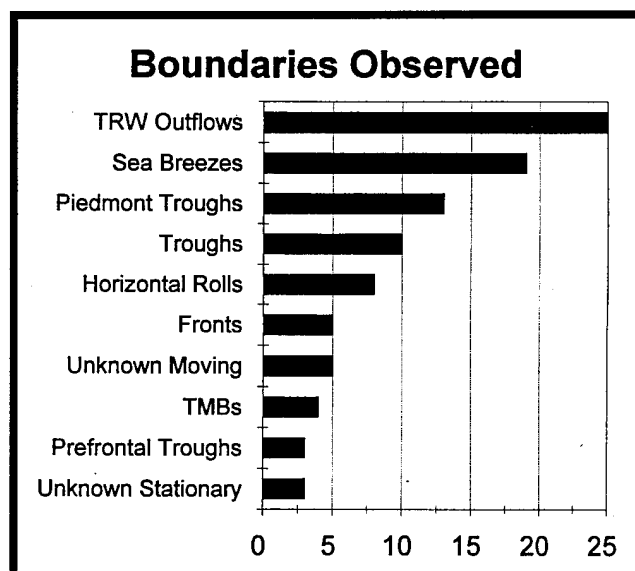


*Figure 4.14. Total number of observed boundaries. Chart indicates absolute number of boundaries observed in each of the ten categories observed.*

As previously discussed, the largest category was thunderstorm outflows. The next largest was sea breezes, followed by Piedmont Troughs (PT)s. Because of the relatively small numbers of individual boundaries in some categories, several will be merged into combined categories in order to make the results statistically more meaningful. For instance, the unknown boundaries (both moving and stationary) will be placed in a category called "Unknown." Troughs and Prefrontal Troughs will be placed in a category labeled

"Troughs" and Fronts and Thermal/Moisture Boundaries will be placed in a category called "TMBs." Due to the relatively high number of Piedmont Troughs observed, and in order to facilitate the study of this category, these features will not be combined with the other troughs. It is felt that the above combinations are valid due to the physical characteristics of the boundaries in each category. Figure 4.15 is the same as Figure 4.14, except it exhibits the boundary combinations discussed above. In order that one can determine the relative importance of each category, Figure 4.16 provides the same information in terms of the percentage of the total number of boundaries.

One of the primary goals of this study was to compare our results to those obtained in the work of Wilson and Schreiber (1986), hereafter referred to as WS, who conducted a study in Colorado to determine the "importance of radar-observed boundary layer convergence lines in initiating convective storms over the Colorado plains." Both studies use Doppler radar to interrogate warm season features, attempt to determine the relative importance of the observed features in their respective PBLs, and study boundary movement and convective activity, as well as boundary interactions.

Even though the studies are similar, the differences are significant. The most basic differences lie in the geology, topography, and climatology of the two states. For example, both regions have mountains to the west, yet the climate is significantly different. In general, there is little moisture in CO and there is abundant moisture in NC due to the Atlantic Ocean to the east. These differences and others too numerous to mention act to produce different features in the two regions. Even when similar features are encountered in both locations, the way they interact with other boundaries is modified by the local environments in such a way that the overall convective patterns are significantly different.

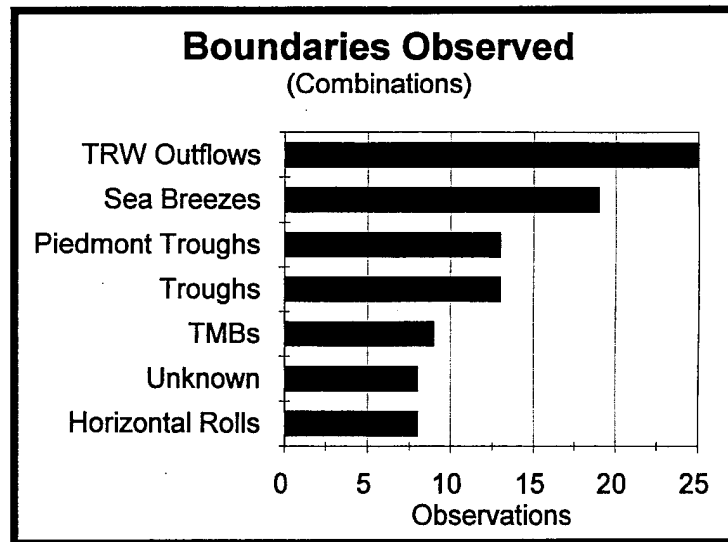


Figure 4.15. Boundaries observed in combined categories (absolute numbers)

Other significant differences in the two studies involve the resources available as well as the basic definitions of features. The WS researchers had access to significantly more resources than were available in the current study. For instance, they had two mesonets, two radars, and chase cars. There were also differences in how the studies defined new convection and boundaries. WS defined a new “cell” as an echo greater than or equal 30 dBZ. The current research began using this same base line, but it quickly became impractical to track the large number of 30+ dBZ cells observed in the NC PBL. The criteria was therefore raised to 40 dBZ. The fact that this change was required is significant, and will be discussed in detail below. WS required that a boundary be greater than 10 km long and limited their study area to between 40 and 50 km. We did not impose any of these restrictions for reasons discussed in Section 3.3.

WS found a total of 166 different boundaries which were divided into six different categories. Their results are summarized in Table 2.2. This is compared to a total of 95 boundaries observed in the current study, divided into 10 separate categories and 7 combined categories. In order that the two studies can be compared, several of the

categories in the WS study must be combined. Gust Fronts and Mountain Outflows are both related to thunderstorm outflows and will therefore be labeled as such. Their unknown moving and stationary boundaries will be combined into an “Unknown” category just as in the current work. Figure 4.17 shows the results of these combinations.

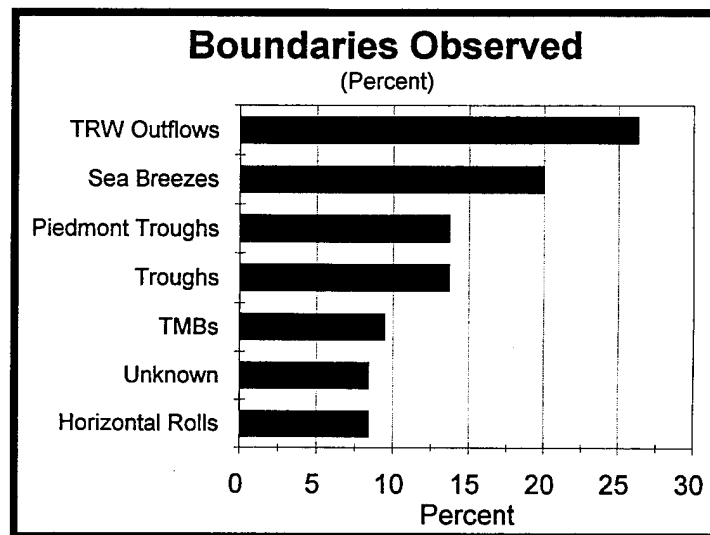


Figure 4.16. Boundaries observed in combined categories of current research (percent).

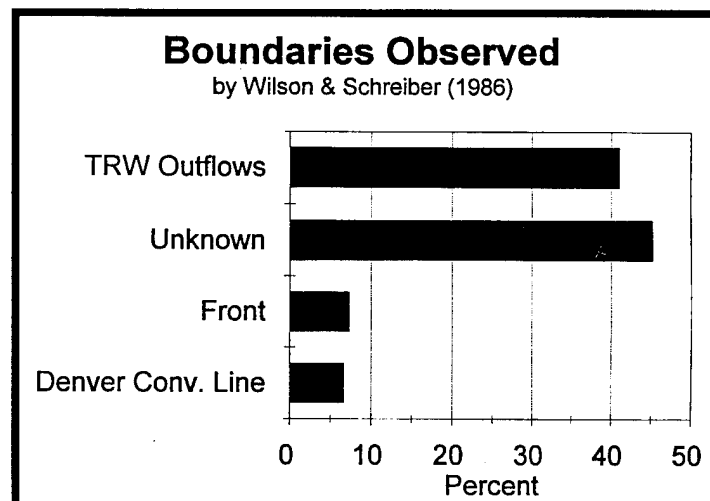


Figure 4.17. Percentage of boundaries in each category (Wilson and Schreiber, 1986)

When the graphs depicting each type of boundary as a percentage of the whole, for each study are considered, there are some interesting similarities and differences. For example, the striking number of unknown boundaries obtained in the WS study is obvious. It is felt that the WS work was primarily a thunderstorm study, since they studied only those days in which they believed there would be deep convection. In contrast, this study was event based; any significant feature observed was studied. It was our desire to present a representative depiction of the summertime PBL in NC. As a result, a significant amount of emphasis was placed on determining the origin of boundaries in this study. This accounts for our relatively low number of "Unknown" boundaries. Also of note is that WS did not consider Horizontal Rolls in their study because they were not often observed to contribute to deep convection in Colorado. As the current study was loosely modeled on their work, we too originally planned to neglect these features, but unlike the results obtained in Colorado, it was found that Horizontal Rolls were very important features in the NC PBL. They were therefore included in the study so that interactions with other boundaries could be examined.

With the exception of the "Unknown" boundaries in the WS study, TRW Outflows dominated both works. This was not a surprise for two reasons. First, as discussed above, WS conducted research only on days in which thunderstorms were expected. Secondly, the importance of TRW outflows in the southeast US has been well documented by Purdom and Marcus (1982). They comprised a total of 41 percent of the WS work and 26 percent of the current research. There is no doubt that if the current research had made use of data collected only on days in which thunderstorms were expected, then these numbers would have been very similar.

As would be anticipated in warm season studies, fronts comprised a relatively small portion of the total number of boundaries. In NC, fronts comprised 5% (does not reflect combination with TMBs) of the total while in Colorado, they comprised 7%.

Both studies included boundaries, whose origins can be traced to topography. The Denver Convergence Line (DCL) (see Section 2.1.1) comprised a total of 7% of the total boundaries and sea breezes comprised approximately 20% of the boundaries observed in NC. Of course mountain outflows are arguably topographically generated boundaries also, and an unknown fraction of our outflow boundaries were ultimately orogenic.

It is interesting to consider the percentage of boundaries in the different categories that in each study initiate storms. Therefore, a graph which combines both studies and like categories is presented as Figure 4.18.

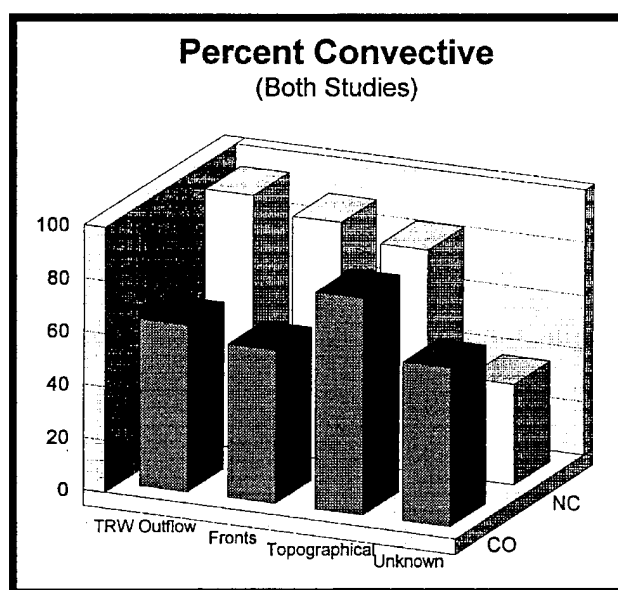


*Figure 4.18. Comparison of convective activity in Colorado and NC.*

The graph shows that thunderstorm outflows and fronts are much more likely to produce convection in NC than in Colorado. The category labeled “Topographical” includes the Sea Breezes of NC and the DCL of Colorado. Topographically induced boundaries in both locations are about equally likely to produce convection. WS found that “Unknown”

boundaries produced convection about 60% of the time, while in NC they produce convection about 38% of the time.

The differences in the numbers of the "Unknown" boundaries will not be considered further. Their unknown origin makes speculation illogical. However, the differences in TRW outflows and fronts can be readily discussed. It is felt that the significantly higher numbers occurring in NC are the result of the increased moisture in the PBL and higher levels of CAPE. Although knowledge of the Colorado climatology is admittedly limited, it is known that often there is an elevated layer of warm, dry air which serves to cap the mixed layer. North Carolina generally has no such cap in the summertime. CAPE values regularly are over  $2000 \text{ J kg}^{-1}$  and there usually is no negative area at all. Therefore, convective plumes and thermals are not hindered as they reach their LCL and LFC. This is the reason that in this study, it was necessary to use a 40 dBZ cutoff instead of the 30 dBZ minimum used by WS. In NC, 30 dBZ showers are often too numerous and too short lived to count, especially in the vicinity of a sea breeze.

One area in which WS placed significant emphasis was on the interactions between boundaries. They divided the different types of boundary interactions into three categories: Intersections, Mergers, and Collisions. The definitions of these categories were previously discussed in Section 2.21 and a graphical depiction of each is included as Figure 2.4. They divided the results of the boundary interactions into three categories: New, Intensified, and None. "New" indicates that totally new convection developed as a result of the interaction. "Intensified" means that preexisting cells grew stronger or expanded, and "None" means that no new convection occurred as a result of the interaction. The results of boundary interactions in the current research were divided into slightly different categories: Intensified, No Change, and Decreased. This was necessary because there was one case in which an interaction between two boundaries decreased the convective activity. As we

compare our results to those of WS, we must combine their “New” and “Intensified” into one category called “Intensified.” This can then be compared to our “Intensified” category.

Figure 4.19 is a graph showing the results of different boundary interactions for the current research only. Note that the absolute numbers are depicted. The obvious point made by the figure is that the number of interactions which *do not* result in increased convection in this area is very small. Overall, 94% of the total number of boundary interactions in NC resulted in increased convection.

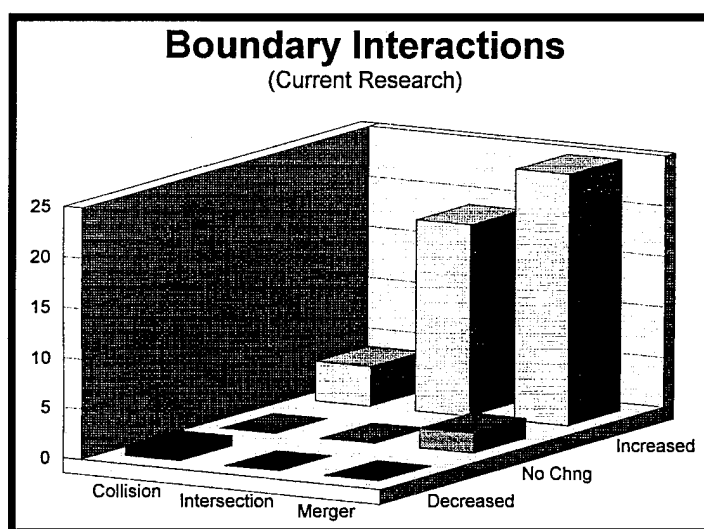
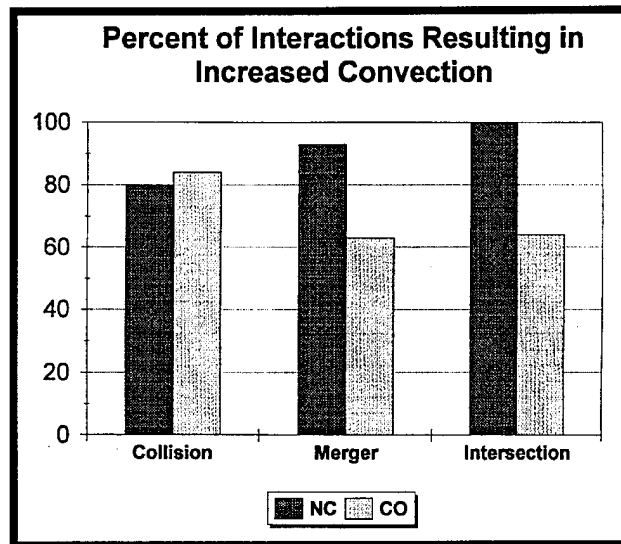


Figure 4.19. Results of boundary interactions (current study).

Figure 4.20 is a representation of the percentage of the different types of boundary interactions which resulted in increased convection in both studies. As expected, in North Carolina, boundaries are significantly more likely to increase in convection when they interact with other features. It should be mentioned that these results were based on a total of 49 boundary interactions in the WS study and on 51 boundary interactions in the current





*Figure 4.20. Comparison of boundary interactions of both studies*

study. This is important considering that the WS study was based on a total of 166 boundaries and the current work was based on a total of 95 boundaries. That means that the ratio of total boundaries to interactions was about 1.9 in NC and about 3.4 in Colorado. This could be taken to mean that for every collision, merger or intersection in the WS case, there were two in the current work. Another perspective on this statistic is that a boundary in NC would be about two times more likely to be involved in an interaction with another boundary than would a feature in Colorado. This is not totally unexpected however. Purdom and Marcus (1982) pointed out the importance of CSI in the southeast US. But this accounts only for thunderstorm interactions. It is felt that the topography in NC serves to focus the boundaries into a relatively small area (the eastern Piedmont and Coastal Plain). This increases the likelihood of boundary interactions. For instance, sea breezes routinely interact with horizontal roll convection and Piedmont Troughs. This happens regularly, almost on a daily basis in the summertime. Based on this and the higher likelihood of features producing convection in NC, it is felt that forecasting new or

intensified convection caused by boundary interactions in NC would be a more direct procedure than doing so in CO. As noted above, there were several significant differences between the two studies concerning boundaries and interactions; however, most of the results are understandable, given the different synoptic environments.

With the completion of the comparison of NC boundaries to Colorado boundaries, it is appropriate to study local features in more detail. Of particular interest is the convective activity of the different types of boundaries. Specifically in question is whether a boundary is capable of producing convection without interacting with another feature. In this work, a boundary which does produce convection without such interaction will be referred to as "autoconvective." Whether a boundary is autoconvective is of interest because these types of features are capable of producing the first thunderstorms of the day. Figure 4.21 is a graph showing the likelihood of a specific category of boundary being autoconvective. For the most part, the majority of the boundaries can be expected to produce convection of 40 dBZ or greater with a probability of at least 50% without any need for boundary interactions. Even the Horizontal Rolls, which WS indicated rarely produced deep convection, produced 40 dBZ showers about 39% of the time. One of the especially interesting aspects of these graphs is that TMBs and troughs can generally be expected to produce convection nearly all of the time.

It should be noted that there is a significant difference in the current study data provided in Figure 4.21 and that data provided in Figure 4.18. Figure 4.18 includes both autoconvective activity as well as interactions between boundaries. This difference is noted because WS did not study separately those boundaries which produced convection upon interaction with another feature and those boundaries which produced convection without such interaction (autoconvective). Figure 4.21 does not take boundary interactions into account, thus resulting in the lower numbers. When all categories are considered, 72% of the boundaries are likely to be autoconvective.

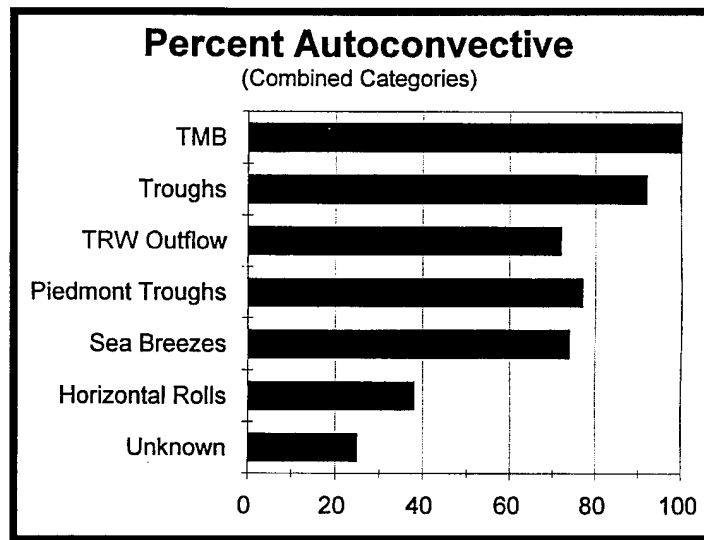


*Figure 4.21. Percent of boundaries autoconvective in NC*

The relationship between boundary movement and whether or not it was autoconvective was also considered. It was expected that moving features would more likely be autoconvective due to the convergence they would tend to generate at the boundary/environment interface. Wilson and Mueller (1993) quoted work from WS which indicated that the movement of the boundary was only weakly correlated with the resulting convective activity. They found that 60% of stationary boundaries are convective and that 65% of moving boundaries are convective. Figure 4.22 shows the results obtained in the current research. Of the total of 95 boundaries studied in NC, 60 were moving and 35 were stationary. Moving boundaries and stationary boundaries were autoconvective 75% and 66% of the time, respectively. It is recognized that this difference is likely not significant due to the small sample size. However, if the figures are taken at face value, this would lead one to believe that there are ample PBL triggers and sufficient CAPE so that the movement-generated convergence (ground relative) is not a necessity for thunderstorm formation in central and eastern North Carolina.

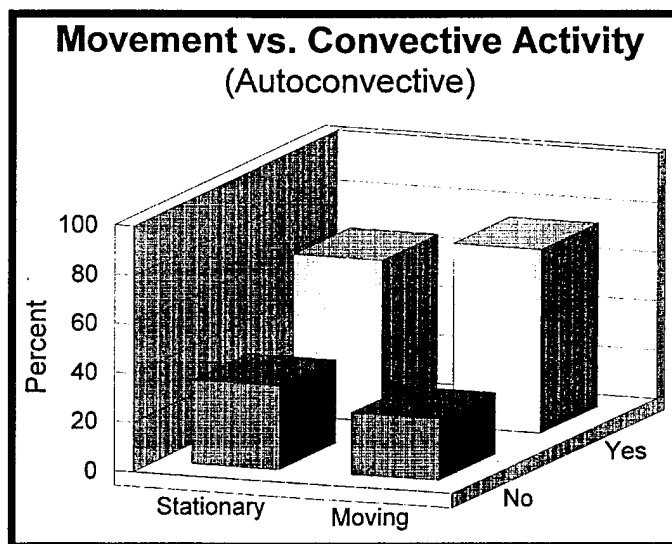


Figure 4.22. Depiction of movement vs. convective activity (autoconvective).

When this research was initiated, it was hoped that there would be some results which would indicate the relative importance of different stability indices in this area. Stability parameters were computed using the NWS SHARP Workstation software (Hart and Korotky, 1991) in an attempt to be as objective as possible. After all, Wilson and Mueller (1993) found that a 1-2 °C difference in temperature or dewpoint was all that was necessary to produce or inhibit convection. The 12Z soundings of Greensboro (GSO) or Cape Hatteras (HAT) were selected for use depending on which appeared to be more representative for the area in which convection eventually occurred. The selected sounding was modified to represent the *worst case* (highest surface dewpoint and temperature) which occurred in the area of concern within three hours of the initiation of convection. The SHARP software was then used to objectively compute the mixing ratio for the lowest 150 mb of the atmosphere and to lift a representative parcel from the surface. There were obviously several different methods which could have been used in the computations;

however, all of them would have been highly subjective. It was felt that based on the findings of Wilson and Mueller (1993), it was necessary to be as objective as possible.

The stability parameters investigated were Convective Available Potential Energy (CAPE), the SWEAT Index, the K Index, Total Totals, the Showalter Index (SI), the Lifted Index (LI) and Convective Inhibition (CIN). A specific goal was to determine if any of these parameters could provide information as to whether a boundary would be autoconvective or not.

It was found that CAPE was not a good indicator of whether or not a boundary would be autoconvective. Most days on which data was collected had over  $1000 \text{ J kg}^{-1}$  of CAPE without any negative area. There were almost equal numbers of autoconvective boundaries and non-autoconvective boundaries with the lowest category of CAPE (201-600  $\text{J kg}^{-1}$ ). Therefore it is not felt that CAPE can be used with any degree of success.

The K Index was found to be slightly more useful. A total of 80% of the autoconvective boundaries occurred when the K Index was greater than 31. However, it is also true that around 80% of the non-autoconvective boundaries occurred with the K-Index was greater than 31. About the only useful result using K Index was that there were no instances of autoconvective boundaries when the K Index was less than 11.

Similarly, when Total Totals (TT) was considered, it was found that about 80% of both autoconvective and non-autoconvective boundaries had TT between 44 and 51. Again, only a lower bound can be provided for autoconvective boundaries. It was found that there were no autoconvective boundaries with TT was less than 36.

To summarize: the modified soundings indicate that thunderstorms will not form when the stability indices fall below a certain threshold. However, when potentially unstable profiles were indicated, thunderstorms did not always form. These conclusions agree with those of Mueller et al. (1993). It is believed that the method of data collection did not lend itself to obtaining an accurate representation of the stability parameters. For

example, data was not collected unless an “interesting” feature was seen. Once data collection started, all boundaries observed on that day were included in the study. But, in general, only one set of stability parameters were applied to each day.

The final goal to be met in this section concerns the relative importance of each of the data acquisition platforms. The reader is reminded of the definition used to define whether or not a platform “detected a feature. A boundary was considered to be detected by a platform if a forecaster, who was aware of the presence of the boundary, could discern the feature. For example, if a trough is found while conducting a mesoanalysis, and the analyst can then examine the satellite or radar imagery and find evidence of the feature, then it has been “detected” by that platform. There was no emphasis placed on which data platform detected the boundary “first” because there were too many subjective variables which must be considered. For example, all mesoanalyses were conducted well after all satellite and radar imagery had been acquired, and all radar imagery was acquired prior to the acquisition of the satellite imagery. Therefore, the “first detection” statistics would have been biased in favor of the radar.

With this in mind, Figure 4.23 shows the relative importance of each of the data acquisition platforms in detecting the features. As shown, the percentages were similar with the radar and satellite detections of 84% and 82% respectively. The surface analyses revealed only 53% of the total boundaries, a result which was not unexpected. The problem with these results is that the figure implies that the radar *misses* 16% of all of the boundaries and the satellite *misses* 18% of all boundaries. This is extremely important because it reveals a weakness of the “system” in general. However, forecasters do not have access to only one or the other of these platforms; they are used together. Therefore statistics were computed to determine how effective different combinations of data

acquisition platforms were in detecting NC PBL boundaries. Figure 4.24 is a graphical depiction of the results.

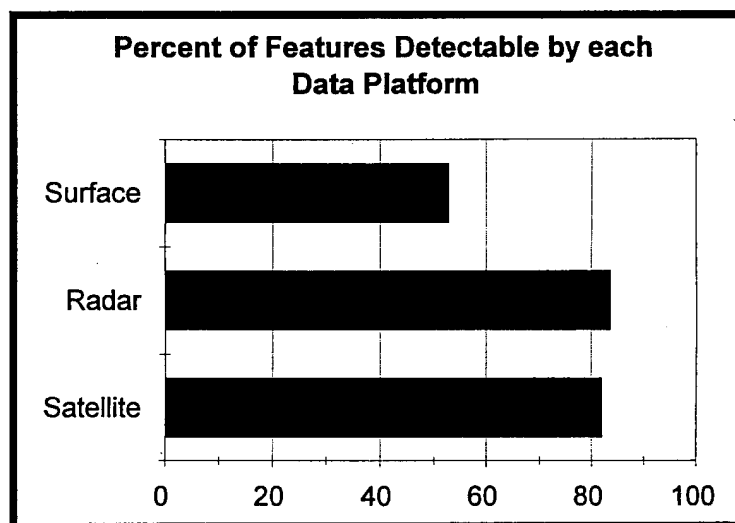


Figure 4.23. Relative importance of each data acquisition platform.

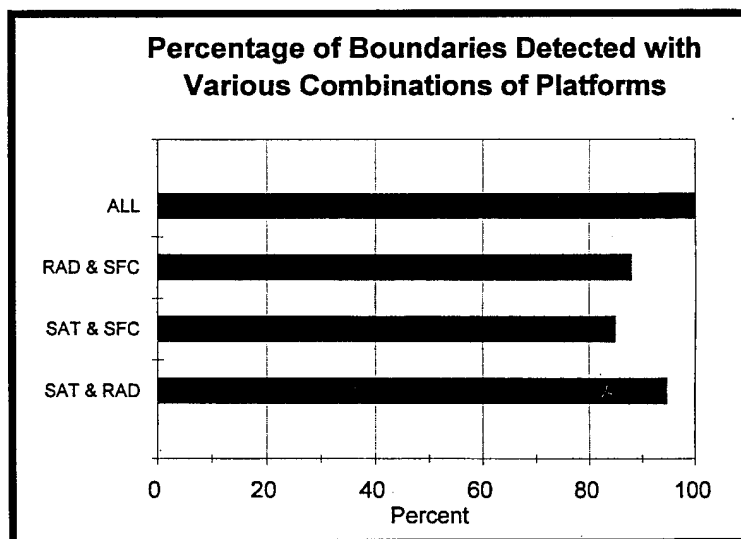


Figure 4.24. Boundary detecting using a combination of platforms.

When the satellite is combined with the radar, 95% of all boundaries are detected, leaving only 5% undetected. Fortunately however, the addition of the surface analysis data to this results in the detection of 100% of the boundaries uncovered.

This is obviously the expected result because all of the boundaries included in this study were obviously detected in some way or other; however, the important point is that each of the platforms has strengths and weaknesses. For example, the radar is extremely good at detecting features, even in the clear air to a distance of about 80 km (50 nm). Beyond that distance the beam is well over the PBL features which are of interest in this work. The satellite is extremely good for detecting features which have produced convection. It is accurate and useful for the detection of cloud-producing boundaries well beyond the range of the radar or the forecasters' area of concern. However, a cloud must be present in order for the satellite to be of use. Previous research has shown that "haze boundaries" are also capable of producing nonclassical mesoscale circulations; however, none of these features were observed in this work.

The final data set is the surface mesoanalysis. Although it was expected that the surface data would be a weak component compared with the remote sensors, it is the surface data which usually allowed us to identify the observed features. The weakness of the mesoanalysis obviously lies in the spatial and temporal coarseness of the data. However, when the coarse data is used in conjunction with the high spatial and temporal resolution of the remote sensors, it is definitely possible to detect and identify mesoscale features using synoptic scale surface charts.

The results of this section may lead one to believe that the added benefit of the radar is only 2%. However, one must remember that this is first and foremost a radar study. Nearly all of the boundaries detected were first seen in the radar imagery. They were then investigated further to determine if other platforms could resolve them.



## **5. CASE STUDIES**

As this research was conducted, several cases were identified which were interesting for one reason or another. Three of them will be examined in greater detail in order to gain a better understanding of what types of interactions occur in the NC PBL. The first to be presented is a very interesting case which involves a large number of boundaries, including a TMB. The second case involves the most perplexing of all of the features encountered in this research, and the final case is a weakly forced situation with few thunderstorms and a sea breeze which propagates well into the interior of the state.

One of the primary objectives of this research is to determine the feasibility of conducting mesoscale analysis in NC using synoptic station reports and radar and satellite imagery. Even under the best of conditions, subjective analysis is very...well, subjective. The previously discussed work of Sanders and Doswell (1995) is testimony to the extreme amount of subjectivity often exhibited in analyses, even in strongly forced, synoptic scale situations. The point is that if the reader does not agree with the analysis, and there will surely be those occasions, then that is not a surprise. Each of the mesoanalyses presented here have been changed numerous times; the final product is felt to best combine all available data products.

### **5.1 Case 1: 16 July 1994**

This event occurred on 16 July 1994 and is interesting for several reasons. First, the radar plainly depicted (in retrospect) a feature which would eventually prove to be important. At the time, the forecasters and the author were unsure as to what the feature was and "wrote it off" to ground clutter and/or atmospheric. Later in the day, the "ground clutter" erupted into large, long lasting thunderstorms which produced localized flash flooding. The radar showed extremely large amounts of precipitation had fallen in the area

of interest, while the regional rain gauge network did not resolve the event. This case is therefore a good example which presents several of the capabilities of the new radar.

Several days prior to the occurrence of the event, middle and long-range forecast products had been predicting a frontal passage through central NC on 15 July 1994. As is usually the case in NC in the summertime, the majority of the energy and upper level support remained well north of the state and only a lower level trough traversed the area.

On the morning of 16 July, initialized upper air and surface products showed a well defined trough situated in the eastern Coastal Plain. A very weak surface frontal boundary was analyzed from the New England states through Pennsylvania, northern West Virginia and northern Kentucky. There was a region of 70% humidity at the 700 mb level and a weak vorticity maximum at 500 mb, both of which were vertically aligned above the surface front. The winds at 850 mb and above were approximately parallel to the front. No further southerly frontal progression was expected and the surface trough in eastern NC was forecast to move off the east coast. The forecast for the day called for the usual afternoon and evening showers and thunderstorms.

The morning sounding from Greensboro (GSO) is shown in Figure 5.1. It displays very weak northerly flow at the surface with winds backing to westerly at about 800 mb and a nocturnal inversion extending up to about 950 mb; the layer from 1000 to 900 mb is statically stable.

The stability parameters for the morning sounding are shown in the upper right hand corner of Figure 5.1. The sounding, modified to reflect the maximum heating and representative dewpoint for the environment producing the thunderstorms, resulted in the following stability parameters: Lifted Index = -5; Showalter Index = -2; and Total Totals = 50. The positive energy increased to  $1858 \text{ J kg}^{-1}$ .

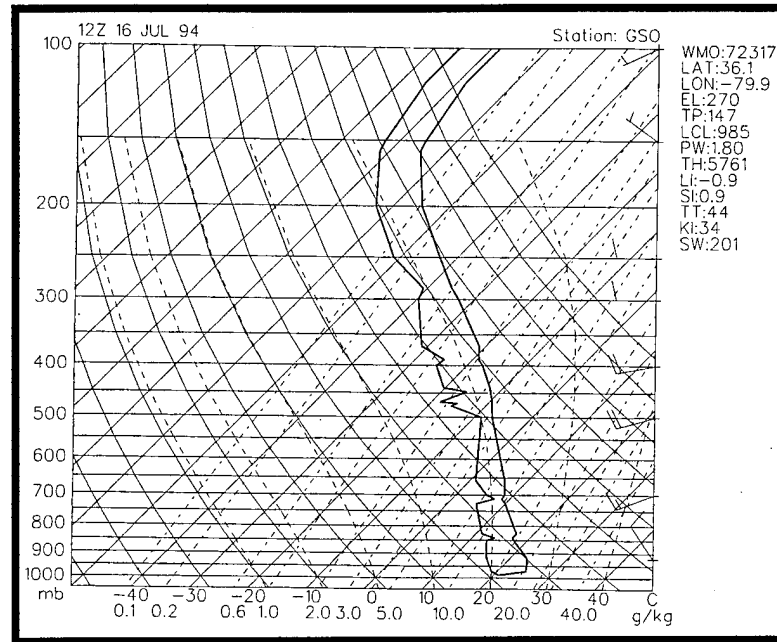


*Figure 5.1. GSO sounding for 12Z 16 July 1994*

Included for reference are Figures 5.2 and 5.3 which are respectively, the NWS morning analysis, and a subjective analysis, both valid at 12Z. The “after-the-fact” subjective analysis shows three features, two of which were not evident in the morning NMC products. The “frontal boundary” shown in NC is actually a TMB and was identified using a surface  $\theta_e$  analysis (see Figure 5.4a). The subjective analysis also shows a weak surface trough just north of the NC/VA border. The third feature, a strong surface trough in the eastern coastal plain of South Carolina, was depicted in the NWS analysis. The same analysis also placed the surface frontal boundary well north of NC, as mentioned previously.

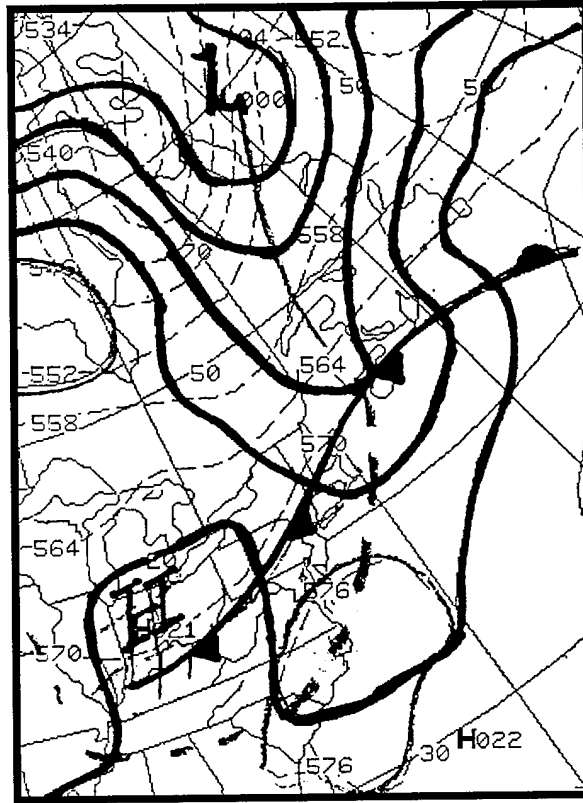


Figure 5.2. NWS 12Z analysis (surface pressure).

Figure 5.4a is an objective  $\theta_e$  analysis for 13Z. The  $\theta_e$  contours give some indication of cooler, drier air from the north moving into the warmer, moister air to the south, forming TMB #1. However, the area along the NC-VA border, from about the middle portion to the coast, is particularly data void. Objective analyses in this region often are not representative of the true meteorological situation. A very weak TMB, hereafter referred to as TMB #2, is also depicted laying through the Sand Hills (SH) region of NC.

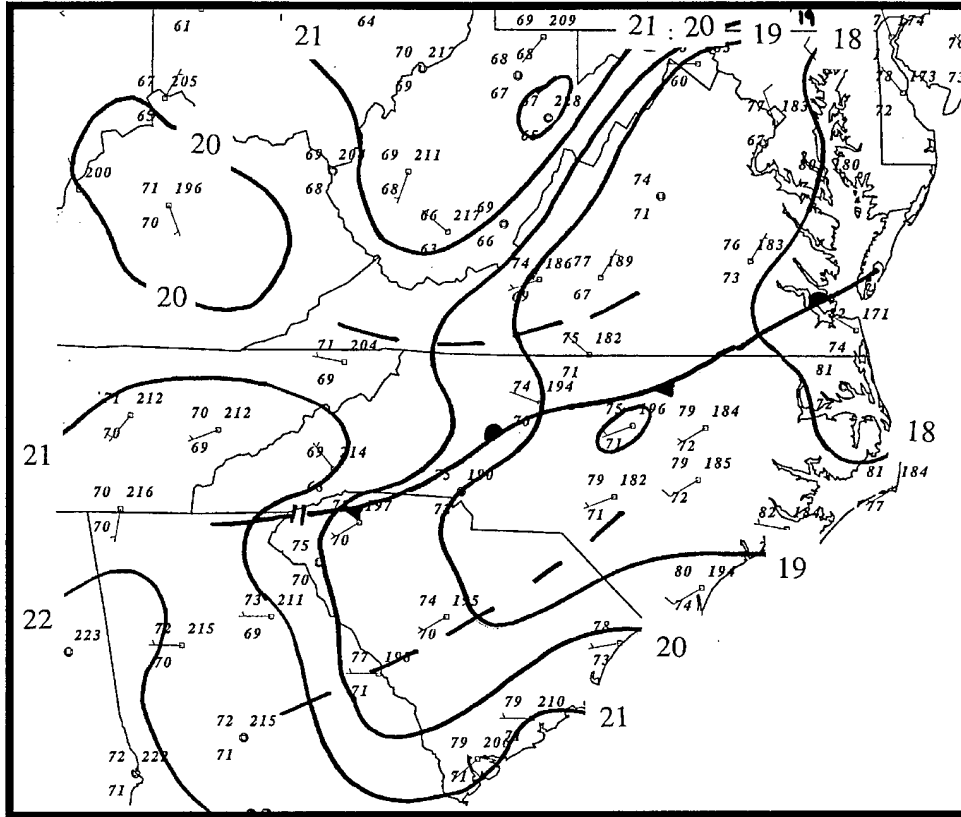


Figure 5.3. Subjective surface analysis for 12Z.

A series of Doppler radar and satellite images as well as surface mesoscale analyses will now be presented to illustrate the sequence of events for the day. The 12Z surface charts and the 13Z  $\theta_e$  analysis have already been discussed. Note that the trough in the Coastal Plain has been replaced by a TMB, as justified in Figure 5.4. The specific relationship between the trough and the TMB is not known. The 13:54Z clear air radar image is shown here (Figure 5.5) to give the reader a reference point for subsequent radar images. Neither boundary depicted in the 13Z  $\theta_e$  analysis is discernible in this image at this time.

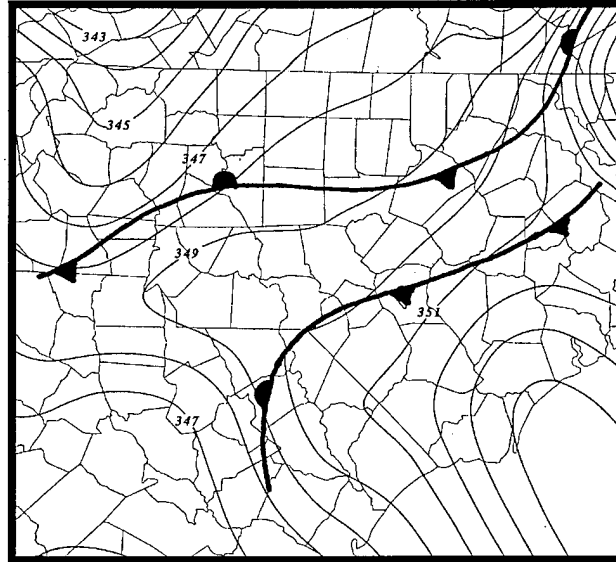


Figure 5.4a. Equivalent potential temperature objective analysis for 13Z. Boundary locations are indicated.

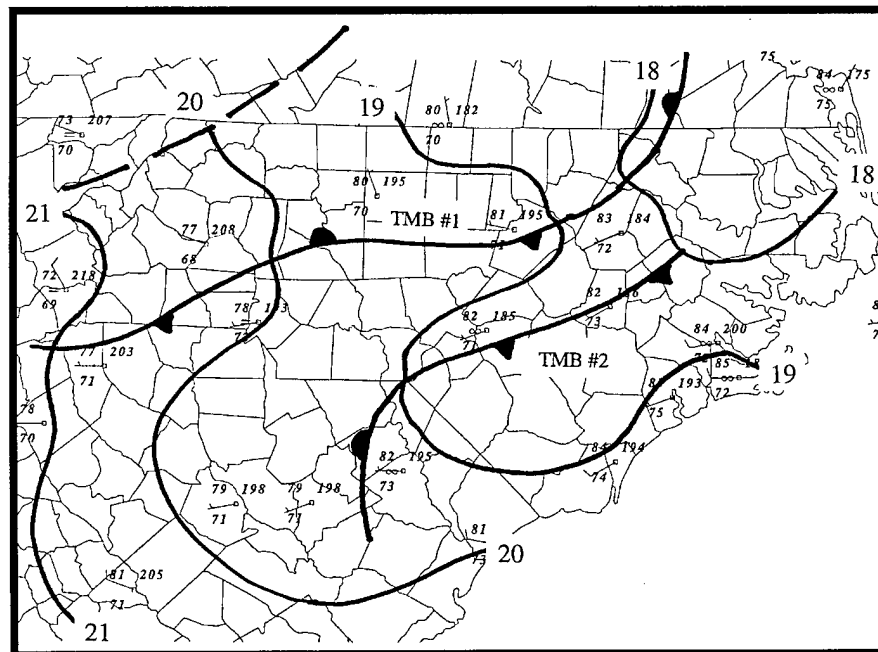


Figure 5.4b. Mesoanalysis for 13Z

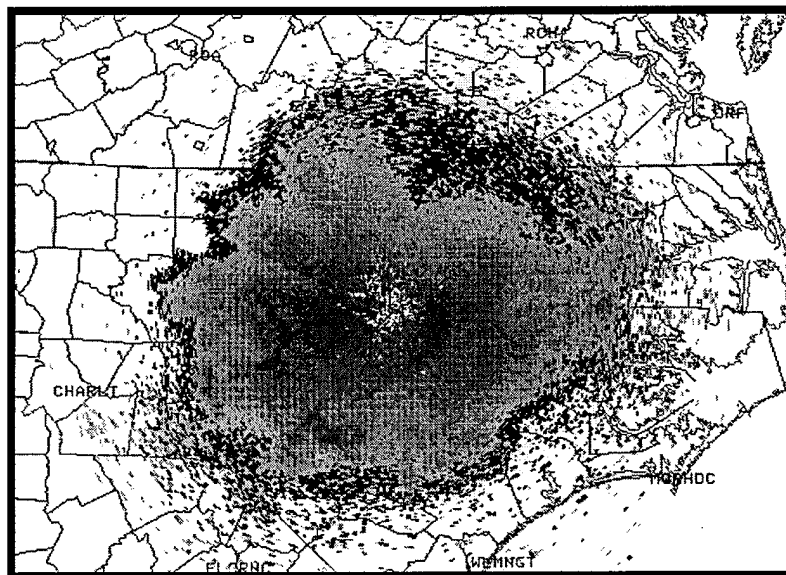


Figure 5.5. 1354Z clear air radar imagery.

By 14Z, the mesoanalysis (Figure 5.6) shows the weak trough which was in southern VA moving into NC. The southern end of TMB #1 appears to be moving slightly to the south.

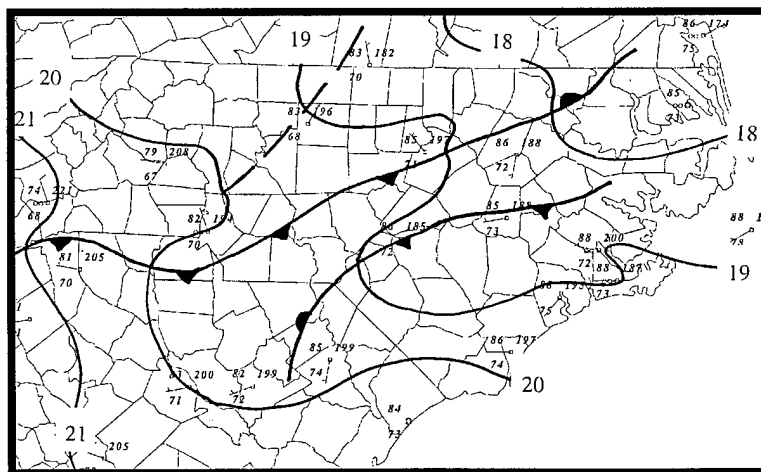


Figure 5.6. Mesoscale analysis for 14Z.

At 16:02Z, the radar provided the first indication that something was indeed occurring just north of the radar site (Figure 5.7). In the radar imagery, TMB #1 is depicted as a linear zone of relatively higher reflectivity (about 8 dBZ in clear air mode) and is located between the arrows. The same feature is also detectable in the satellite imagery. The feature is located approximately 30 nm from the radar site and the radar beam intersects it at about 914 m above ground level. In the surface data, the feature appears to have broken due to localized pressure rises and/or discontinuous movement. The radar also depicts the northern end of TMB #2. It is located approximately 55 nm southeast of the radar, a location which places the center of the radar beam around 1676 m above the surface the earth. Originally, it was believed that this zone of discontinuous reflectivity was due to the radar beam penetrating through the top of the mixed layer. However, if this were the case, there would be an approximately circular pattern around the radome at the distance from the radar (height above the ground) this occurred. It is speculated that the convergence along the TMB is enhanced due to its location near the easternmost edge of a convective roll cloud field. This hypothesis is weakly supported in the satellite imagery. Perhaps this easternmost edge of the convective roll field is a preferred zone for deeper convection because of the large amount of water in the tidewater region just to the east. Differential heating would produce a thermally direct circulation with flow towards the west, increasing convergence along this line.

By 17Z, the radar has shifted out of clear air mode in response to the thunderstorms forming to the north and west, yet no deep convection has been initiated in the immediate area (Figure 5.8). The satellite imagery shows the sea breeze moving slowly inland and the some enhancement of the convection along the TMB #2. It is obvious at this point that TMB #2 and the sea breeze are two separate features.

Convection develops rapidly during the next hour. By 18Z (Figure 5.9), cells are beginning to grow along TMB #1 (see zoom box, Figure 5.10) and showers are forming





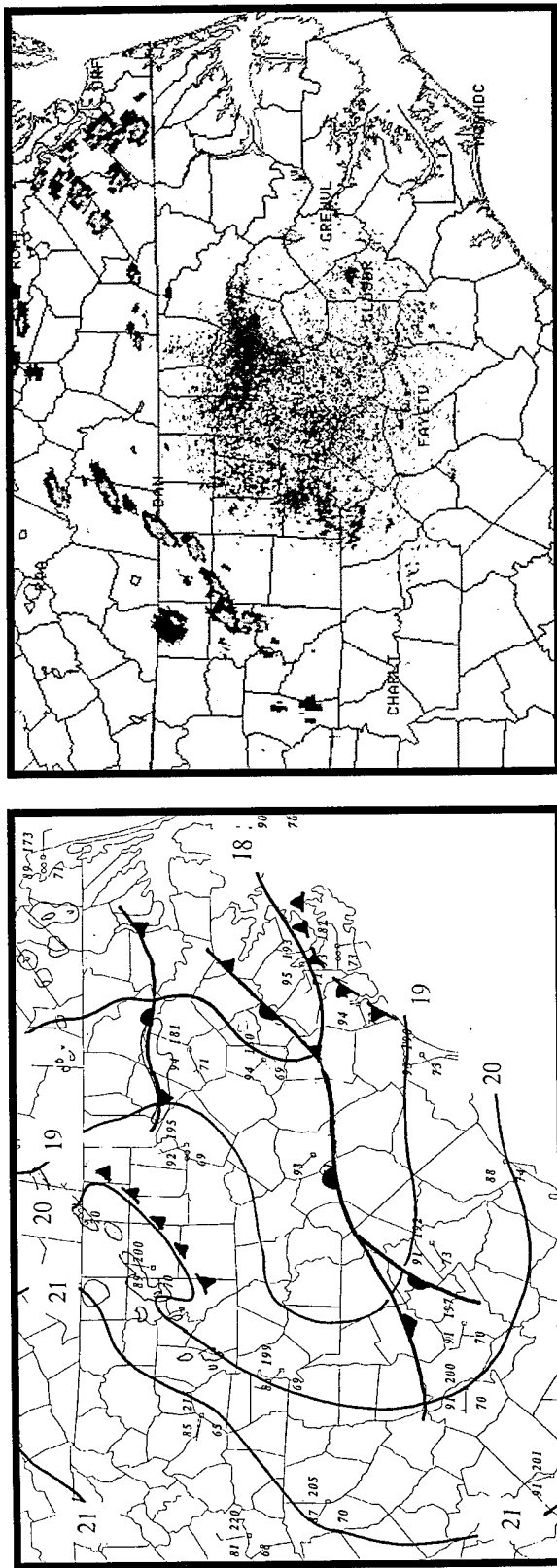


Figure 5.8 a, b, and c. Mesoanalysis, radar, and satellite imagery for 17Z.

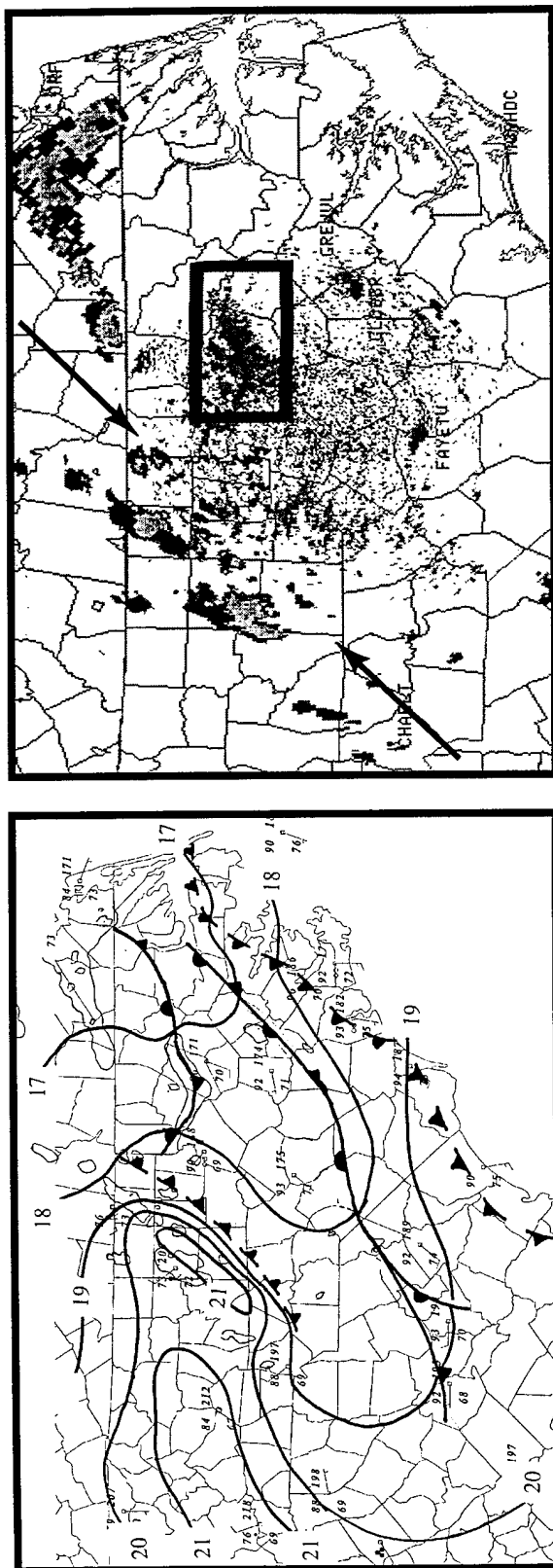
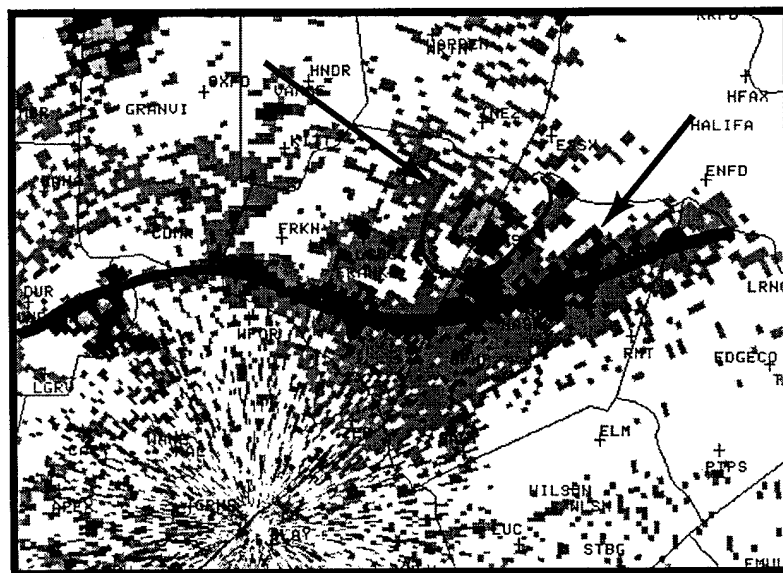


Figure 5.9 a, b, and c. Mesoanalysis, radar, and satellite imagery for 18Z.

along the outflow boundary northwest of the radar as depicted by the region between the arrows in Figure 5.9b. A weak shower has also occurred along TMB #2, in South Carolina (not shown in radar). At this point, 5 to 15 dBZ echoes can be seen occurring in discrete areas along the boundaries, located just north of Fayetteville and between Goldsboro and Greenville. This general increase in reflectivity was noticed by Eilts et al. (1991) and Wilson and Mueller (1993) who note that this is often the first sign that deeper convection is occurring in that area. The zone of relatively higher reflectivity just north of Fayetteville erupts into 40+ dBZ thunderstorms about one hour later.

Figure 5.10 is a zoom (from zoom box in Figure 5.9) of TMB #1 and the showers forming along it at 18:11Z. The cells appear to be forming just to the north of the boundary as indicated by the arrows. It is believed that the lifted air parcels are being moved to the east and north by the weak southwest winds as they are lifted along the surface boundary. Konrad (1970) also found indications of this occurring as he studied cloud streets which were sometimes not aligned directly over the maximum surface reflectivity.



*Figure 5.10. Zoom of TMB just north of Rocky Mount (RMT) at 18Z.*

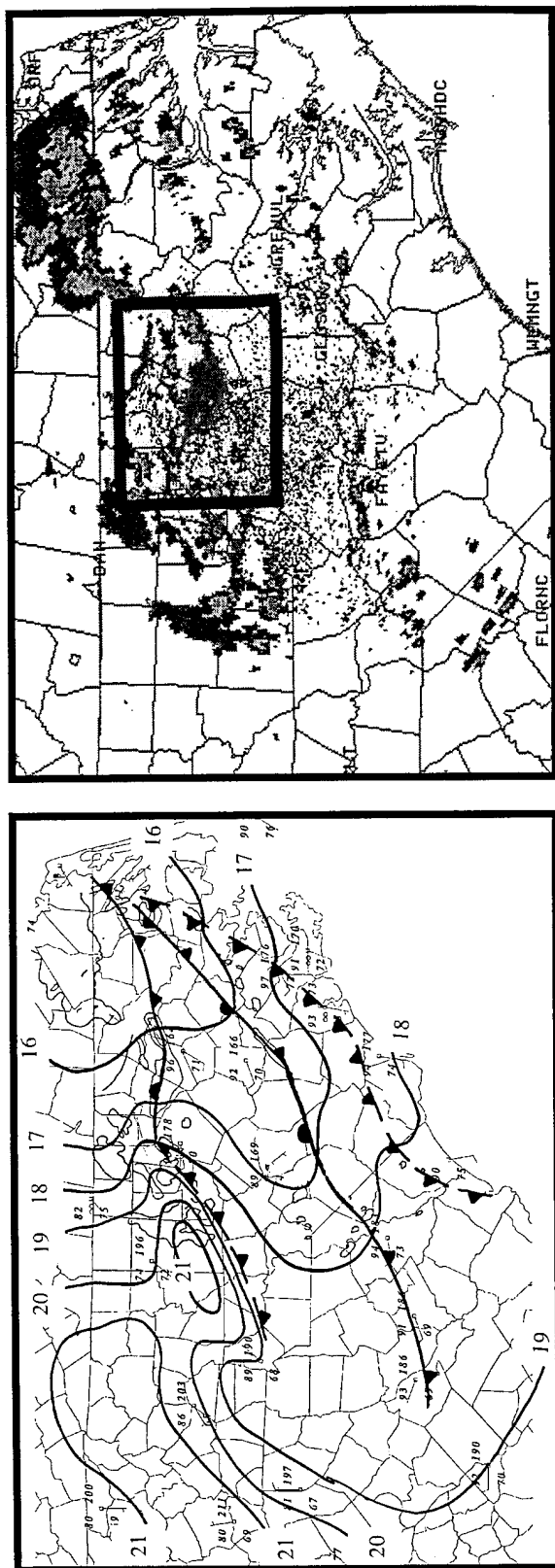
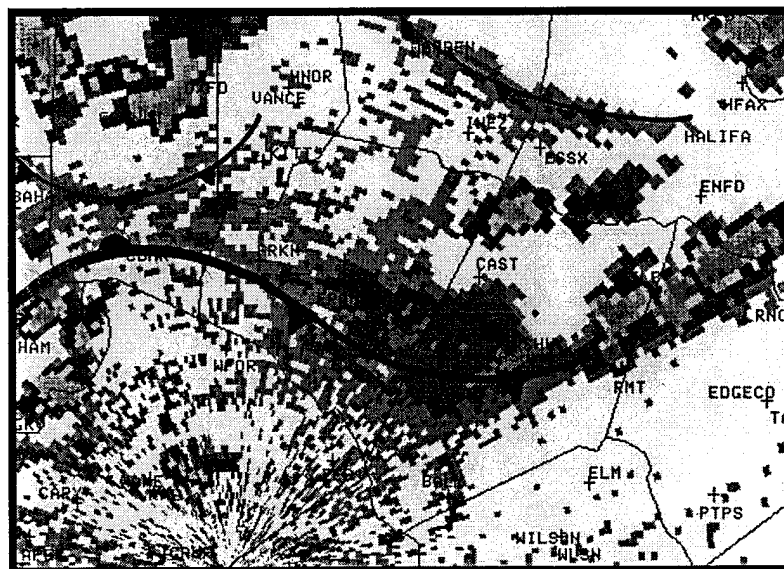


Figure 5.11 a, b, and c. Mesoanalysis, radar, and satellite imagery for 19Z.

The 19Z (Figure 5.11) figures show that development is occurring preferentially along TMB #1. Figure 5.12 (see zoom box in Figure 5.11) shows that outflow boundaries are very obvious in the radar imagery as the Convective Scale Interaction (CSI) discussed by Purdom and Marcus (1982) becomes one of the primary forcing mechanisms for convection in this event. Note that in general, TMB #2 has become convectively active while the other horizontal roll-like features have weakened (Figure 5.11c). Subsidence on either side of the vigorously growing cumulus suppresses convection in those areas (Houze, 1993) producing zones of significantly reduced convective growth on either side. The thunderstorm outflow from the west continues to propagate into the interior of the state, producing large thunderstorms as it moves.



*Figure 5.12. Zoom of 19Z radar imagery. Showers are just beginning at RMT.*

By 20Z (Figure 5.13), the south-eastward moving TRW outflow (see Figure 5.9) has reached TMB #1, which has been stationary throughout the day. Convection occurs when the two boundaries collide (within zoom box). TMB #2 is continuing to produce

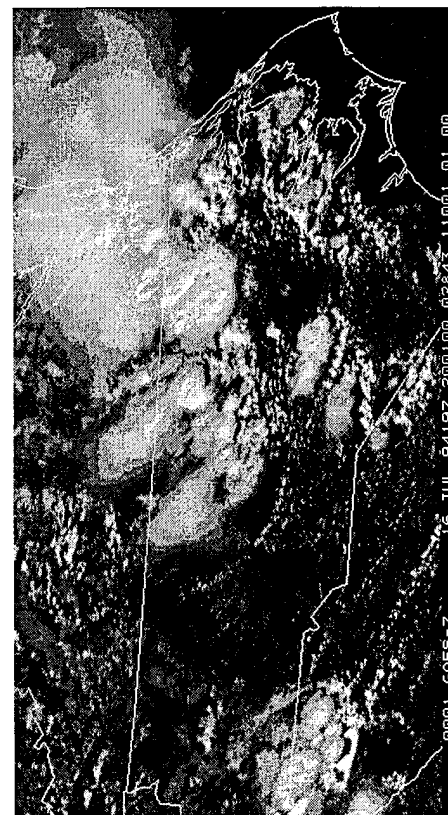
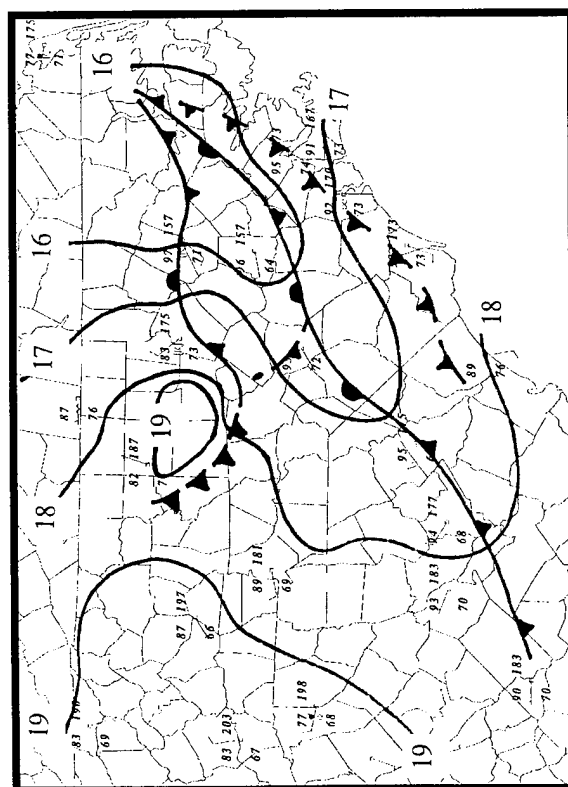
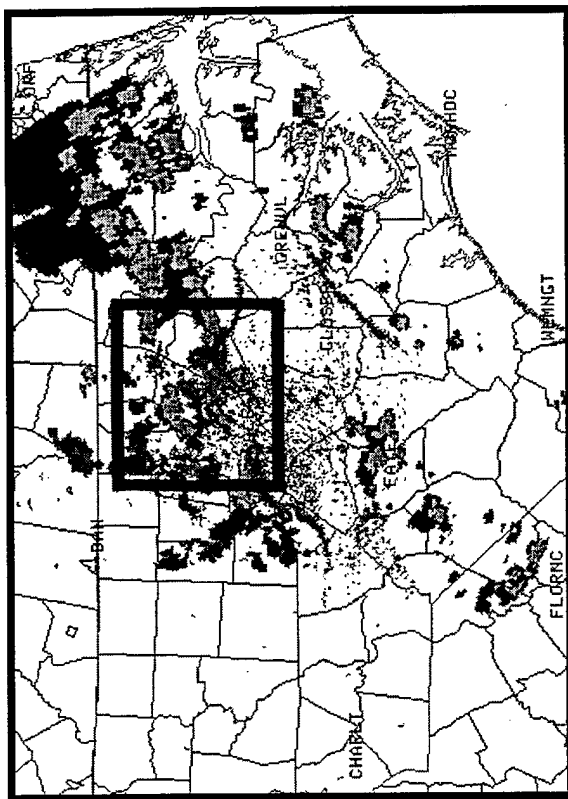
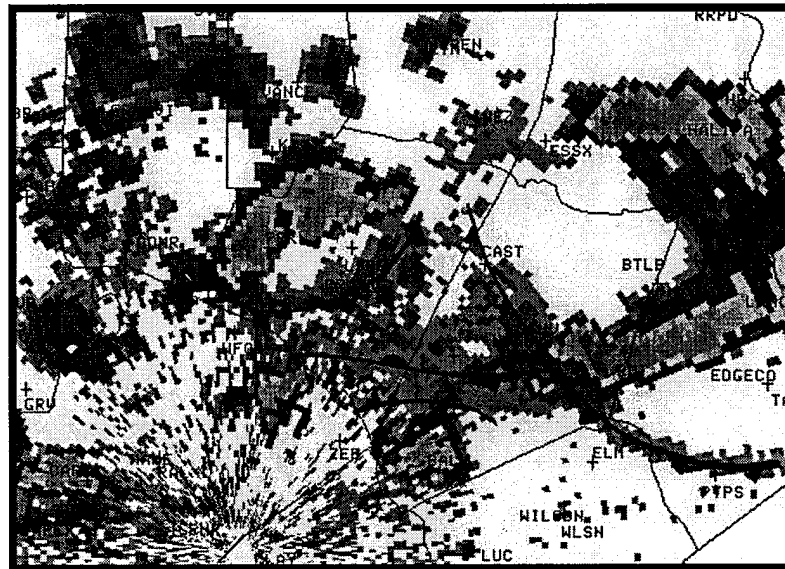


Figure 5.13 a, b, and c. Mesoanalysis, radar, and satellite imagery for 20Z.

deep convection in the Coastal Plain and Sand Hills. In the northeastern part of the state, the sea breeze and both TMBs are interacting and producing deep convection. Figure 5.14 is a zoom (see zoom box in Figure 5.13) of the radar imagery which vividly depicts the convective scale interaction described by Purdom and Marcus (1982). Notice in particular the 50 dBZ cell located over Rocky Mount, NC (white dot). The thunderstorms along this line are the result of the interactions between TRW outflows and TMB #1. Since the TMB is stationary and convergence continues along it, thunderstorms continue to build and collapse, resulting in localized flash flooding in this area. This is interesting considering this is the only point at which the boundaries intersect at a relatively large angle.



*Figure 5.14. Zoom of 20Z radar image.*

At 21Z (Figure 5.15), it appears that the northernmost TMB #1 has lost its original character as thunderstorm outflows dominate the local environment. Just to the west of Pamlico Sound, the sea breeze has merged with the TMB #2 and the convection increased preferentially in that area. Further to the north, the sea breeze and the two TMBs are continuing to interact, producing locally severe storms.



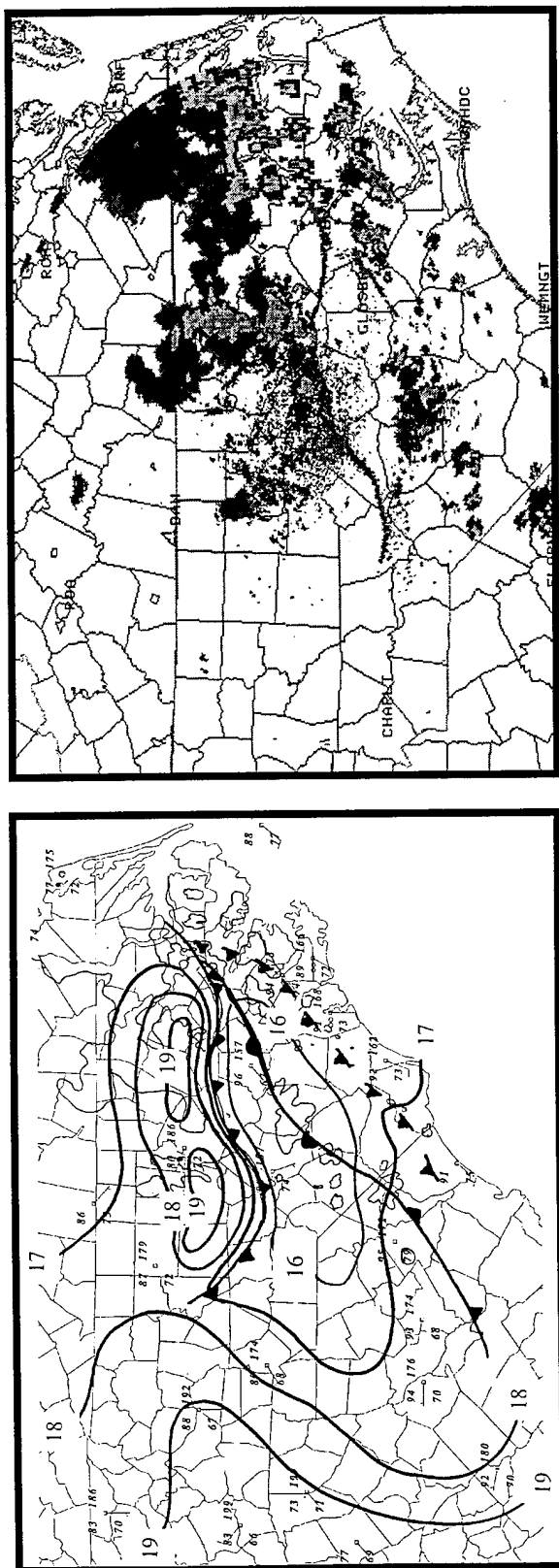


Figure 5.15 a, b, and c. Mesoanalysis, radar, and satellite imagery for 21Z.

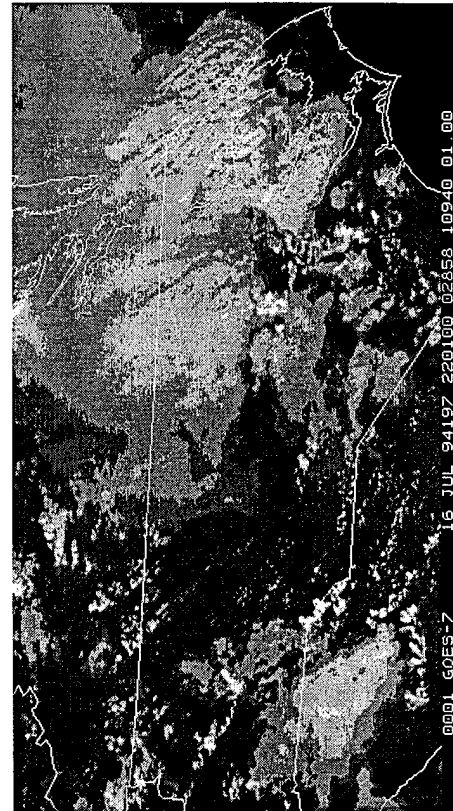
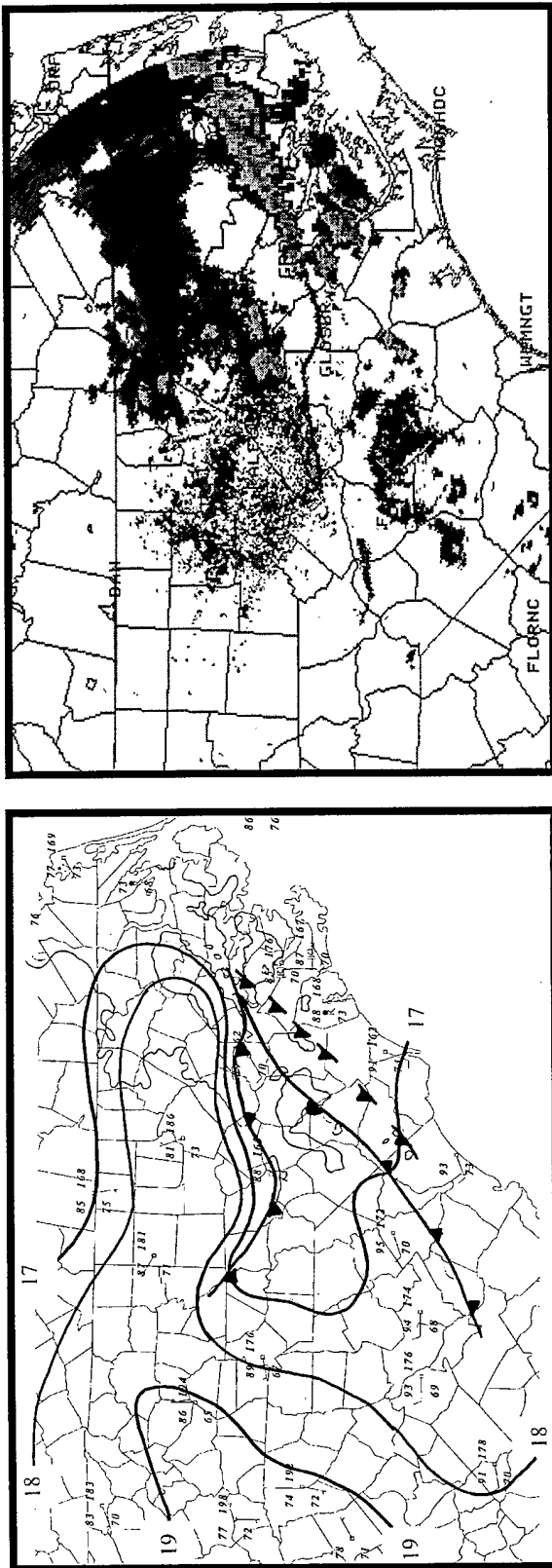


Figure 5.16 a, b, and c. Mesoanalysis, radar, and satellite imagery for 22Z.

By 22Z (Figure 5.16), the strongest showers are still located where the sea breeze, the TMBs, and the thunderstorm outflows are interacting. A line of showers just to the south of the radar site is weakening. It appears that all of the features without strong surface forcing are now beginning to dissipate. This is the last time period for which radar and visible satellite data are available.

The radar estimate of storm total precipitation showed that in a very small area in north Rocky Mount, NC, there was between 4 and 5 inches of rainfall in just 3 hours. However, when the records from the National Climatic Data Center (NCDC) were studied, it was found that the rain gauge nearest the event (6 nm southwest of Rocky Mount) recorded only 1.4 inches of rain during the period. This is significantly different from the totals estimated by the radar. However, since emergency management officials in Nash and Edgecombe Counties reported flash flooding to the NWS Raleigh Office, it is expected that the remotely sensed rain rates were more representative of the total amount of precipitation than was the coarse rain gauge network.

In summary, there are numerous reasons that this case was interesting. First and foremost, it taught forecasters and researchers that persistent features revealed by the radar are significant and should be investigated. In this case, the radar depicted the TMB in the clear air at 16:02Z. At the same time it showed evidence to support the northern end of TMB #2. The radar did not show the southern end of this boundary, probably because the radar beam was overshooting the feature. The first 40 dBZ cells formed along TMB #1 about 17:36Z, which means the radar provided over 90 minutes of lead time for this severe local event. The first showers did not form along TMB #2 until 18:05Z, which gave the radar a lead time of just over 2 hours. Although this case study does not provide evidence which would warrant immediate issuance of flash flood warnings or severe thunderstorm warnings for those areas near a suspicious feature, it does show that the radar can provide

forecasters with information which they can use to narrow down their broad "afternoon and evening thunderstorm" forecasts.

This case also provides an example of the utility of using the storm total precipitation product. Although some effort should be expended to "calibrate" the system with a rain gauge network, it appears to be much more useful than using *individual* rain gauges to estimate precipitation amounts.

This study would be incomplete if it did not compare the output of the WSR-88D with that of the older system, the WSR-57. Although WSR-57 data is not available here, there is information available which would allow us to estimate the relative sensitivities of the two radars in an applied situation such as this. Technical specifications indicate that the minimum detectable signal for the older system is 13 dBZ (Alberty and Crum, 1991) and -32 dBZ for the 88D (OTB/OSF Training Manual). However, when used outside of the "laboratory" and in the presence of ground clutter and atmospheric noise, the minimum detectable signal is generally agreed to be about 25 dBZ and -25 dBZ respectively.

The first features detected by the WSR-88D at 16:02Z were about 8 dBZ and 4 dBZ for TMB #1 and TMB #2 respectively. Obviously, these are well below the threshold that would be detected by the WSR-57. It is interesting to consider just when in this event a WSR-57 would have detected echoes and what a forecaster using that system would have seen. When the interior of the state is considered (that area approximately bounded by the two features of interest), then the first echo which was strong enough to be detected by the WSR-57 occurred at about 17:36Z. At this point, the cells would have appeared to be so scattered that they would have been considered "air mass" showers since there would have been no prior knowledge of the structure of the triggering boundaries. Also of note, in this case, which was dominated by what appear to be very strong thunderstorm outflows, not one of the outflows was stronger than 15 dBZ. Therefore, forecasters utilizing the older

unit would have been unable to "nowcast" future storms based on the movement of the outflow boundaries. Even those strong storms which resulted from the interaction between the sea breeze and the TMBs would have been a mystery for the most part.

There are several very interesting questions which should be considered in the study of this case. First, it is of significant interest to this researcher why the TMBs, which were visible in the 16:02Z imagery, were not depicted in the earlier clear air imagery. It is felt that northern end of TMB #2 probably was not visible because there had not been enough sensible heating to establish a thermally direct circulation, resulting in the low level convergence. However, the "sudden" appearance of TMB #1 is not quite as easily explained. The feature was obviously in place because its presence was supported by the 12Z mesoanalysis. Even with strong diurnal heating later in the day, the feature did not move significantly, so it is assumed that it remained approximately stationary from 12Z to the time it was finally detected at 16Z.

Rabin and Doviak (1989) studied meteorological and astronomical influences on radar reflectivity in the convective boundary layer and found that radar reflectivity increased as solar radiation increased. They note that this is because all atmospheric motion is ultimately linked to energy obtained from the sun. In the case of Bragg scatter, the reflectivity depends on centimeter scale eddies which mix thermal and moisture discontinuities (see Section 2.1.5 and the discussion of Bragg scatter). If no mixing occurs, no reflectivity due to Bragg scatter occurs. So we should consider the origin of these eddies. For a moving boundary, the part of the motion contributed by centimeter scale eddies can be detected in the radar reflectivity (assuming appropriate moisture and/or thermal discontinuities are present). In this case however, there was no movement. Therefore, the detection of the feature depended upon the absorption of incident solar radiation, which ultimately produced the turbulent eddies which the radar could observe. It

is believed that the convective turbulence increased with solar insolation and reached the level/intensity which could be detected by the radar at approximately 16Z.

So, why is this important? First of all, it tells us that an echo-free radar in the morning does not necessarily mean that there are no boundaries in the area. The radar should be monitored through the morning hours and weak reflectivity fields should be compared with a pressure and  $\theta_e$  analysis. If this case is representative of our PBL, then sometime between late morning and noon, we can expect that very weak features will begin to appear. Note that this is often the case with horizontal rolls as well. The convective rolls resulting from thermal instability are seldom visible early in the day. As solar insolation increases, we tend to see more of these very weak features in the PBL.

There are other situations in which a boundary may be difficult to detect. A feature which is oriented approximately along a radial from the radar, such as the southern end of TMB #2, is very difficult to discern. This is because as the beam moves along the boundary, the beam continuously changes elevations, so that the feature is only intersected by the beam in one discrete location.

The analysis of this case tested the use of several techniques which proved to be quite productive. It was found that the surface  $\theta_e$  data was the most useful tool for locating the weak TMBs observed in this study. Often, in weakly forced conditions, there is only a degree or two difference in the temperature and dewpoint fields. When standard analyses were conducted of these fields, no features could be detected. By using the  $\theta_e$  analysis, the small differences in temperature and moisture were combined and the features became evident.

Research by Eilts et al. (1991) and Wilson and Mueller (1993) showed that the development of thunderstorms could often be linked to an increase in reflectivity aloft. In this particular case, it was shown that the same technique could be used to forecast storms

in NC. The 18Z radar imagery clearly depicts an area of enhanced reflectivity (5-10 dBZ) just north of Fayetteville. The area is approximately 3300 ft above the ground. The above mentioned researchers, as well as Knight and Miller (1993) indicate that these areas are primarily caused by Bragg scatter as the radar beam intersects warm, moist, vigorously growing thermals. By 19Z, the area of interest intensifies into strong thunderstorms. These cells were "forecast" by the radar with almost one hour lead time. Although the emphasis of this research was not placed on determining just how many large thunderstorms form from enhanced reflectivities aloft, it appears that the technique may work well in NC.

## 5.2 Case 2: 26 May 1994

One of the primary goals of this research was to investigate as many different types of boundaries as possible. This interesting event definitely helps to fulfill that goal. In this case, a front moving toward the coast interacted with an "Unknown Moving Boundary" (UMB) which was coming from the coast. This is the only situation in which a moving boundary collided with another moving boundary, and the net result was a decrease in the convection.

In order to adequately resolve the sequence of events which transpire in this case, a mesonet would be required. Unfortunately, all of the observations reported hereafter are based only on four stations located along the NC coastline and one inland station, all of which report hourly. The stations of interest are Wilmington (ILM), Jacksonville (NCA), Cherry Point (NKT), Newbern (EWN) and Goldsboro (GSB) and their locations are indicated on Figure 5.18a. Meteograms for each of the stations, which show the approximate time of passage of each boundary, are included as Figure 5.26.

The 12Z synoptic surface map (Figure 5.17) shows a well-defined frontal boundary entering western Kentucky. Associated with the surface front were several troughs, both ahead of and behind the primary front. There also appears to be lee side troughing in the NC foothills. Later in the event, several troughs were evident and it was impossible to distinguish between lee side troughing and prefrontal troughing. In order to reduce confusion, the troughs were categorized as "prefrontal" when statistics were tabulated.

At the 300 mb level, there was a 115 kt jet maximum working eastward around the base of the long wave trough, over Illinois and Indiana. There was significant diffluence over NC as the Polar Jet curved cyclonically to the north and the Subtropical Jet curved to the south over the Bermuda High, with rather strong westerly flow over the Appalachian Mountains, as is required for lee troughing to occur.



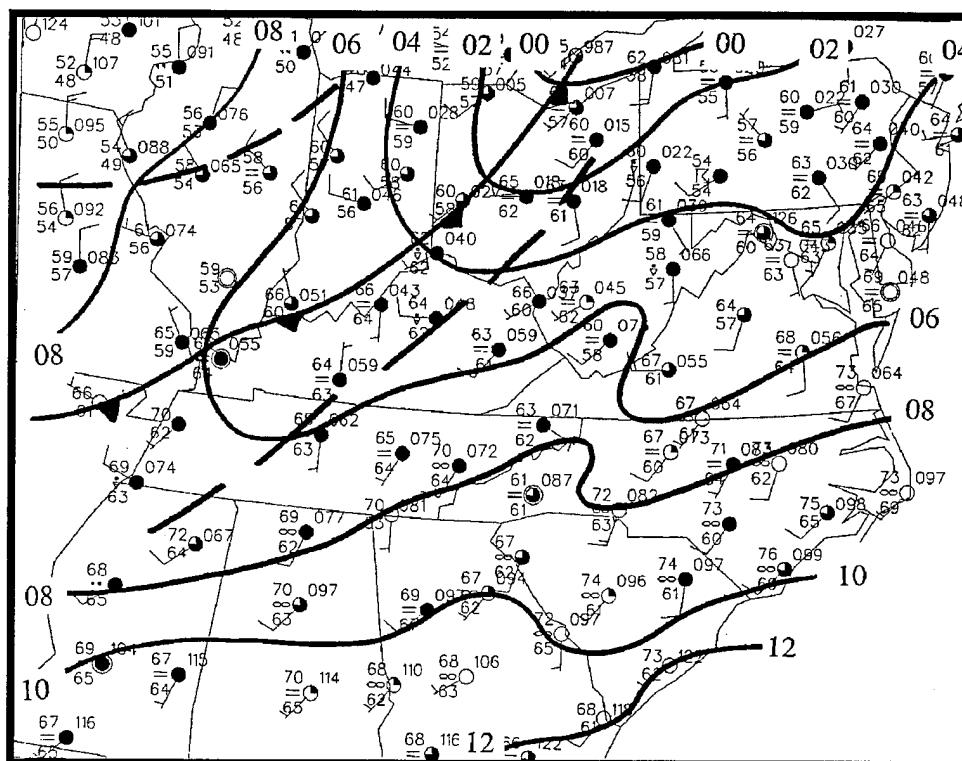


Figure 5.17. Synoptic-scale subjective analysis for 12Z, 26 May 1994.

The GSO morning sounding showed a well developed nocturnal inversion, up to about 925 mb. There was a weak inversion from about 725 mb to about 675 mb, with dewpoint depressions of about 4-6 °C in the layer. The unmodified stability parameters were as follows: Lifted Index = 1; Total Totals = 47; K Index = 31; Showalter Index = 1; Sweat Index = 216, CAPE = 6 J kg<sup>-1</sup>, and CIN = 42 J kg<sup>-1</sup>. The modified sounding, which reflects the afternoon environment in which the thunderstorms formed, yielded the following indices: Lifted Index = -4, Total Totals = 52; K index = 36; Showalter Index = -2, Sweat Index = 276, CAPE = 818 J kg<sup>-1</sup>, and CIN = 0.

A series of mesoanalyses and satellite and radar imagery have been included and will be referred to throughout the following discussion. The 13Z subjective mesoanalysis (Figure 5.18a) shows a weak trough over west central NC; the surface winds are generally from the southwest at about 10 kts. Satellite imagery (Figure 5.18b) shows a cloud layer

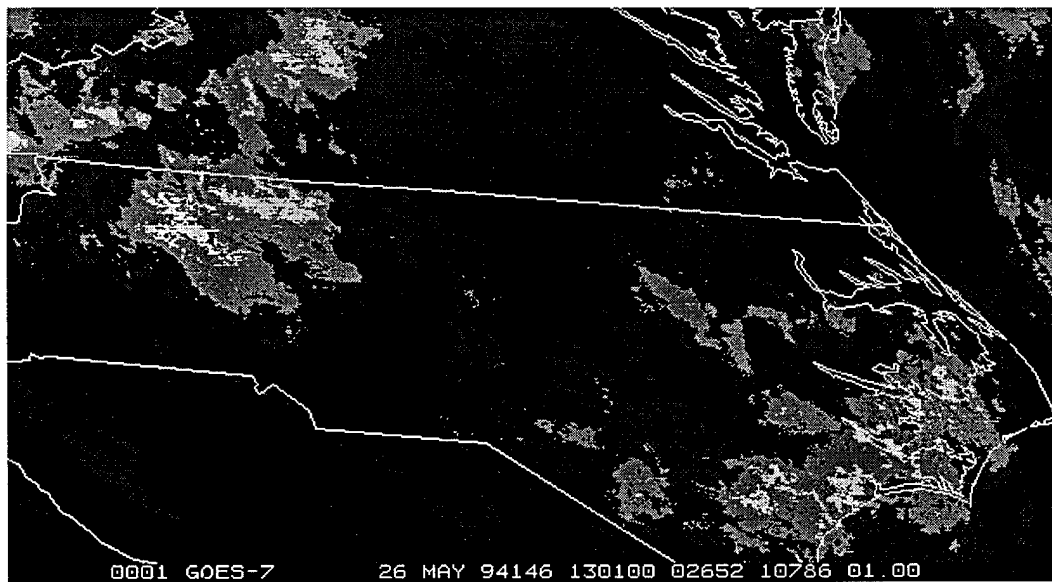
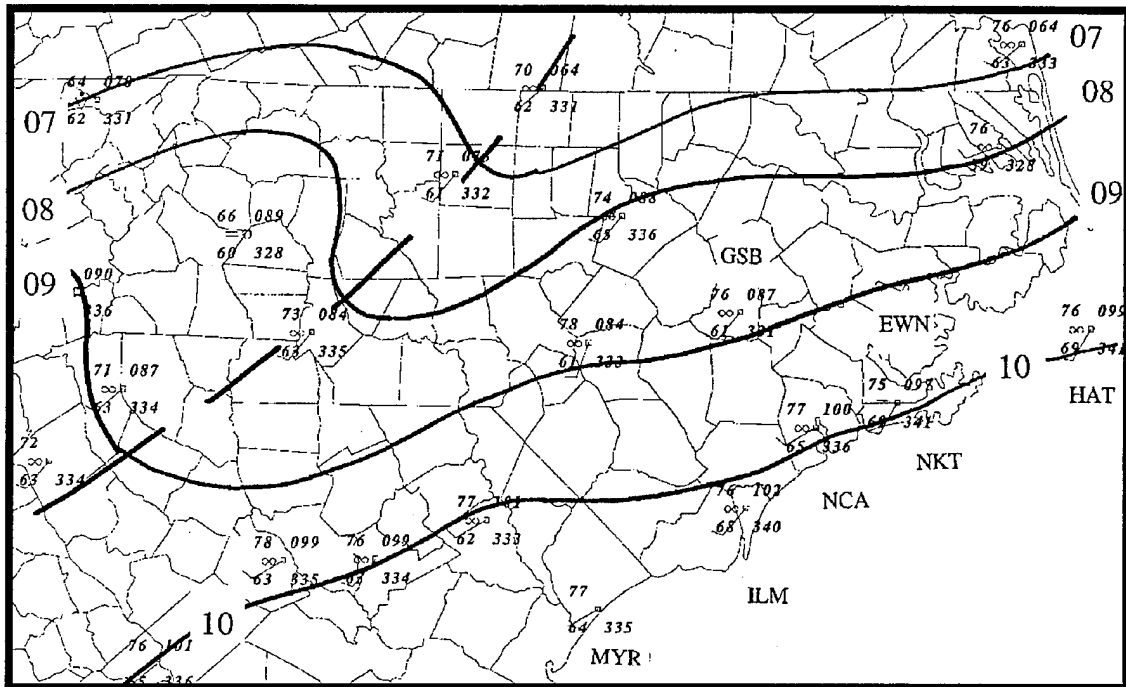
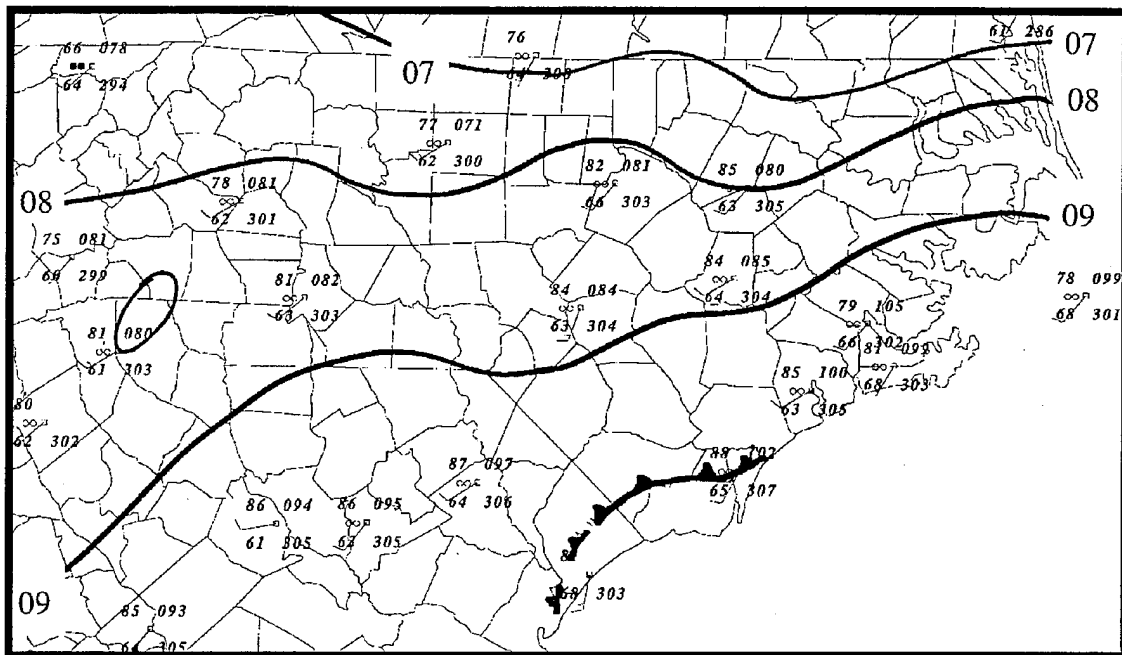


Figure 5.18 a and b. Mesoanalysis and satellite imagery for 13Z.

along the NC coastline, which is probably being capped by the weak subsidence inversion shown on the 12Z HAT sounding (Figure 5.25). The surface dewpoints along the coastline are between 8 to 12°F less than the temperatures, which indicates that the clouds are elevated. With the inversion at about 950 mb, and the significant dewpoint depressions at the surface, it is estimated that the thickness of the cloud deck is from about 400 feet to 1800 feet.

By 14Z, the clouds are beginning to evaporate from the edges. The southeast coast including Wilmington (ILM) is beginning to break out from under the cloud deck. Temperatures across the interior of the state are generally above the 75°F which the GSO sounding indicates is necessary to break the nocturnal inversion, although the elevated inversion over HAT requires a temperature of approximately 82°F to develop a well-mixed PBL. With the cloud cover in that area, the temperatures are not climbing as fast as they are in the interior of the state.

Wilmington (ILM) and Jacksonville (NCA) reached convective temperature (assuming the HAT sounding (Figure 5.25) is representative for the entire east coast of NC) by 15Z. At 16Z, a feature is just becoming visible in the satellite imagery, as indicated by the arrow in Figure 5.19b. At first glance at the mesoanalysis and satellite imagery, it appears this feature is a sea breeze. The winds at Myrtle Beach, SC (MYR) have become on-shore, the temperature decreased 4°F, and the dewpoint increased 4°F. However, at ILM, the temperature has increased 4°F and the dewpoint has decreased 3°F. This is exactly opposite of what is expected to occur during a sea breeze passage. The winds at ILM never become on-shore. Due to the unusual shape of the coastline however, it is difficult to determine just how much of a response would be expected, especially considering the significant synoptic forcing present on this day. Based on this and evidence to be presented, the feature originating from ILM is not believed to be a sea



breeze. This unknown moving boundary (UMB) will be depicted using cold front symbols throughout the analyses.

Between 16 and 17Z, the temperature at ILM increases 1°F, the dewpoint falls another 2°F, and the satellite imagery depicts the UMB propagating inland fairly rapidly. There are some shallow cumulus clouds forming along the front edge of the boundary as it moves inland, but no deep convection is initiated. ILM winds actually have a weak offshore component at this time. If all of the classic indicators of a sea breeze passage are considered (falling temperature, rising dewpoint, onshore winds), then at this point, exactly the opposite has occurred at ILM. The sea breeze is also beginning to propagate inland in the vicinity of Cherry Point (NKT).

At 18Z, a boundary has apparently passed NCA and ILM (see Figure 5.20). An examination of the station reports reveal that the winds at NCA have become onshore; the temperature at both stations has decreased and the dewpoint has dropped at both stations.

At 19Z, the UMB very difficult to detect in the satellite imagery because of the cirrus originating from the thunderstorms to the west. It is obviously not producing deep convection for that would be detectable. Showers and thunderstorms are beginning to form along two prefrontal troughs which are moving into the interior of the state. At this point, the temperature and dewpoint at ILM decreased 2°F while the temperature and dewpoint at NCA decreased 1 and 3°F respectively. NKT experiences significant changes through this hour with an increase in temperature from 84 to 85°F and a drop in dewpoint from 68 to 63°F. It is believed that the UMB passing the station is responsible for the decrease in moisture.

As thunderstorms begin to build in the interior of the state, the first radar images become available at 19:42Z as shown in Figure 5.21. In reflectivity, the only evidence for



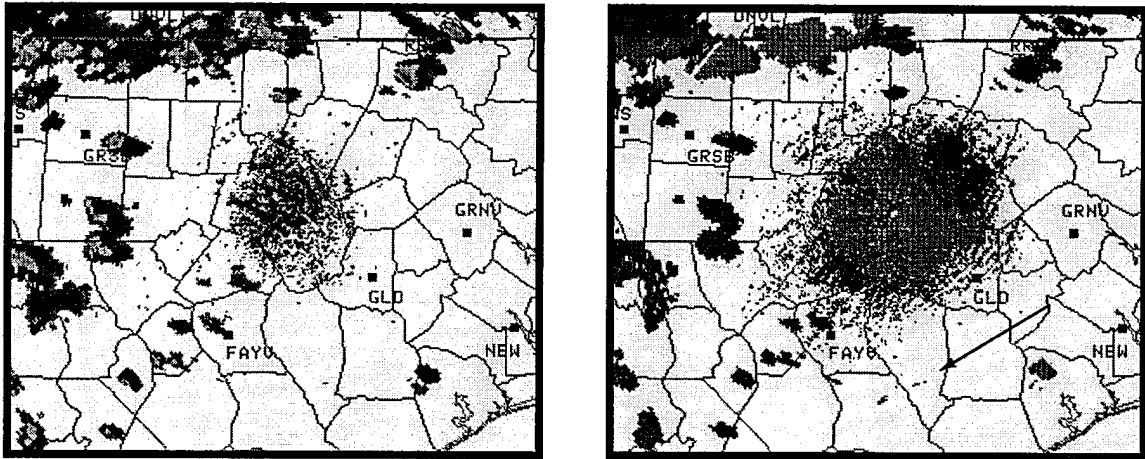


*Figure 5.21a and 5.21b. Radar reflectivity and velocity at 1942Z. Note that UMB is not visible in reflectivity but is just becoming visible in velocities southeast of Fayetteville.*

the UMB is one weak, shower; however, the feature is just becoming visible in Doppler velocity, as indicated by the arrow in Figure 5.21b.

At 20Z, the pressure gradient is tightening significantly throughout the state as the frontal system has crossed the mountains and now lies just northwest of GSO. The UMB continues to propagate inland and the dewpoints at ILM, NCA, and NKT (see Figure 5.26) continue to fall. Both boundaries (sea breeze and UMB) are located in a data void area at this point and the satellite imagery is not helpful in determining the locations of the features. The UMB is located about 55 nm from the radar at this point, and is visible only in Doppler velocities and not the reflectivity field (Figure 5.21). The radar beam appears to be intersecting the top of the feature which indicates the boundary is about 5500 feet deep.

By 21Z, the feature has moved to within 40 nm of the radar site. It is estimated that its rate of movement is about  $5\text{--}7\text{ ms}^{-1}$  (12-15 mph) at this point. To the south, we can detect the feature up to about 5500 feet as mentioned earlier. However, when the radar beam is directed to the east, the feature is visible up to about 6200 feet (Figure 5.22).

Also of interest is that just ahead of the feature by about 16 km, there appears to be a similarly shaped feature that cannot be resolved due to the proximity to the radar. This is most clearly depicted in the Doppler velocity field shown as Figure 5.22. It is felt that this is an area of increased convergence resulting from the close proximity of the UMB to the trough depicted in the Figure 5.23 mesoanalysis. This is not the only possible explanation for this feature. It may be a shallower feature which has just become visible to the radar as it moved inland. Alternatively, the UMB may actually be a pulsed type of phenomenon and the radar now resolves two features, the new shallow one and the deeper one which has been visible for some time. It is impossible to determine for sure.

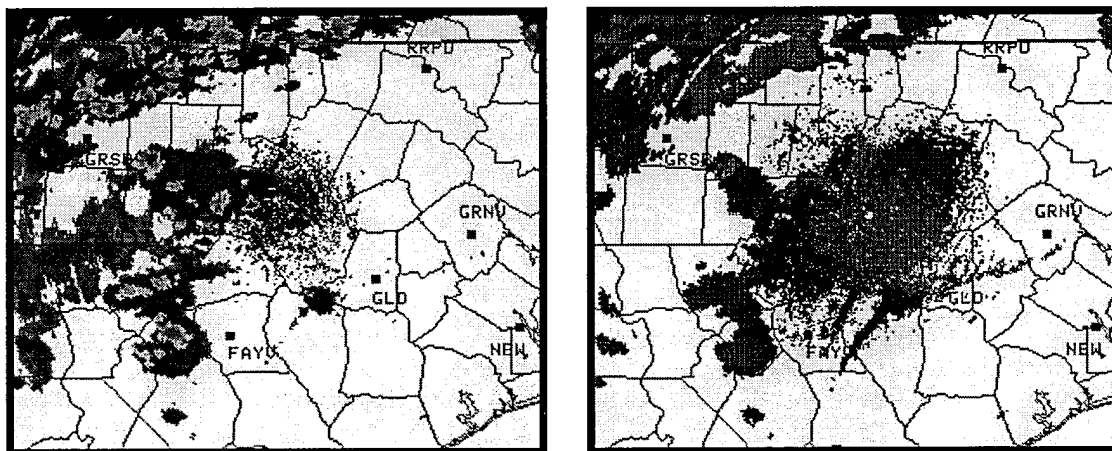


*Figure 5.22a and 5.22b. Radar reflectivity and velocity at 21Z. UMB is clearly depicted in velocity field and is just becoming discernible in reflectivity.*

During this time period, the UMB interacts with the prefrontal trough and produces a shower which rapidly decreases in intensity. Behind the boundary, the temperature at ILM dropped 2°F in the last hour and the dewpoint dropped 7°F. At NCA and NKT, the dewpoint dropped 2°F and 4°F respectively. At Newbern (EWN) the dewpoint dropped 5°F while the temperature was unchanged, indicating the feature has just passed that location.





By 22Z, it appears that the UMB moved through the first trough and is beginning to interact with the front. It is still very difficult to detect in the reflectivity field but is very obvious in the Doppler velocities (Figure 5.24b). A drop in dewpoint occurs during the next hour at GSB from 60 to 44°F. During the same time period, the EWN dewpoint decreases from 58 to 50!

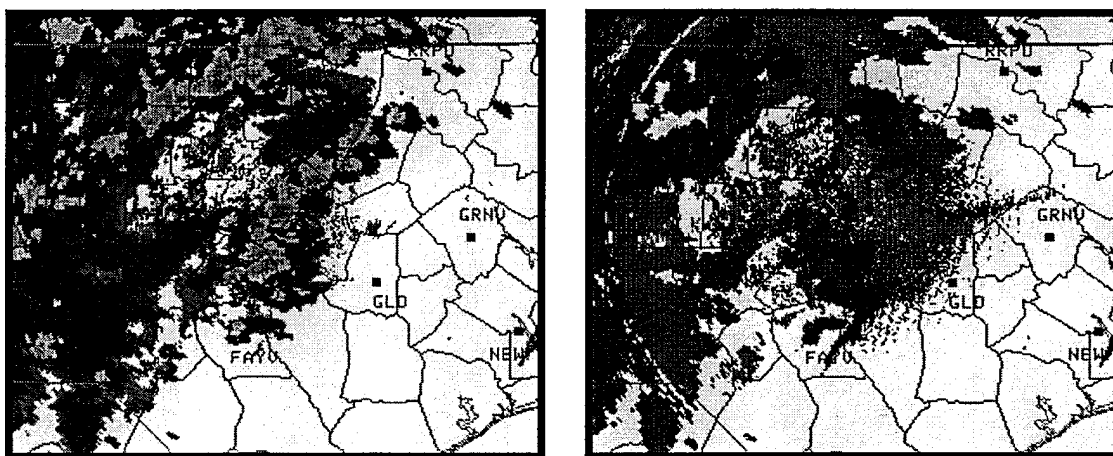


*Figure 5.24a and 5.24b. Radar reflectivity and velocity at 22Z.*

By 23Z, the UMB and prefrontal trough and the front are interacting. It appears that the collision actually weakened the frontal system as the showers decreased both in intensity and rate of motion. It is believed that the entrainment of low  $\theta_e$  air, which characterizes the UMB, was responsible for diminishing the convection. At this time, the dewpoints along the coast are beginning to increase. ILM rose from 60 to 63, NCA rose from 50 to 58.

Now that the satellite imagery, radar data, and the mesoanalysis have been presented, the most obvious question concerns the identification of the feature. Without the aid of a mesonet, it is difficult to resolve this type of boundary, however, there is some data available which will allow at least some speculation.

As previously mentioned, it is likely that someone viewing the satellite data would come to the conclusion that the UMB was a sea breeze. However, the above discussion documents the highly abnormal characteristics associated with the boundary such as the extremely dry air and the diminishing of all convection with which it comes into contact. The meteograms in Figure 5.26 show the approximate time the UMB passed each station. At this time, it is not known whether the UMB is a result of the sea breeze or if the two are independent of each other.

It would appear that the first step in resolving the question of the identity of the UMB would be to determine the source of the dry surface air because the drying was significant. ILM began the day with a dewpoint of 69°F, which corresponds to a mixing ratio of approximately 14.2 g kg<sup>-1</sup>. The lowest dewpoint recorded at ILM for the day was 53°F, which corresponds to a mixing ratio of about 8.2 g kg<sup>-1</sup>. In comparison, EWN and NCA, which began the day with dewpoints of 65 and 66°F respectively, both went down to 50°F for a mixing ratio of 7.5 g kg<sup>-1</sup>.

In an attempt to “find” the dry air, Sea Surface Temperature (SST) data was acquired for the days in question. Although much of the 26 May SST data was contaminated by cloud cover, the 25 May temperatures could be substituted since they should be representative of the temperatures for the next day. It was found that the temperature along the coast from MYR to NKT ranged from about 65 to 70°F (the HAT dewpoint ranged from 67 to 70°F throughout the event). If we assume that the dewpoints over the ocean are within two or three degrees of the temperature, then it is unlikely that air parcels with dewpoints of 50°F and less came from over the ocean. If we look upwind, we find that the minimum dewpoints were in the middle to upper 60s. Again, it appears unlikely that the low moisture parcels were advected into the area horizontally. For these reasons, the only location from which the air could have come is from above.

Assuming that the HAT sounding (Figure 5.25) was representative for all of the coastal stations, this means that in order for this air to have come from above, it would have originated from between 800 and 850 mb. This is not totally unreasonable since drier air is usually mixed down from above when the nocturnal inversion is broken. However, this is considered to be a turbulent/random process. In this case, it would appear that the breaking inversion actually created a coherent, long lived feature which propagated for 130 km and which could be detected on radar moving at speeds over 10 mph.

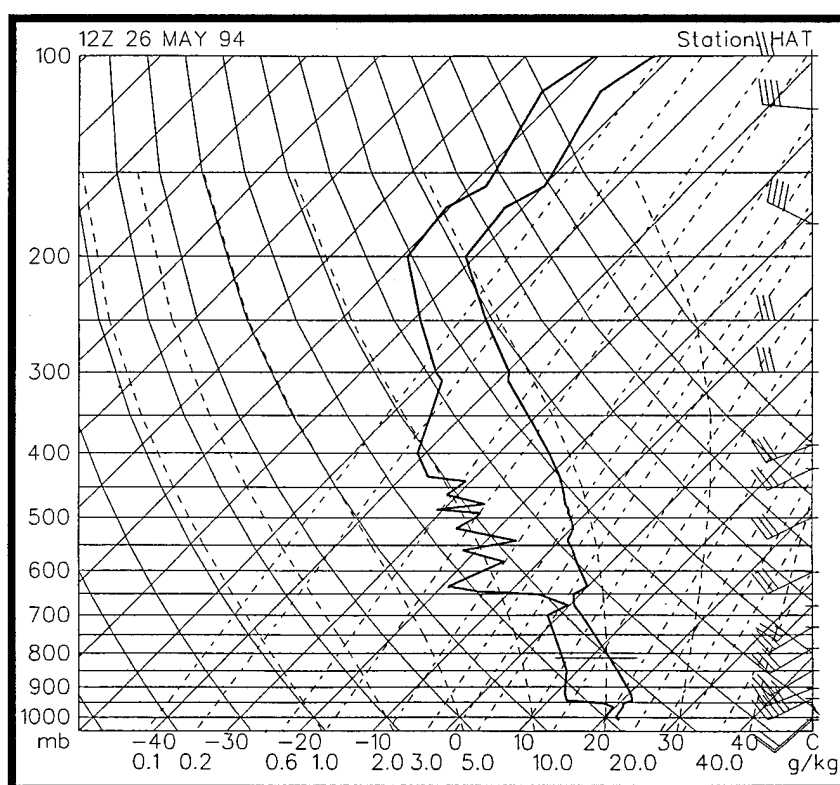


*Figure 5.25. 12Z HAT sounding.*

If the breaking inversion was responsible for the formation of the UMB, it is instructive to consider how the temperature profile would have changed with surface heating. Using the HAT 12Z sounding, and assuming it was representative for the east coast, the temperatures at the surface must rise to about 81 to 82°F in order to break the inversion. The first coastal station to reach that convective temperature was ILM with a temperature of 84°F by 15Z. It is interesting that this is the approximate time we have the first indication of the UMB in the satellite imagery. This is also the point at which the ILM dewpoint started its downward trend. The temperature at each station was examined to determine if the boundary appeared to "pass through" the station at the time the temperature reached the convective temperature of 81°F. This definitely was not the case because the boundary did not pass through NCA until 1900Z which was 4 hours after the convective temperature was reached.

This brings up one of the most interesting aspects of this case. We could actually see this feature in the radar imagery as it moved inland at a significant pace. Yet the reflective properties of the feature were very unusual. For instance, it was not visible in the reflectivity field until it was very close. This indicates that there were few or weakly reflecting scatterers or that the reflectivity was the result of Bragg Scatter. Since other boundaries during the event were reflective, it is felt that the Bragg Scatter hypothesis is probably most correct. This is supported by the well known and previously discussed dependence of the atmospheric refractive index on the moisture of the air. This feature was extremely dry as compared to the ambient environment; the resultant mixing of the different air parcels could easily contribute to Bragg Scatter.

It has been noted that the feature was weakly reflective; however, it would probably have appeared as approximately -10 to 0 dBZ if the radar had been in clear air mode. Since the precipitation mode will only display reflectivities of 5 dBZ or greater, it was just barely

discernible. This does not mean the radar did not “detect” the feature. To the contrary, the radar vividly displayed the feature in the velocity field.

At this point, we cannot definitively say what the feature was or was not, but there are a few statements which can be made with some certainty:

1) The feature was associated with the entrainment of drier air from aloft which was reflected in the surface station reports.

2) The feature effectively terminated all convective activity with which it became associated, even in a highly dynamic environment.

3) The UMB moved quickly inland as a coherent entity; its progress was tracked using both satellite and radar imagery.

4) The top of the boundary was approximately 1676 m high.

5) The feature was surface based as evidenced both by the drying at the surface and the fact that the radar continued to slice the feature at successively lower levels as it moved closer to the radome. Therefore, the feature was about 5500 feet deep.

6) The radar imagery revealed that the feature was at least 80 nm in length.

7) It moved inland toward falling pressures ... (like a density current). It may have moved in other directions too (seaward) but we could not track it.

8) It moved perpendicular to the ambient winds and had no obvious “following flow” (like a gravity wave).

9) The boundary lifted parcels to the LCL as it moved because there were clouds associated with the feature in the satellite imagery; however, the clouds were not deeply convective and dissipated quickly.

10) The boundary was not a sea breeze, at least in the classical sense of the term.

11) The feature appears to be a substantial boundary. Radar imagery shows that for at least one hour beyond the intersection of the UMB and the front, the environmental flow still “feels” the presence of the boundary (unlike a gravity wave). The intricate detail

depicting this would be lost in the black and white imagery used in this discussion and is therefore not included.

With these thoughts in mind, a hypothesis follows. The 1231Z satellite imagery (not shown) clearly shows the early morning low level clouds along the NC coast. Just 30 minutes later, the imagery (Figure 5.18b) shows that the cloud layer is being eroded away by surface heating. By 1400Z, the clouds over ILM have completely dissipated, leaving the more northerly stations under rapidly decreasing clouds. At this point, it is expected that surface thermals are penetrating the nocturnal inversion as previously discussed.

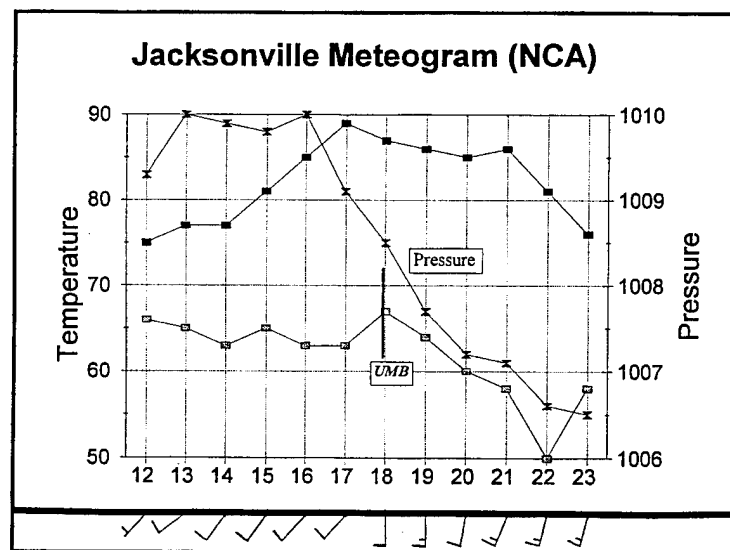
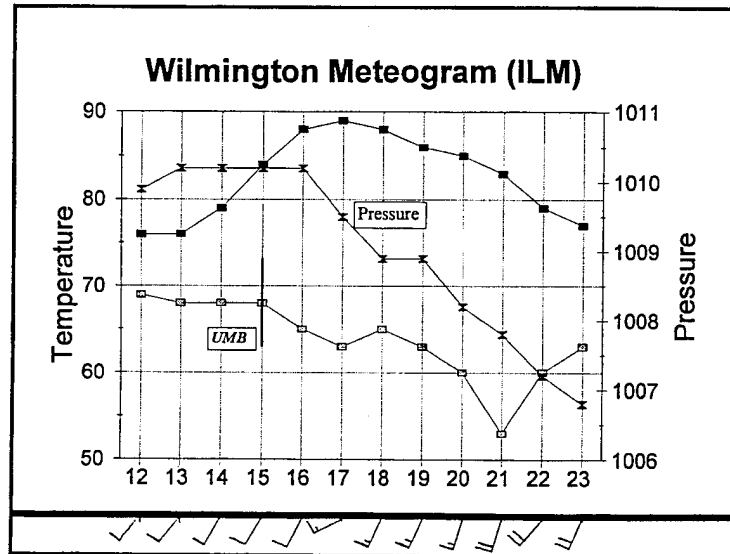
It is believed that the penetration of the inversion actually is occurring in a discrete location (over ILM) and that it has not been eroded away further north. This "puncture" in the "cap" allows the drier air aloft to be funneled downward, much like water going down a drain. It is believed that this high momentum, low  $\theta_e$  air contacts the ground and spreads out, much like a thunderstorm outflow. This is how the UMB is able to propagate against a gentle upslope at the speeds recorded. If the inversion had been broken at nearly the same time along the coast, there would have been no "funneling" of the energy and no significant acceleration downward.

Once the "penetration" of the inversion occurs, the dry air starts mixing down, eroding the inversion along the edges of the puncture and evaporating the moisture contained in the lower levels (clouds). At this point, there is no longer a focusing point through which the air moves toward the ground.

It is not believed that the movement of this feature resulted in significant convergence at the surface, which would have made the feature more highly reflective to the Doppler radar. It is felt that as it moved, the drier air rapidly mixed with the environmental air and the radar detected the centimeter scale eddies associated with this

mixing process (Bragg scatter). This would definitely explain the low reflectivity of the feature.





Figures 5.26 a, b, c, d, e, and f. Meteograms. Pressure, temperature, dewpoint and winds are depicted. Times shown are local.

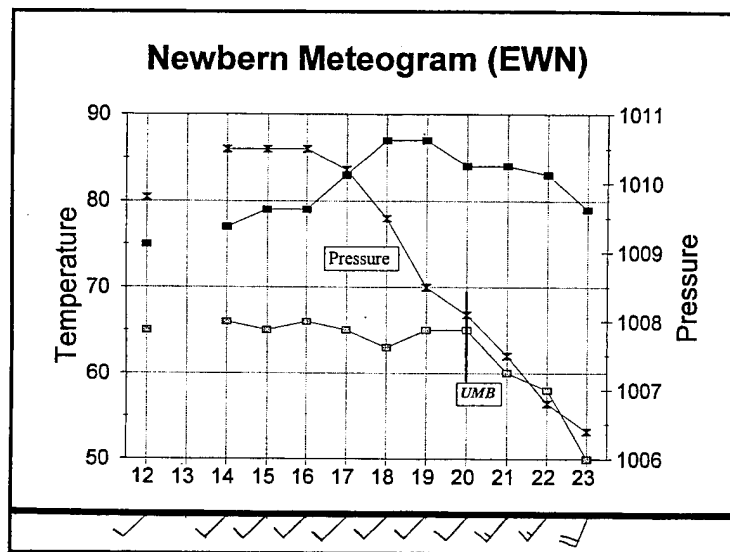
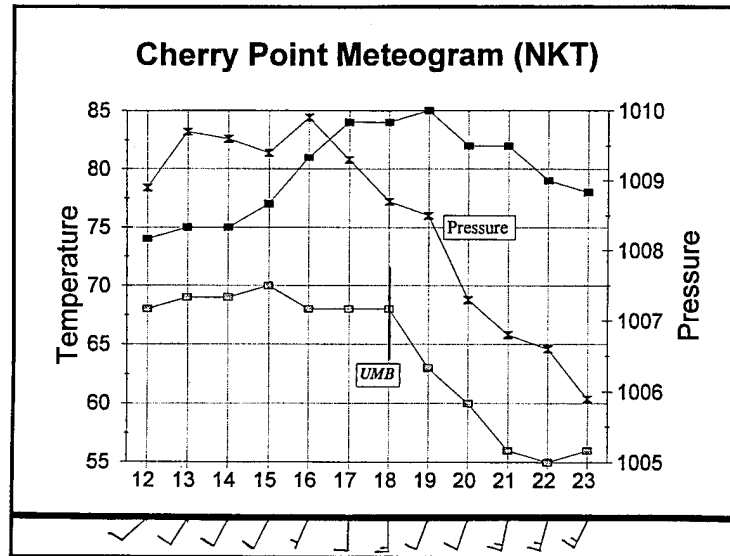


Figure 5.26 c and d.

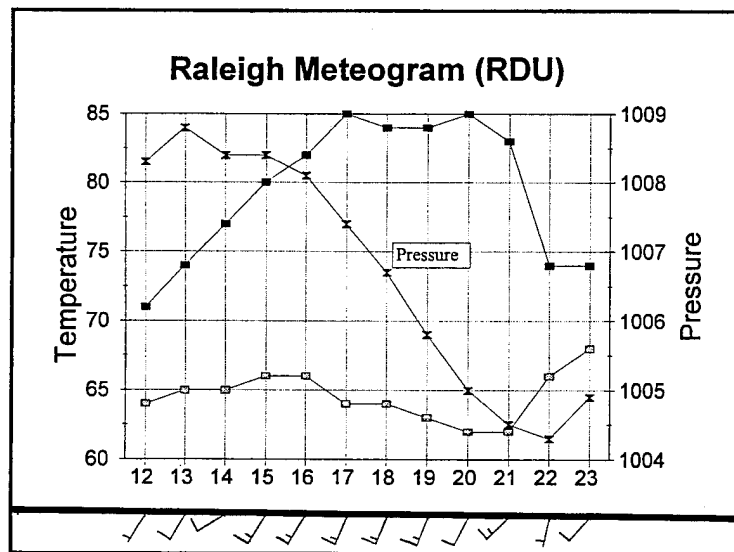
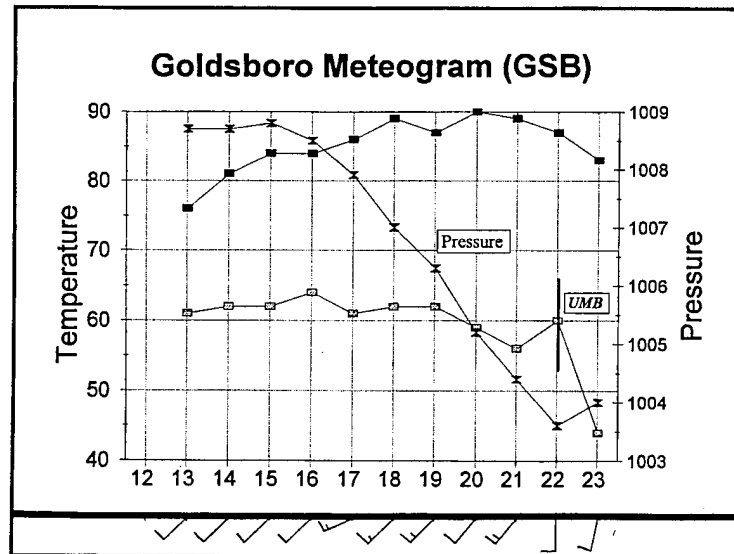


Figure 5.26 e and f.

### 5.3 Case 3: 12 June 1994

This case has been selected for inclusion in this work because it is an excellent example of typical summertime weather in North Carolina. It also provides an example of a sea breeze which propagates significantly further inland than is normally thought likely. On the morning of 12 June, 1993, the Bermuda High was the dominant feature affecting the weather in NC. The axis of the ridge extended from west to east across the center of the state is shown in the 12Z mesoanalysis (Figure 5.27). Also depicted are two very weak stationary troughs embedded in the ridge. As expected, flow on the north side of the ridge axis is generally from the west and widely varying. On the southern side of the ridge, the winds are generally easterly and variable.

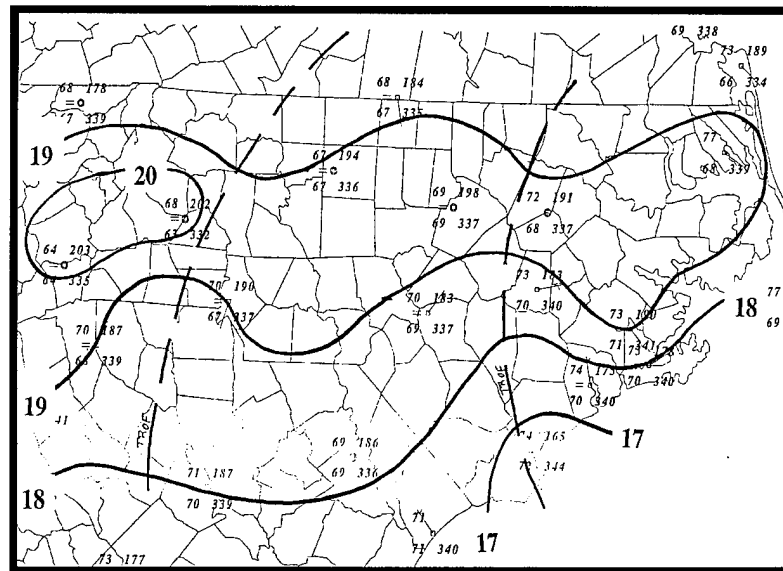


Figure 5.27. Mesoscale analysis for 12Z, 12 June 1994.

Unfortunately, the morning sounding data from HAT is unavailable for this case, but data from GSO is available. The GSO sounding is used and modified to represent the environment in which the sea breeze moves ashore. It is recognized that due to the orientation of the ridge axis, the low level flows at HAT and GSO are directed opposite

each other. The stability parameters for the maximum heating in the afternoon are as follows: Lifted Index = -4; Showalter Index = -1; Total Totals = 49; CAPE = 1151; K Index = 36; Sweat Index = 235; and CIN = 10.

The upper level charts showed that the ridge was also found at the 700 mb level and was associated with dry air. At 500 mb, weak negative to neutral vorticity advection is occurring. With evidence of weak instability, the surface ridge, and dry air aloft, it was expected that there would be very few showers during the day, but a weak sea breeze was expected to be present along the coast.

The first time for which all three data sets are available is 17Z; Figure 5.28 depicts the radar and satellite imagery, as well as the mesoanalysis. The showers along the sea breeze front shown in the radar imagery are generally about 40 to 45 dBZ. The mesoanalysis shows that the ridge axis is weakening as the sea breeze advances toward the easternmost trough.

Figure 5.29, which is a radar derived vertical wind profile at 1747Z, clearly shows easterly flow *ahead* of the sea breeze. This type of synoptic flow was studied by Eilts et al. (1991) and Wakimoto and Atkins (1994). Their research showed that this type of flow results in (1) a sea breeze which sets up early; (2) a weak, diffuse sea breeze; and (3) a sea breeze which propagates a significant distance inland.



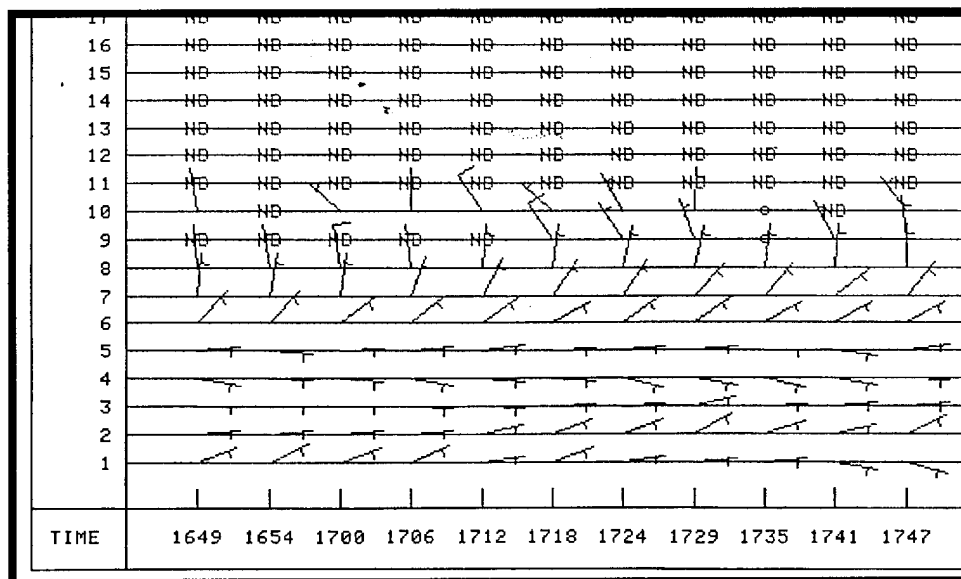


Figure 5.29. Radar wind profile at 1747Z from the Raleigh WSR-88D. Wind barbs depict knots.

The 18Z data show that the strongest and most persistent showers produced by the sea breeze were actually the result of the interaction of the sea breeze with the “sound breeze” as discussed in section 4.1.2 and shown in Figure 5.30. This is often seen to occur on one side or the other of Pamlico and Albermarle Sounds. In this event, both sound breezes were evident. The 18Z satellite imagery shows approximately parallel bands of slightly enhanced cumulus and towering cumulus associated with the surface troughs.

By 20Z (19:43Z radar image) the easternmost trough is producing weak convection and the sea breeze continues to move westward. The sea breeze is about 40 nm from the radar and the density current is just becoming visible to the radar (see Figure 5.31). This means that the feature is approximately 3500 ft deep. Figure 5.32 is a radar image at 20:24Z which clearly depicts the sea breeze in Doppler velocities. However, the speeds indicated are 0 to 1 kt inbound. Even in the color imagery, the majority of the flow field is depicted as “zeros.”

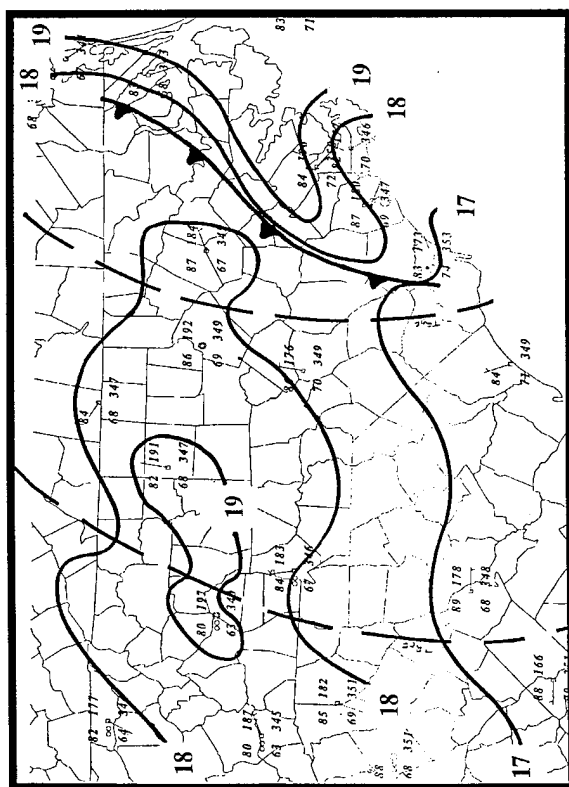
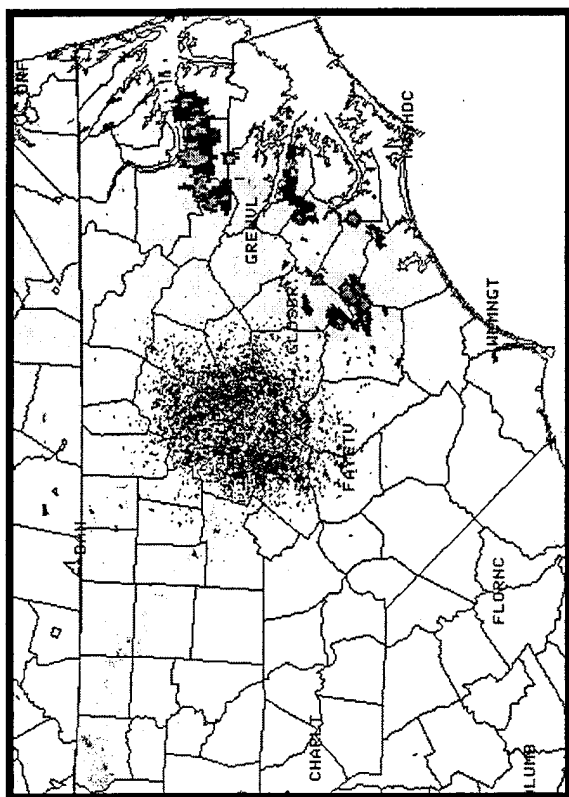


Figure 5.30. Mesoanalysis, radar, and satellite imagery for 18Z.



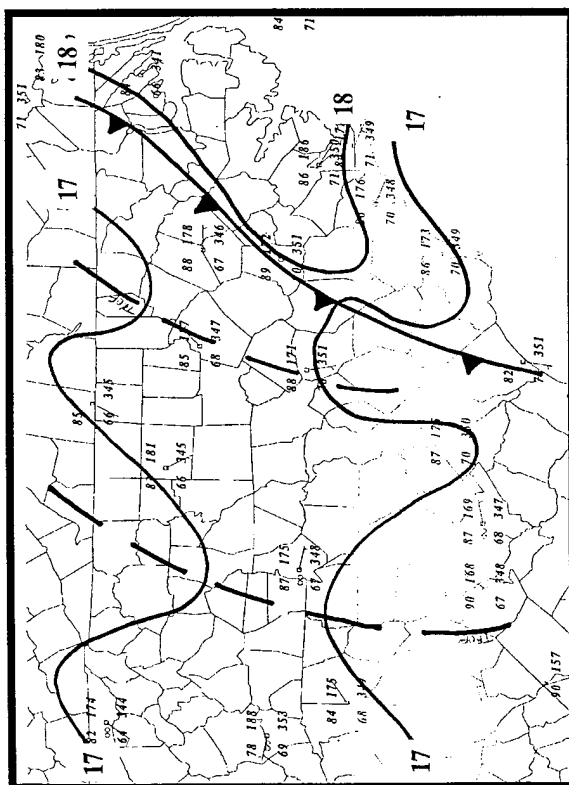
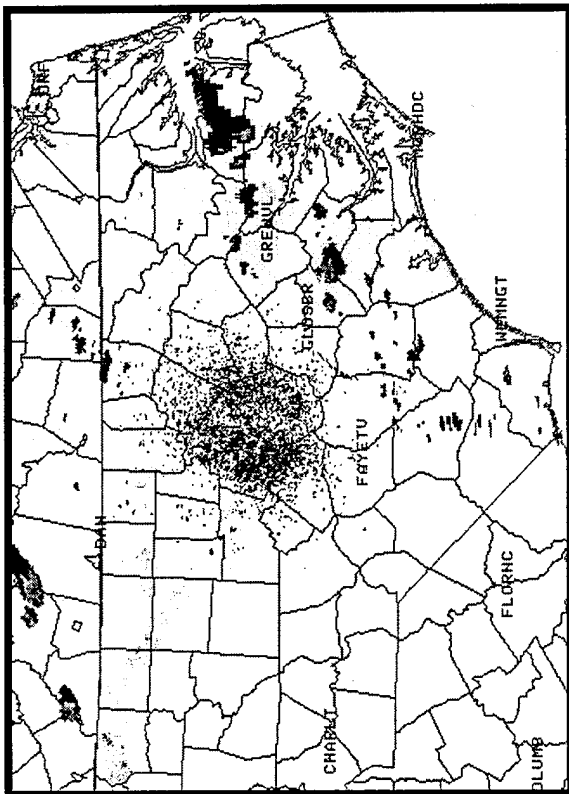


Figure 5.31. Mesoanalysis, radar, and satellite imagery for 20Z.

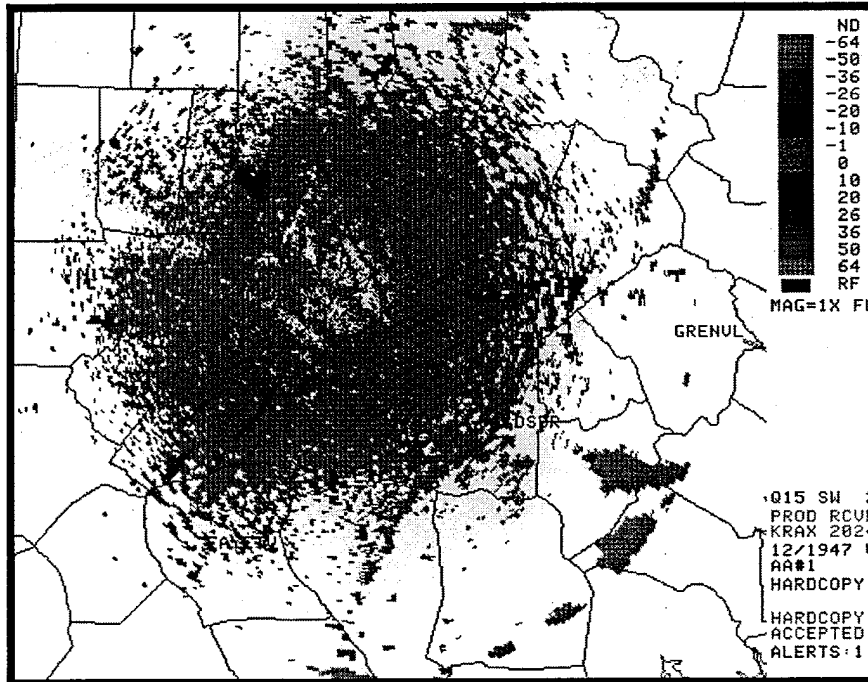


Figure 5.32. Depiction of sea breeze in Doppler velocity.

This is one of the primary problem areas discovered with the WSR-88D during this research. As shown in Figure 2.1, the Doppler velocity display is not symmetric about zero. The system will display speeds as low as 1 kt inbound, but will not display outbounds until the speeds are above 10 kts. The result is that on a weakly forced day, such as shown in this case, the only velocities depicted are -1 kts and 0s. The radar is displaying the boundary because there are scatterers present due to the convergence at the surface.

By 22Z, the sea breeze has merged with the easternmost trough with no significant increase in convection noted (Figure 5.33). At this point, it appears that the density current has moved into the area of lowest pressure in the area. The current is traveling at about  $3.9 \text{ ms}^{-1}$  (8.5 mph).

At 23Z, the visible satellite imagery does not provide any significant information due to the low sun angle. The radar data however (Figure 5.34), shows that the sea

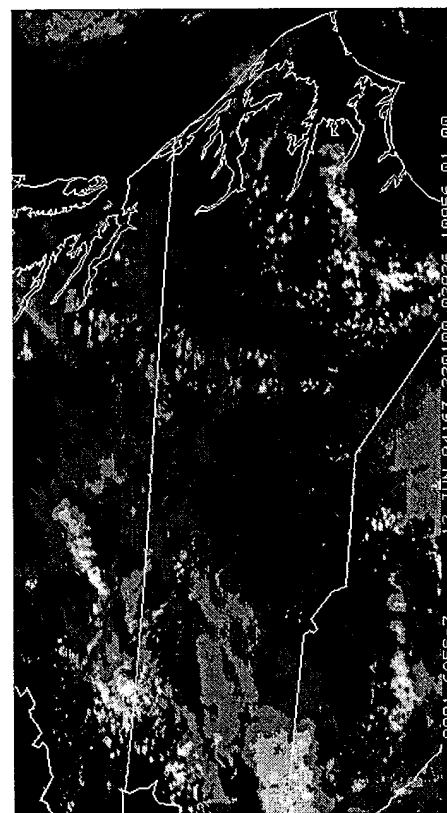
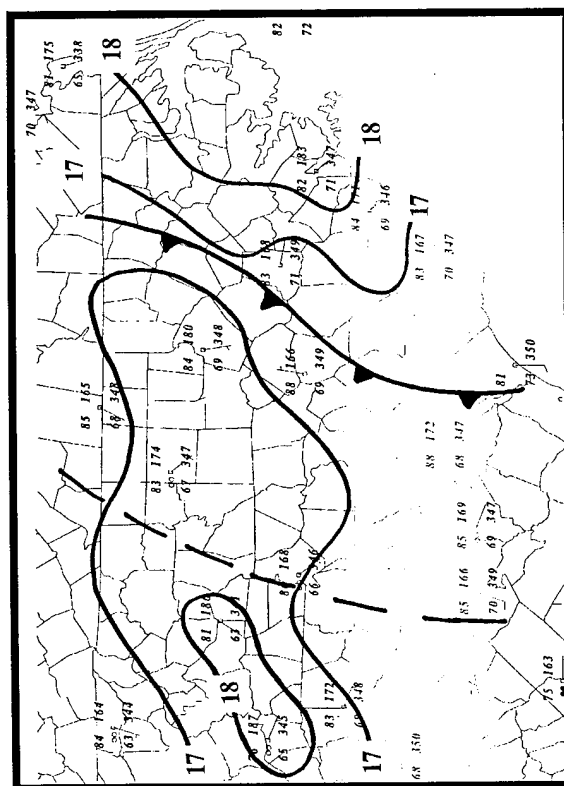
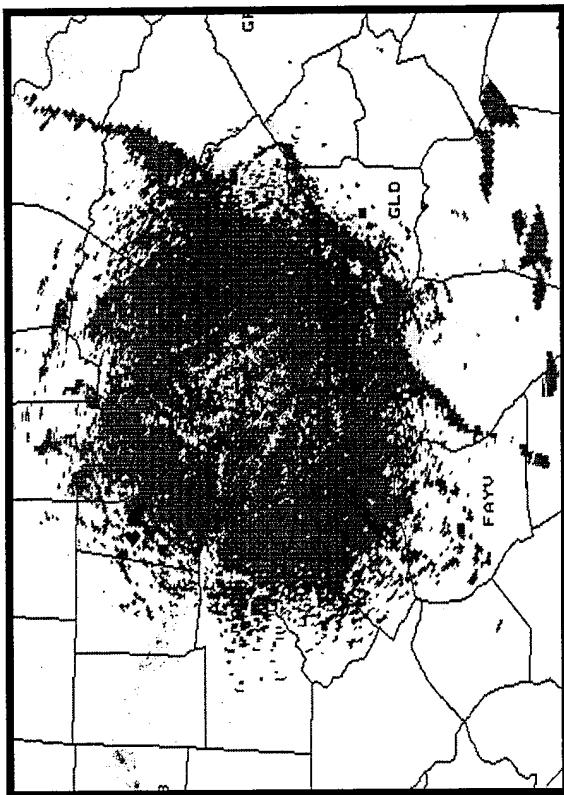
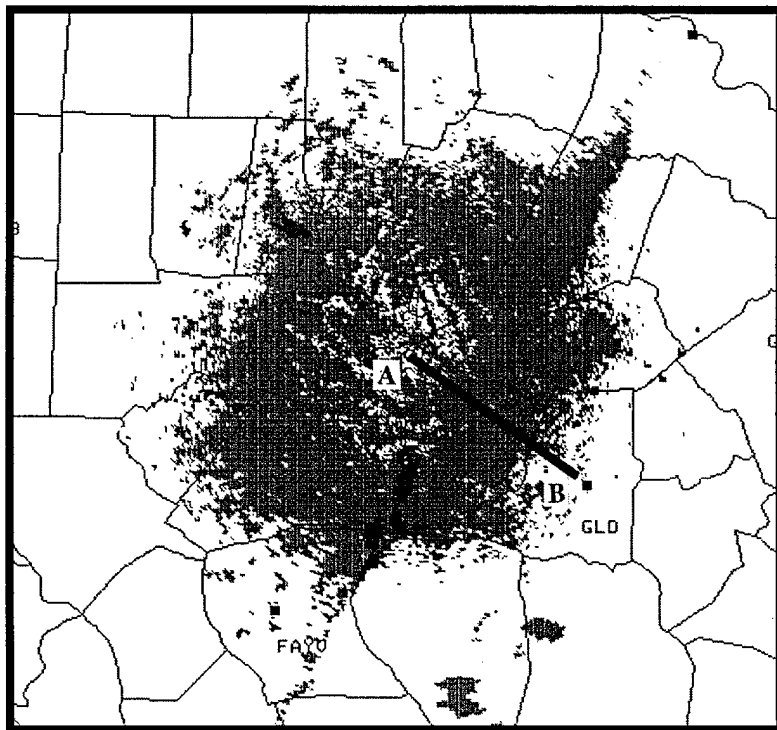


Figure 5.33. Mesoanalysis, radar, and satellite imagery for 22Z.

breeze is located just to the east of the radome. The mesoanalysis (Figure 5.35) shows that the trough into which the sea breeze moved appears to be propagating to the west with the boundary. The results of a cross section along a radar radial and perpendicular to the boundary is depicted in Figure 5.36. The head of the density current, which is indicated by -1 kt inbound velocities (obviously not discernible in the black and white imagery) is outlined. Above the density current, there are two pixels representing outbound velocities of 10 kts. The vertical profile indicates the winds at 10,000 ft are westerly at 10 to 15 kts. This is the approximate height at which the two outbound pixels are located. This is important because one could easily interpret the outbound velocities to be the return flow of the density current. That would put the top of the density current at about 7000 ft.



*Figure 5.34. Doppler velocity imagery at 2305Z showing sea breeze just to the east of the radome. Solid line A-B depicts cross section shown in Figure 5.36.*

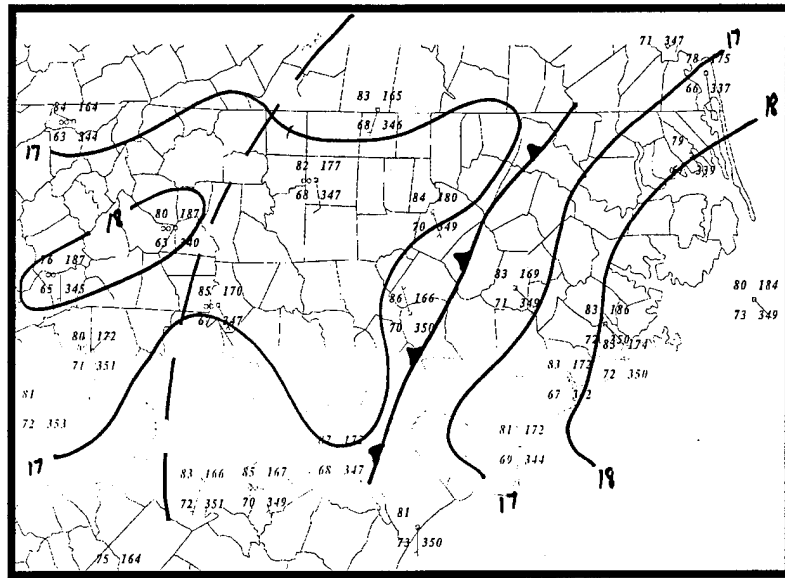


Figure 3.35. Mesoanalysis at 23Z.

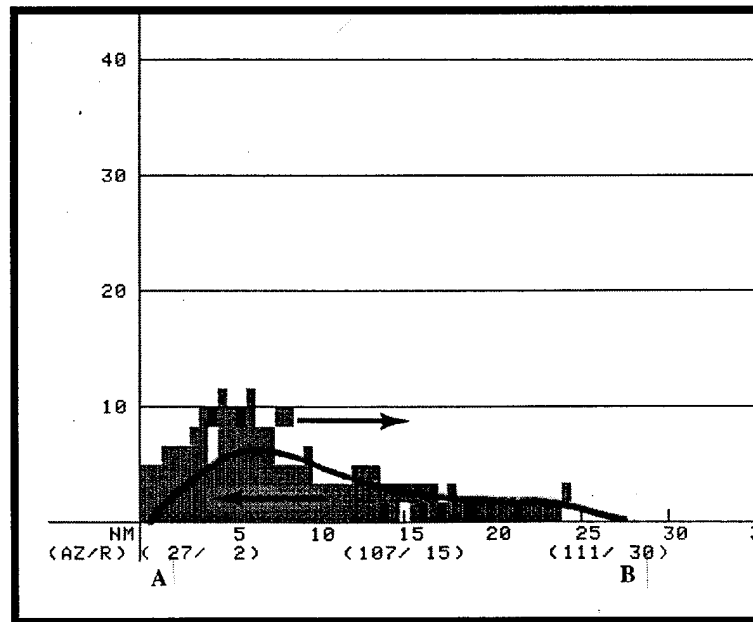
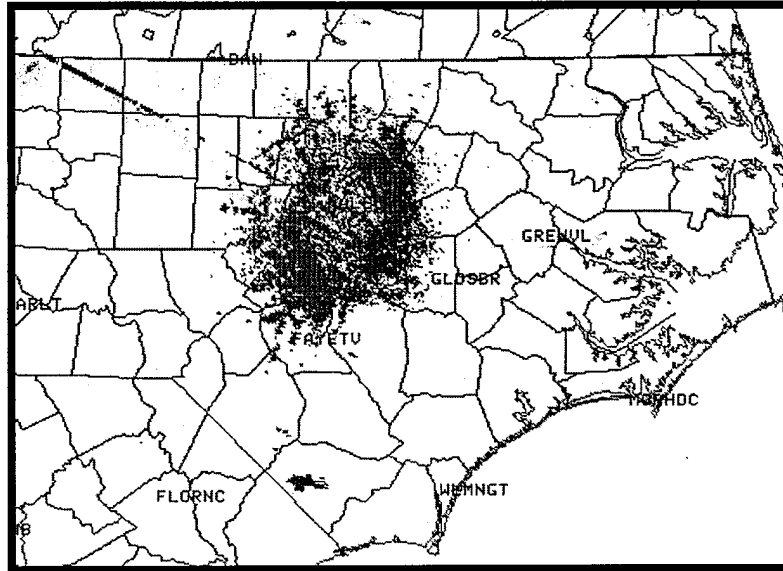


Figure 5.36. Cross section through sea breeze.

The last image (Figure 5.37) at 00:27Z shows the sea breeze directly over the radar site. This means that feature has traveled at least 120 nm inland or nearly 200 km!



*Figure 5.37. Depiction of sea breeze directly over radome.*

As discussed in the section on sea breezes, the normal propagation distance is usually considered to be 30 to 60 nm (50 to 90 km) (Zhong and Takle, 1992). It is interesting to consider just what caused the feature to move inland so far. In this situation, the general synoptic situation resulted in weak onshore flow. As discussed earlier, this type of situation often results in a significant propagation distance. It is believed that the series of troughs in the ridge, which were parallel to the coast and the sea breeze, served to “guide” the sea breeze inland. Density currents propagate due to the differences in density of the fluid ahead of and behind the boundary. With the trough ahead of the sea breeze, the densities were less than those behind the boundary. Therefore, there was a net acceleration toward the trough. Once the boundary “dropped into” the trough, the westward progression seemed to be slowed. It was unlikely at that point that the density current would move “against the gradient” into the area of relatively higher pressure.

## **6. SUMMARY AND CONCLUDING REMARKS**

This work was necessarily very broad since it was really the first time that such research has been conducted in eastern NC. The work took several directions which included a basic study of radar theory, a study of the different types of features which exist in the NC PBL, and a comparison of the relative utility of data acquisition platforms in NC.

### **6.1 SUMMARY**

An investigation was conducted of the NC PBL in search of boundaries which are common in this region. The following types of features were found and documented: thunderstorm outflows; sea breezes; piedmont troughs; troughs; horizontal rolls; fronts; thermal/moisture boundaries; prefrontal troughs; and moving and stationary boundaries of unknown origin. Although no case was studied based solely on thunderstorm outflows, these features were found to be the most prevalent in the NC PBL, comprising about 26% of the 95 boundaries studied. Sea breezes were found to be the next most important feature, comprising about 20%. One of the interesting factors uncovered about the sea breezes is that they appear to propagate significant distances inland, more frequently than previously thought. The piedmont troughs, which made up about 14% of the total boundaries, were features which we did not expect to find. They appear to be "heat lows" or actually "heat troughs" which form in the western Piedmont/eastern Coastal Plain region under intense diurnal heating. The features were characterized by a pressure deficit of about 1.5 to 2 mb and were capable of producing convection without any interaction with other features. The piedmont troughs were identified after-the-fact in mesoscale analyses and as such were not primary features on which the data was collected. This makes them even more significant since they occurred on 13 out of the 23 days studied.

The convective activity of all of the boundaries was studied and the results were compared to those results from Wilson and Schreiber (1986). In general, it was found that

any type of boundary which occurred in NC was more likely to be convective in NC than in CO. It was also found that NC boundaries were nearly twice as likely to be involved in a collision with another feature as those in CO. These differences were attributed to differences in CAPE and geology in the two regions.

The *type* of boundary interaction, defined by Wilson and Schreiber (1986) as "collision," "merger," and "intersection" was studied as well. The CO study revealed that collisions, which result in more vigorous interaction, resulted in increased chances for convection. The results of such a test in NC were not conclusive and it is believed that the type of collision is not a good indicator of whether or not convection will form in NC. Indeed, one interesting finding about boundaries in NC is that they were often *autoconvective*. That is, they often produced convection without any interaction whatsoever with other features.

The movement of the boundaries was studied in the hopes that it would provide some information on whether a feature could be expected to be autoconvective. It was hypothesized that moving boundaries would be more likely to produce convection without interaction with other features. Although there were too few features studied in each category for the results to be conclusive, the results tend to show that there is no dependence of movement on autoconvective activity. It is believed that other factors, such as winds aloft and thermodynamics, are more important predictors of convective activity.

One of the goals of this work was to determine the "utility" of the WSR-88D as compared to other tools at hand as well as the older radar system. Because of the way in which the data were collected (the radar was the primary tool used to locate boundaries) an objective comparison of the relative importance of the radar, satellite, and mesoscale analysis could not be conducted. However, it was found that in order to gain the maximum



amount of information about any one specific boundary, it was necessary to use *all three platforms*.

The new radar was compared to the older WSR-57 by using known thresholds of each of the systems. As expected, the increased sensitivity of the WSR-88D, even in the precipitation mode, allows forecasters and researchers to have a more complete understanding of the convective activity which is occurring around them. The majority of the features observed in this research would not have been displayed on the older system.

Three case studies were conducted. The first involved the clear air detection of a weak thermal/moisture boundary by the radar. It was found that the radar gave over 1.5 hours of lead time on a severe-local event, which would have been impossible if the older system were used. The second study involved a feature which is still categorized as "unknown moving." This boundary moves inland from the coast and is associated with very dry air which is believed to be entrained from aloft. The feature was weakly reflective and was only identifiable using the Doppler velocity field. Obviously, this feature would have escaped detection had the WSR-88D not been in use. The final case involved a sea breeze which moved 200 km inland. While this occurrence was not the norm, neither was it unique.

## **6.2 CONCLUDING REMARKS**

There were several interesting radar-related findings which occurred throughout this research. A discussion has already been conducted on the difficulty of switching the radar into clear air mode and keeping it there, and also on the asymmetric Doppler velocity scale. In barotropic conditions such as those present in NC in the summertime, the clear air mode and the ability of the radar to depict 1 kt outbound velocities are of extreme importance if subtle features are to be routinely detected. In the summertime, the default mode of the radar should be the clear air mode, from sunset (as diurnal convection diminishes) until

thunderstorms threaten part of the warning area the next day. This mode is most capable of providing the maximum amount of information about subtle PBL features in the pre-convective environment and should be routinely used.

One thing that this researcher learned during a summer of working with the radar was that *everything* depicted by the radar was important for one reason or another. Even the ducting and ground clutter observed in the mornings, caused by the nocturnal inversion, provides information on the relative depth and strength of the inversion. Looping these images shows the speed at which the inversion is being eroded away. This can be translated to an approximate time of inversion breakdown. With the radar in clear air mode, the distance out to which there are radar returns gives some indication of the depth of the mixed layer (Wilson and Mueller, 1993). Zones of enhanced reflectivity aloft, which often are unnoticed, at times have been seen to be precursors of thunderstorm activity. This was observed in the current research as discussed above. Horizontal roll features, even if they are not producing clouds, are creating weak zones of convergence at the surface and transporting moisture to the top of the PBL. These weak features therefore are "priming" the atmosphere for deep convection later in the day. In short, it was found that just about *any* linear feature shown by the radar has some meteorological significance and should be investigated.

Often, the investigations of weak PBL features made use of the  $\theta_e$  fields. These were found to be much more useful in detecting weak boundaries than was moisture convergence, especially in weakly forced regimes. Forecasters who are genuinely interested in understanding the state of the PBL should spend some time conducting a mesoscale subjective  $\theta_e$  analysis once the nocturnal inversion breaks.

### 6.3 RECOMMENDATIONS FOR FUTURE RESEARCH

Since this research was the first of its type in the mid-Atlantic region, many interesting features were observed which should be further investigated. Obviously one of the surprises of this work involved the distance of propagation of some sea breeze events. It is believed that by using GOES 8 imagery and Doppler radars at Morehead City and Raleigh, much insight can be gained concerning this phenomenon. As shown, sea breezes are very important in NC, and there simply is not enough known about how and why they propagate in the manner observed.

Another of the interesting and unexpected features observed during this work was the Piedmont Trough (PT). This boundary was observed to produce convection on numerous occasions. It is thought that the feature is related to both diurnal heating and to local geology. There is probably a strong association with this feature and the sea breeze as well. It is believed that a modeling study of the eastern Piedmont and Coastal Plain would be of immense value to local meteorologists. Such a study must be able to resolve the heterogeneities observed in the NC soil types and include microphysics describing the soil air interface. This would prove invaluable to the study of the NC sea breeze and local PBL features such as the PT and horizontal rolls, and their interaction.

Interesting work could be conducted using reflectivities aloft to forecast convection. No emphasis was placed on this in the current work, but researchers in some parts of the country (primarily Florida) have had some success using these features to forecast thunderstorms. In the current work, several of these features were observed to precede thunderstorms up to one hour.

The Storm Total Precipitation product was used several times during this research; however, it has yet to be calibrated against "known" precipitation amounts. An appropriate study would be to conduct this calibration.

It appears that the future for remote sensors and Doppler radar in particular is certain. Relationships have already been derived for the dependence of reflectivity on the structure parameter (although significantly more study is needed in this area as well). The structure parameter is actually a function of moisture, temperature, velocity, and obviously the refractive index. It is only a matter of time before radars of variable wavelength and high power will be able to routinely sample the PBL and provide accurate information on temperature, humidity, turbulence, and the resulting turbulent fluxes. This will allow us to learn more about the microphysics involved in the lower part of the atmosphere, thereby allowing us to improve our prognostic models.

## LIST OF REFERENCES

- Ahrens, C. Donald, 1985: Meteorology Today, An Introduction to Weather, Climate, and the Environment. West Publishing Company, St. Paul, MN, 524 pp.
- Alberty, R., and T. Crum, 1991: The NEXRAD Program: Past, present, and future: A 1991 perspective. *Preprints, Int'l Conference on Radar Meteorology*, Paris, Amer. Meteor. Soc., 1-8.
- Battan, L. J., 1959: Radar Observation of the Atmosphere. Univerisity of Chicago Press, Chicago, 324 pp.
- Benjamin, Stanley, G. and Toby N. Carlson, 1986: Some effects of surface heating and topography on the regional severe storm environment. Part 1: Three-dimensional simulations. *Mon. Wea. Rev.*, **114**, 307-329.
- Biggs, W. G. and M.E. Graves, 1962: A lake breeze index. *J. Appl. Meteor.*, **1**, 474-480.
- Bluestein, Howard B., 1993: Synoptic-Dynamic Meteorology in Midlatitudes Vol II: Observations and Theory of Weather Systems. Oxford University Press, New York, 594 pp.
- Brown, R. A., 1972: On the inflection point instability of a stratified Ekman Boundary Layer. *J. Atmos. Sci.*, **29**, 850-859.
- , 1980: Longitudinal instabilities and secondary flows in the planetary boundary layer: A review. *Rev. Geophy. Space Phy.*, **18**, 683-697.
- Businger, S., W.H. Bauman III, and G.F. Watson, 1991: The development of the Piedmont front and associated severe weather on 13 March 1986. *Mon. Wea. Rev.*, **119**, 2224-2251.
- Christian, T.W., and R. M. Wakimoto, 1989: The relationship between radar reflectivities and clouds associated with horizontal roll convection on 8 August 1992. *Mon. Wea. Rev.*, **117**, 1530-1544.
- Cione, J. J., S. Raman, and L. J. Pietrafesa, 1993: The effect of Gulf Stream-induced baroclinicity on U.S. east coast winter cyclones. *Mon. Wea. Rev.*, **121**, 420-430.

- Daniels, R.B., H.J. Kleiss, S. W. Buol, H. J. Byrd, and J.A. Phillips, 1984: Soil Systems in North Carolina, Bulletin 467.
- Doviak, R. J. and Dusan S. Zrnic', 1993: Doppler Radar and Weather Observations. Academic Press, San Diego, 562 pp.
- Eilts, M. D., E. D. Mitchel, and K. Hondl, 1991: The use of Doppler radar to help forecast the development of thunderstorms. *Preprints, 25th Int'l Conference on Radar Meteorology*, Paris, Amer. Meteor. Soc., 63-66.
- Fankhauser, J. C., and A. R. Rodi, 1989: Kinematic and thermodynamic structure of radar-detectable clear-air boundary-layer convergence zones, *Preprints, 24th Conference on Radar Meteorology*, Tallahassee, 130-133.
- Fujita, T. T., 1963: Analytical mesometeorology: A review. *Meteor. Monogr.*, No. 27, Amer. Meteor. Soc., 77-128.
- Goff, R. C., 1976: Vertical structure of thunderstorm outflows. *Mon. Wea. Rev.* **104**, 1429-1440.
- Gossard, E. E., and R. G. Strauch, 1983: Radar Observation of Clear Air and Clouds. Elsevier Science Publishers B.V., Amsterdam, 280 pp.
- \_\_\_\_\_, 1990: Radar research on the atmospheric boundary layer. *Radar in Meteorology*, D. Atlas Ed., Amer. Meteor. Soc., 3-6.
- Hart, J.A. and J. Korotky, 1991: The SHARP Workstation v1.50: A Skew T/Hodograph Analysis and Research Program for the IBM and compatible PC. NOAA/NWS Forecast Office, Charleston WV.
- Hartfield, Gail, 1995: Cold-Air Damming: A classification and recognition scheme -- Preliminary notes and request for comments. National Weather Service Forecaster Memo.
- Houze, Robert A. Jr., 1993: Cloud Dynamics, Academic Press, Inc., San Diego, 573 pp.

- Keeter, K. K., S. Businger, L. G. Lee, and J. S. Waldstreicher, 1995: Winter weather forecasting throughout the eastern United States. Part III: The effects of topography and the variability of winter weather in the Carolinas and Virginia. *Weather and Forecasting*, submitted for publication.
- Klingbe, D. L. and D. R. Smith, 1987: Gust front characteristics as detected by Doppler radar. *Mon. Wea. Rev.*, **115**, 905-918.
- Knight, C. A. and L. J. Miller, 1993: First radar echoes from cumulus clouds. *Bull. Amer. Met. Soc.*, **74**, 179-188.
- Koch, S.E., M. DesJardins, and P. J. Kocin, 1983: An interactive Barnes objective map analysis scheme for use with satellite and conventional data. *J. Clim. App. Meteor.*, **22**, 1487-1503.
- , P. B. Dorian, R. Ferrare, S.H. Melfi, W.C. Skillman, and D. Whiteman, 1991: Structure of an internal bore and dissipating gravity current as revealed by Raman lidar. *Mon. Wea. Rev.*, **119**, 857-887.
- , J.T. McQueen, and V.M. Karyampudi, 1994: A numerical study of the effects of differential cloud cover on cold frontal structure and dynamics. *J. Atmos. Sci.*, **52**, 937-964.
- , A. Aksakal, and J. T. McQueen, 1995: The influence of mesoscale humidity and evapotranspiration fields on a model forecast of a cold frontal squall line. *Mon. Wea. Rev.* (accepted).
- Konrad, T. G., 1970: The dynamics of the convective process in clear air as seen by radar. *J. Atmos. Sci.*, **27**, 1138-1147.
- Korotky, J. D., 1990: The Raleigh tornado of November 28, 1988: The evolution of a tornadic environment. *Preprints, 16th Conference on Severe Local Storms*, Kananaskis Park, Alberta, Canada, Amer. Meteor. Soc., 532-537.
- Kuettner, J. P., 1971: Cloud bands in the earth's atmosphere: observations and theory. *Tellus*, **23**, 404-425.
- LeMone, M. A., 1973: The structure and dynamics of horizontal roll vortices in the planetary boundary layer. *J. Atmos. Sci.*, **30**, 1077-1091.

- Maddox, R. A., L. R. Hoxit, and C. F. Chappell, 1980: A study of tornadic thunderstorm interactions with thermal boundaries. *Mon. Wea. Rev.*, **108**, 322-337.
- Mahfouf, J., E. Richard, and P. Mascart, 1987: The influence of soil and vegetation on the development of mesoscale circulations. *J. Cli. Appl. Meteor.*, **26**, 1483-1495.
- McCumber, M.C. and R.A. Pielke, 1981: Simulation of the effects of surface fluxes of heat and moisture in a mesoscale numerical model. Part 1: Soil layer. *J. Geophys. Res.*, **86**, 9929-9938.
- Mueller, C. K. and R. E. Carbone, 1987: Dynamics of a thunderstorm outflow. *J. Atmos. Sci.*, **44**, 1879-1898.
- \_\_\_\_\_, J. W. Wilson, and N. A. Crook, 1993: The utility of sounding and mesonet data to nowcast thunderstorm initiation. *Weather and Forecasting*, **8**, 132-146.
- Ookouchi, Y, M. Segal, R.C. Kessler, and R.A. Pielke, 1984: Evaluation of soil moisture effects on the generation and modification of mesoscale circulations. *Mon. Wea. Rev.*, **112**, 2281-2292.
- Operational Training Branch/Operational Support Facility, WSR-88D student guide, April 1994.
- Pielke, R.A., J.H. Rodriguez, J.L. Eastman, R.L. Walko, and R.A. Stocker, 1993: Influence of albedo variability in complex terrain on mesoscale systems. *J. of Clim.*, **6**, 1798-1806.
- Purdum, J. F. W., 1973: Meso-highs and satellite imagery. *Mon. Wea. Rev.*, **101**, 180-181.
- \_\_\_\_\_, 1976: Some uses of high-resolution GOES imagery in the mesoscale forecasting of convection and its behavior. *Mon. Wea. Rev.*, **104**, 1474-1483.
- \_\_\_\_\_, 1979: The development and evolution of deep convection. *Preprints 11th Conference on Severe Local Storms*, Kansas City, MO, Amer. Meteor. Soc., 143-150.



- \_\_\_\_\_, and K. Marcus, 1982: Thunderstorm trigger mechanisms over the southeast United States, *Preprints, 12th Conference on Severe Local Storms*, San Antonio, Amer. Meteor. Soc., 487-488.
- Rabin, R. M. and R. J. Doviak, 1982: Prestorm observations in the clear air boundary layer with a Doppler radar. *Preprints, 12th Conference on Severe Local Storms*, San Antonio, Amer. Meteor. Soc., 425-429.
- \_\_\_\_\_, 1989: Meteorological and astronomical influences on radar reflectivity in the convective boundary layer. *J. App. Meteor.*, **28**, 1226-1235.
- Ralph, F. M., 1994: Using radar-measured radial vertical velocities to distinguish precipitation scattering from clear-air scattering. *J. Atmos. Ocean. Tech.*, (In press).
- Rinehart, R. E., 1991: Radar for Meteorologists, Knight Printing Company, Fargo, North Dakota, 334 pp.
- Riordan, A.J., 1990: Examination of the mesoscale features of the GALE coastal front of 24-25 January 1986. *Mon. Wea. Rev.*, **118**, 258-282.
- Sanders, Frederick and C. A. Doswell III, 1995: A case for detailed surface analysis. *Bull. Amer. Meteor. Soc.*, **76**, 505-521.
- Schreiber, W. E., 1986: Case studies of thunderstorms initiated by radar-observed convergence lines. *Mon. Wea. Rev.*, **114**, 2256-2266.
- Scofield, R. A. and J. F. W. Purdom, 1986: The Use of Satellite Data for Mesoscale Analysis and Forecasting Applications, Mesoscale Meteorology and Forecasting, P.S. Ray, Ed., Boston, Amer. Meteor. Soc., 118-150.
- Segal, M. J.F.W. Purdom, J.L. Song, R.A. Pielke, and Y. Mahrer, 1986: Evaluation of cloud shading effects on the generation and modification of mesoscale circulations. *Mon. Wea. Rev.*, **114**, 1201-1211.
- \_\_\_\_\_, and R. Avissar, 1988: Evaluation of vegetation effects on the generation and modification of mesoscale circulations. *J. Atmos. Sci.*, **45**, 2268-2292.

- Sha, W., T. Kawamura and H. Ueda, 1991: A numerical study on sea/land breezes as a gravity current: Kelvin-Helmholts billows and inland penetration of the sea-breeze front. *J. Atmos. Sci.*, **48**, 1649-1665.
- Stull, Roland B., 1993: An Introduction to Boundary Layer Meteorology. Kluwer Academic Publishers, Boston, 666 pp.
- Tant, P. L., H. J. Byrd, and R. E. Horton, 1990: General Soil Map of North Carolina. Soil Conservation Service, U.S. Department of Agriculture.
- Vescio, M.D., K.K. Keeter, G. Dial, P. Badgett, and A.J. Riordan, 1993: A low-top weak-reflectivity severe weather episode along a thermal/moisture boundary in eastern North Carolina. *Preprints, 17th Conference on Severe Local Storms*, St. Louis, MO, Amer. Meteor. Soc., 629-633.
- Wakimoto, R. M., 1982: The life cycle of thunderstorm gust fronts as viewed by Doppler radar and rawinsonde data. *Mon. Wea. Rev.*, **110**, 1060-1082.
- \_\_\_\_\_ and N. T. Atkins, 1994: Observation of the sea-breeze front during CaPE. Part I: Single Doppler, satellite, and cloud photogrammetry analysis. *Mon. Wea. Rev.*, **122**, 1092-1113.
- Weaver, J.F. and S.P. Nelson, 1982: Multiscale aspects of thunderstorm gust fronts and their effects on subsequent storm development. *Mon. Wea. Rev.*, **110**, 707-718.
- Weisman, R. A., 1990: An observational study of warm season southern Appalachian lee troughs. Part II: Thunderstorm genesis zones. *Mon. Wea. Rev.*, **118**, 2020-2041.
- Wilson, J. W., and W. E. Schreiber, 1986: Initiation of convective storms by radar-observed boundary layer convergent lines. *Mon. Wea. Rev.* **114**, 2516-2536.
- \_\_\_\_\_, G. B. Foote, N. A. Crook, J. C. Fankhauser, C. G. Wade, J. D. Tuttle, C. K. Mueller, S. K. Krueger, 1992: The role of boundary-layer convergence zones and horizontal rolls in the initiation of thunderstorms: A case study. *Mon. Wea. Rev.*, **120**, 1785-1815.
- \_\_\_\_\_, and C. K. Mueller, 1993: Nowcasts of thunderstorm initiation and evolution, *Wea. Forecasting*, **8**, 113-131.

- \_\_\_\_\_, T M. Werkwerth, J. Vivekanandan, R. M. Wakimoto, and R. W. Russel, 1994: Boundary layer clear-air echoes: Origin of echoes and accuracy of derived winds. *J. Ocean. Atm Tech.*, **11**, 1184-1206.
- Zhang, D. and R. A. Anthes, 1982: A high resolution model of the planetary boundary layer - sensitivity tests and comparisons with SESAME-79 data. *J. App. Meteor.*, **21**, 1594-1608.
- Zhong, S. and E. S. Takle, 1992: An observational study of sea- and land-breeze circulation in an area of complex coastal heating. *J. App. Meteor.*, **31**, 1426-1438.